1974

RNA and Cell Volume Distribution Analysis of VEE Virus Infected Mosquito Cell Cultures

Clayton Werner Naeve

RNA AND CELL VOLUME DISTRIBUTION ANALYSIS OF VEE VIRUS INFECTED MOSQUITO CELL CULTURES

BY

CLAYTON WERNER NAEVE

A thesis submitted
in partial fulfillment of the requirements for the
degree Master of Science, Major in
Microbiology, South Dakota
State University
1974

RNA AND CELL VOLUME DISTRIBUTION ANALYSIS OF VEE VIRUS INFECTED MOSQUITO CELL CULTURES

This thesis is approved as a creditable and independent investigation by a candidate for the degree, Master of Science, and is acceptable as meeting the thesis requirements for this degree, but without implying that the conclusions reached by the candidate are necessarily the conclusions of the major department.

Thesis Advisor Date

Head Date
Microbiology Department

ACKNOWLEDGMENTS

I wish to extend my sincere appreciation to my major professor, Dr. George C. Parikh, for his advice, counsel, and patience during the course of this study and the preparation of this thesis.

I wish to express my sincere thanks to the staff of the Veterinary Science and Diagnostic Laboratory, S. D. S. U.; the Northern Grain Insect Research Laboratory, U. S. D. A., Brookings; and the Station Biochemistry Department, S. D. S. U., for their advice, their techniques, and the use of their facilities.

Sincere appreciation is extended to Dr. Sonja M. Buckley, Yale Arbovirus Research Unit; Dr. Imogene Schneider, Walter Reed Army Institute of Research; Dr. A. J. Machatt, National Animal Disease Laboratory, and the Veterinary Science and Diagnostic Laboratory for providing the cell cultures and culture techniques employed in this study.

I wish to extend my thanks to Dr. T. Sreevalsan, Georgetown University, and Sylvia Bunting, National Institute of Health, for their patience and kindness in my training in RNA extraction and in polyacrylamide gel electrophoresis. I wish to extend sincere appreciation to my cell culture technicians, Ms. Kathy Veal and Ms. Linda Talley.

The computer expertise of Mr. Stan Carlson is gratefully acknowledged - in addition to his advice regarding data analysis.

The assistance of Dr. T. R. Wilkinson with proofreading of this manuscript is gratefully acknowledged.

I thank the Microbiology Department faculty and graduate students for their continued advice and discussions regarding this research.

Appreciation is extended to Mrs. Charlotte Dennis for typing this thesis. The friendship and understanding of Ms. Carol Lunder is also appreciated.

I wish to thank my parents, Mr. and Mrs. Werner J. Naeve, for their continued support, understanding, and encouragement.

CWN

LIST OF ABBREVIATIONS

Aal	*Aedes albopictus*
arbovirus	Arthropod-borne virus
BHK-21	Baby hampster kidney cells
C6	Control day 6
C8	Control day 8
DNA	Deoxyribonucleic acid
DNase	Deoxyribonuclease
EEE	Eastern equine encephalomyelitis
FBS	Fetal bovine serum
iFBS	Inactivated fetal bovine serum
GKN	Glucose, potassium, and sodium chloride solution (Calcium and magnesium-free saline)
HBSS	Hank's balanced salt solution
LD_{50}	50% lethal dose
MCM	Mosquito culture medium
MEM	Minimum essential medium
Na-EDTA	Ethylenediamine tetraacetate disodium salt
PAGE	Polyacrylamide gel electrophoresis
p.f.u.	Plaque forming units
RF	Replicative form
RI	Replicative intermediate
RNA	Ribonucleic acid
RNase	Ribonuclease
SDS	Sodium dodecyl sulfate

LIST OF ABBREVIATIONS (Con't.)

SFV	Semliki Forest virus
SLE	Saint Louis encephalomyelitis
SV	Sindbis virus
TCA	Trichloroacetic acid
TEB	Tris-EDTA-borate buffer
U.V.	Ultraviolet
VEE	Venezuelan equine encephalomyelitis
VERO	African Green Monkey Kidney cells
WEE	Western equine encephalomyelitis

TABLE OF CONTENTS

TABLE OF CONTENTS (Con't.)

LIST OF TABLES

LIST OF FIGURES

LIST OF FIGURES (Con't.)

INTRODUCTION

In terms of cellular pathology cultured cells may respond to virus infections in several ways. Three common types of response are a) steady-state noncytocidal infections, in which the virus multiplies in the cell without inflicting obvious morphological damage, b) transformation, also noncytocidal but in which the virus induces cellular change to a neoplastic state, and c) cytocidal infections, in which the virus inhibits cellular metabolism leading rapidly to the destruction of the cell.

Each of these responses is biochemical in nature and is due to the action of virus-specified metabolic products. Many times these biochemical changes lead to functional disturbances and often to histopathologies, commonly called cytopathic effects (CPE). Cytopathic effects are generally microscopically visible and consist of one or more of the following: cell lysis, vacuolization, appearance of inclusion bodies, and cell fusion resulting in polykaryocytes. In addition, one of the earliest cytopathic effects is what histopathologists call "cloudy swelling", associated with changes in the permeability of the plasma membrane. Such slight swelling, however, is very difficult to detect in cell cultures by microscopic observation.

The purpose of this investigation, based on the above observations, is two-fold: (i) to shed some light on the sequence of virus-specific biochemical events occurring in cells exhibiting a steady-state noncytocidal response to virus infection (in this case the mechanism of ribovirus genome replication), and (ii) to develop a

rapid means of detecting such inapparent noncytocidal infections (in this case the detection of post-infection "cloudy swelling"). Hence, two separate yet related studies were undertaken - an analysis of virus-specific RNA species isolated at various times post-infection and electronically gathered, computer assisted analysis of cell volume distribution profiles.

The subject of this investigation is the Aedes albopictus (Aal) cell line infected with Venezuelan equine encephalomyelitis (VEE) virus, a group A arbovirus. This cell-virus system is an ideal choice for both types of analysis. Certain of the group A arboviruses have been looked at as "models" for ribovirus replication and thus have several advantages for an RNA study. The genome is a single strand of RNA containing only about a dozen cistrons, the virions contain only one polypeptide in the nucleocapsid and one in the envelope, and infectious RNA is easily isolated and titrated by sensitive plaque assay. In addition, VEE infected Aal cells exhibit a noncytocidal response and are thus ideally suited for the volume distribution profile study.

The A. albopictus cells were employed for several reasons. First, the A. albopictus mosquito can function as a vector for the VEE virus. Second, the A. albopictus cell line was a recent development and little was known about virus replication in these cells. Third, these cells do not exhibit CPE upon infection with VEE. Fourth, this cell-virus system provided a model by which other noncytocidal cell-virus systems could be compared.

There is a definite need for the RNA analysis. The mechanism of single-strand RNA virus replication has been under intensive study in recent years; the results of which could possibly lead to the means by which RNA virus infections could be prevented. Certainly some of the most destructive viruses, in terms of human misery and economic considerations, are the single-strand RNA viruses. These include polio, rabies, yellow fever, influenza, mumps, measles, and encephalitis viruses. In addition, a large number of the known animal cancer viruses are single-strand RNA viruses.

Virtually all the experimental evidence supporting the current hypothesis of ribovirus replication is based on virus infections in cell lines exhibiting a cytocidal response. The function of the RNA analysis in this investigation is to determine if the mode of ribovirus replication in cells exhibiting the noncytocidal response is similar to the mechanism of ribovirus replication in cells exhibiting a cytocidal response.

In order to accomplish this goal, infected Aal cells were treated with Actinomycin D to inhibit DNA dependent RNA replication, treated with tritiated uridine supplemented media, and allowed to incubate. At various times post-infection the virus-specific RNA was extracted from the cells with phenol-SDS. The different types of RNA isolated was determined by polyacrylamide gel electrophoresis of the molecules. The gels were then sectioned and each section assayed for radioactive RNA species.

There is also a need for a rapid means of detecting noncytocidal virus infections. This need is felt in several areas of virology all of which involve a noncytocidal response to virus infection. Cell-virus systems which fall into this category include the "unconventional slow viruses" in brain tissue cultures, most RNA tumor viruses in various cell systems, and many species of arboviruses in several vector cell lines.

The "unconventional slow viruses" have been implicated in the etiologies of numerous degenerative nervous system diseases. These severe neurological disorders - as required by the definition of "slow" infection, are characterized by a long incubation period and then a protracted course of disease that almost invariably culminates in death. These include kuru and Creutzfeld-Jacob disease in humans, scrapie and transmissible mink encephalopathy in animals. These are called "unconventional slow viruses" in the sense that, although caused by a transmissible infective agent, they are not typical viruses and may in fact be more closely akin to viroids (naked nucleic acid molecules).

Research on the unconventional slow viruses is handicapped by the lack of a fast, reliable method of detecting their presence. Although the agents can be propagated in cell cultures derived from the brains of infected animals, they do not noticeably damage the cells. Investigators must now depend on their infectivity in susceptible hosts in which the minimum incubation period of the "viruses" is several months.

In the case of the known RNA tumor viruses, it has been shown that several species can be assayed by observation of their transforming abilities. Thus, with suitable agar overlays on the cells to prevent diffusion of virus, these transforming assays can be quantitative. The avian RNA tumor viruses fall into this category. However, cytopathic effect has not been observed with the murine viruses, nor has it with the avian leukosis viruses and Rous Sarcoma virus. Similarly, in the case of mouse mammary tumor virus, there is as yet no satisfactory in vitro system for assaying the virus.

Finally, several studies have shown that many arboviruses replicate in vector cell lines such as Aedes albopictus mosquito cells, Aedes aegypti mosquito cells, and Antheraea eucalypti moth cells. However, few produce a cytocidal infection. In other words there is no satisfactory, rapid means of detecting their presence in infected cells.

The cell volume distribution profile study, then, is an attempt to develope a rapid method to detect such noncytocidal virus infections. The method employed, based on the detection of "cloudy swelling" and other virus mediated cell changes, utilizes an electronic counting and sizing apparatus - the Coulter Counter. The Coulter Counter data is stored on magnetic tape and is analyzed in a multitude of ways by a mini-computer - the Hewlett-Packard Model 9830A.

The general concept of this investigation is best illustrated by a flow diagram as outlined in Figure 1.

Fig. 1. Schematic Representation of Thesis Research.

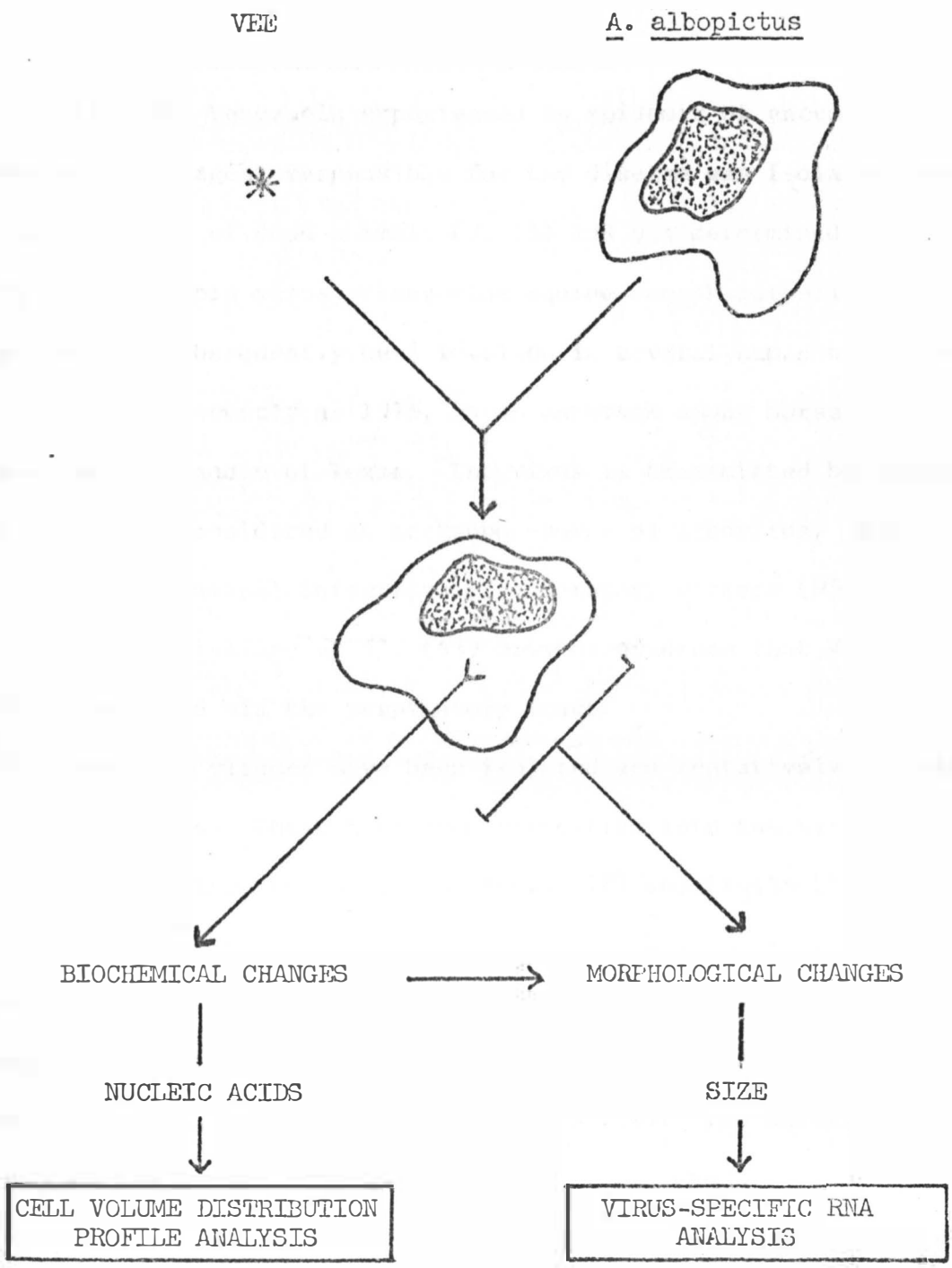

LITERATURE REVIEW

Venezuelan Equine Encephalomyelitis Virus

In 1938, Venezuela experienced an epidemic of encephalitis in horses; the agent responsible for the disease was isolated from the brain tissues of dead animals (7, 45) and was determined to be viral in nature. This virus, Venezuelan equine encephalomyelitis (VEE) virus, has subsequently been involved in several human outbreaks (65, 78) and, as recently as 1971, in an outbreak among horses in the southern panhandle of Texas. The virus is transmitted by mosquitoes and is thus considered an arthropod-borne or arbovirus. Moreover, numerous accidental infections of laboratory workers (95) and the findings of Kissling et al. (43) provide evidence that VEE may also be transmitted via the respiratory tract.

Over 200 viruses have been isolated and tentatively classified as arboviruses. These have been classified into twenty-one antigenic groups as defined by Casals and Brown (18) and Casals (17) with two major groups - group A and group B. The VEE virus is considered a group A arbovirus and shares this distinction with approximately eighteen other viruses, including Western equine encephalitis (WEE), Sindbis virus, and Semliki Forest virus (18). The natural or suspected vectors for all group A arboviruses are mosquitoes.

The group A arboviruses, as all arboviruses, contain ribonucleic acid (RNA) genomes. They are easily inactivated by heat, formalin, and beta-propiolactone (19). The VEE virus has been shown, by electron microscopy, to be approximately spherical and between 40-45

millimicrons in diameter (61). In addition, Klimenko et al. (44) have shown the VEE virion to be enveloped; the diameter then being 60-75 millimicrons. This envelope is of a lipoprotein nature; the total lipid content of VEE being 24.3 percent (38). The total RNA content of the virus is 6.2 percent and the total protein content is 69.5 per cent (100).

The VEE virus replicates and produces cytocidal infection in mammalian and avian cell cultures. The cytocidal effect and cytopathic effects produced by VEE in these cultures provide the basis for assay methods. Venezuelan equine encephalomyelitis virus will also replicate in invertebrate cell cultures (41); however, in this case the infection is noncytocidal. Thus, the virus has the ability to destroy animal or bird host cells resulting in disease, yet fails to damage the cells of the mosquito vector. This effect is important in the survival of the virus and is thus worthy of investigation.

Development of Aedes albopictus Mosquito Cell Culture

The in vitro culturing of mosquito cells began in 1938 (97) and was continued with difficulty until relatively recently. At that time little growth was obtained in vitro although the tissues survived for many weeks as evidenced by muscular contractions. Grace established the first continuous mosquito cell line in 1966, developed from larvae of the mosquito Aedes aegypti in a medium containing moth hemolymph. Initially there were a number of morphologically distinct types of cells in the cultures. However, after the cultures had been growing for three months, many of the cell types disappeared leaving

predominately spindle-shaped cells, 40-50 microns long and 8-10 microns wide. These cells grew in clumps and remained attached to the vessel walls. It was not possible to determine from which tissues the cells arose (33).

Media composition was at first a problem since it was necessary to formulate the media to suit the particular cell line. The addition of insect hemolymph was used as a supplement to provide the cells with essential nutrients. Obviously, insect hemolymph is not in abundance and the search for a suitable replacement continued until 1967. At this time Nagel et al. (62) and Converse and Nagel (21) adapted Aedes aegypti cells to fetal bovine serum supplemented media. Virtually all subsequent dipteran lines have been initiated and maintained in media supplemented with vertebrate sera.

To date, several workers have established continuous cell lines originating from mosquito tissues (9, 71, 80, 84, 94, 99). These investigators used a variety of mosquitoes including Aedes aegypti, Aedes albopictus, Anopheles stephensi, Aedes vexans, and Culiseta inornata. At the present time there are over a dozen continuous mosquito cell lines available.

The cell line employed in this investigation, Aedes albopictus (Singh), was developed in 1967 by Dr. K. R. P. Singh (84). Several hundred freshly hatched larvae were cut into pieces, incubated in trypsin, and placed in a growth promoting medium that Mitsuhashi and Maramorosch (58) described in 1964 for the propagation of leafhopper tissue culture, supplemented with fetal bovine serum for ease of maintenance.

The A. albopictus cells grew well in monolayer culture and exhibited three morphologically distinct cell types. The majority are either round, 6 to 20 microns in diameter, or spindle-shaped, 7 to 10 microns wide and 15 to 90 microns long. In addition, round binucleate cells were also observed.

A subculture of Singh's Aedes albopictus was brought to the United States by Dr. Singh of the Virus Research Center, Poona, India and given to Dr. Sonja M. Buckley at the Yale Arbovirus Research Unit. These cells are kept in liquid nitrogen storage and serve as a source for other investigators. This investigation employs cells obtained from Buckley in their forty-second passage.

Growth of Arboviruses in Mosquito Cell Culture

Mosquito cell cultures were employed in arbovirus research immediately after their development in 1966. Indeed, many cultures were initiated for the singular purpose of delving into the nature of host-virus and vector-virus relationships.

Several studies have been done to determine the growth characteristics of arboviruses in Aal cells, the cell line of interest in this investigation. Singh and Paul detected the growth of several group A, group B, and ungrouped arboviruses, including chikungunya and Sindbis viruses of group A, dengue type 1 to 4, Japanese B encephalitis and West Nile viruses of group B, and Sindbis virus in the ungrouped category (85, 86). Cytopathic effects were observed only with the group B arboviruses: dengue types 1, 2 and 4, West Nile, and Japanese B encephalitis. In 1969, Paul and Singh (67) and Paul

et al. (68) determined that Aal cells are highly sensitive to infection by the group B viruses and described cytopathic effects for a group A arbovirus, chikungunya. Yunker et al. (105) reported results of inoculation of Aal cultures with Japanese B encephalitis, Saint Louis encephalitis, and West Nile viruses, all group B arboviruses; in this case CPE was not observed. An investigation by S. M. Buckley (13) included twenty-three different arboviruses. Of these twenty-three viruses, screened for their ability to produce CPE or replicate in Aal, only nine were found to do so. That is, four group A viruses replicated (chikungunya, EEE, Semliki Forest, and VEE), three group B viruses replicated (SLE, West Nile, and yellow fever), and the Indiana and New Jersey strains of vesicular stomatitis virus replicated in the mosquito cell culture. Only one virus, mosquito-borne West Nile, produced CPE. In the early nineteen seventies, three separate studies demonstrated the ability of dengue type 2 virus to infect Aal cells without causing apparent damage to the host cells (20, 83, 91); however, persistent infection was established with continued virus production for at least six months (83). Davey et al. (25) compared the growth kinetics of Semliki Forest virus in four cell lines, one invertebrate and three vertebrate, and found no difference in the latent period, growth rate and virus yield per cell (25).

Venezuelan equine encephalomyelitis virus, the virus of interest in this investigation, replicates in but does not produce a cytocidal infection in Aal cells (13). In addition, the same effect has been seen in primary cultures of other mosquito species (41, 42).

Although results are sometimes ambiguous, it appears that two generalizations can be drawn relative to arbovirus replication in Aal mosquito cell cultures (i) most viruses of group A and group B, and several ungrouped viruses can replicate in Aal cells; however only four viruses (all in group B) have been found to be cytocidal, and (ii) of those arboviruses inducing noncytocidal response to infection in Aal cells (including VEE), most are cytocidal in vertebrate host cells. These observations suggest a difference in the mechanism of replication or maturation insofar as it affects the two types of cells.

Arbovirus Ribonucleic Acid Replication

In order to determine if the mechanism of VEE virus replication in Aal cells (a noncytocidal response) is similar to the mechanism of single-strand RNA virus replication in vertebrate cells (a cytocidal response) it is important to understand the current hypothesis of single-strand RNA virus replication.

Obviously, the semi-conservative replication scheme of double-stranded DNA by Watson-Crick base pairing has little merit when dealing with single-strand RNA molecule replication. Indeed, the use of specific inhibitors led to the conclusion that the replication of small RNA viruses is not dependent on the integrity of host cell DNA, nor does it require DNA synthesis (75, 82). In addition, Actinomycin D, which inhibits DNA-dependent RNA synthesis (76), does not prevent single-strand RNA virus replication (54, 81, 87). Moreover, replication of several single-strand RNA viruses follows the appearance of an enzyme able to synthesize RNA from an RNA template, i.e.

RNA-dependent RNA polymerase (5, 103). These observations led Montagnier and Sanders (59) to speculate on and demonstrate the existence of a double-stranded intermediate form of RNA analogous to the double-stranded intermediate species of DNA found in the replication of the single-strand DNA phage X174. This species was entitled the "replicative form (RF)" of viral RNA. Subsequently, Haruna et al. and Haruna and Spiegelman isolated the enzyme RNA-dependent RNA polymerase in 1963 (35, 36). This enzyme has been found to catalyze the synthesis of a complementary (-) strand from the virus parental (+) strand, forming the double-strand RF molecule (12, 102). The RF is resistant to the action of ribonuclease (RNase) which is specific for single-strand RNA species (11).

Additional study demonstrated the existence of a species of polydisperse, partly double-stranded RNA species in poliovirus infected HeLa cells (6). This was termed the "replicative intermediate (RI)" and was found to exist in several cell-virus systems (6, 32, 90). Finally, intact progeny strands were isolated and found to be the equivalent of the parental strands (27).

Thus, to summarize, the current view of single-strand RNA virus replication is as follows: The infecting virus RNA genome acts both as messenger RNA and as a (+) template for transcription. Early during infection the parental RNA molecule, acting as messenger RNA, codes for the production of a high molecular weight protein. Post-translation cleavage (14) of this large molecule produces two capsid and three noncapsid proteins. One of the noncapsid proteins is the

enzyme RNA-dependent RNA polymerase. This enzyme is then available to catalyze the synthesis of the double-strand RF from the parental strand. The RF then serves as a template for progeny molecules. In doing so, it becomes the partly double and partly single-strand RI molecule. Finally, from the RI molecule comes the completed progeny RNA virus molecules. A schematic diagram of this process is illustrated in Figure 2.

The majority of the investigations undertaken to determine the sequence of events occurring in single-strand RNA virus replication were performed with enteroviruses. However, once the concept began taking shape, investigations involving arboviruses continued rapidly. Sonnabend et al. first demonstrated in 1964 the existence of the RF in Semliki Forest virus infected chick embryo fibroblast cells (87). In 1966, Friedman et al. isolated three forms of Semliki Forest virus RNA: the RF, the RI, and progeny molecules (32). Dengue virus infected BHK-21 cells exhibited the progeny (45S), the RF (20S), and the RI (26S) actinomycin D resistant, virus-specific RNA species (92). Two closely related group A arboviruses, Semliki Forest (SFV) and Sindbis (SV), became and remain the mainstay of arbovirus RNA replication research. In 1968 Robert Friedman at the National Cancer Institute isolated three viral RNA species from SFV infected chick fibroblasts by sucrose density gradient centrifugation. They were identified as progeny 42S species, 20S RF species, and 26S RI species RNA (31). The same results were obtained by Cartwright and Burke in 1970 (16). Sindbis virus infections also produced the three virus-

Fig. 2. Schematic Representation of the Single-strand RNA Virus Replication Hypothesis.

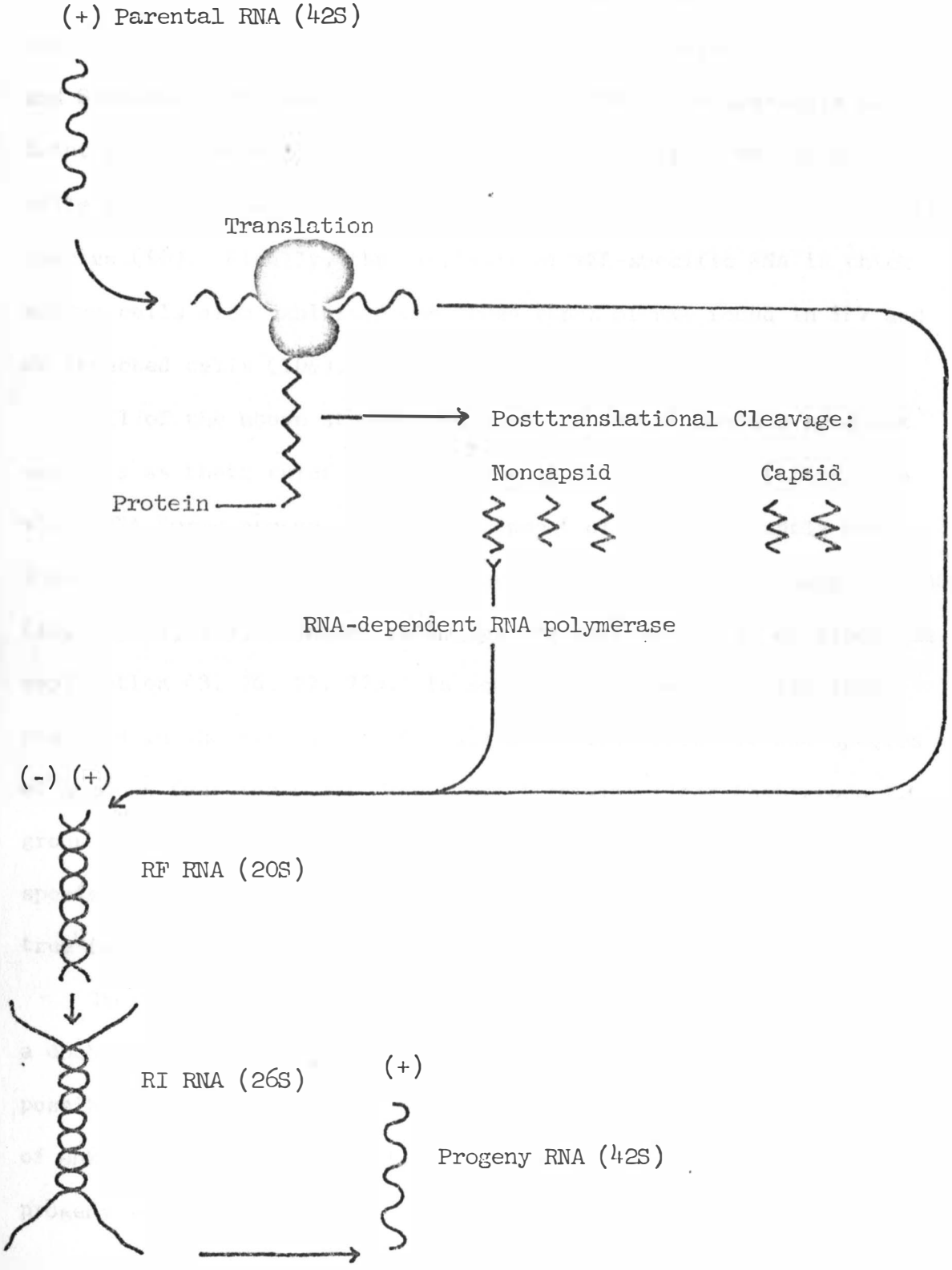

specific RNA species isolated from chick fibroblasts in 1967 (72). The RNA-dependent RNA polymerase involved in double-strand RF production was isolated from SV infected chick fibroblasts by Martin and Sonnabend (56) and Sreevalsan et al. (89). The synthesis of Saint Louis encephalitis virus (a group A arbovirus) RNA in BHK-21 cells involved the production of the 42S, 20S, and 26S virus-specific species (98). Finally, the synthesis of VEE-specific RNA in chick embryo cells also exhibited the three types of RNA found in SFV and SV infected cells (106).

All of the above studies employed the use of density gradient analysis as their chief method for separating and quantitating the viral RNA forms present. The development of a significantly more sensitive method of analysis, polyacrylamide gel electrophoresis (PAGE) (10, 29, 55, 69), resulted in higher resolution studies of arbovirus replication (3, 26, 27, 77). In some cases these investigations resulted in the resolution of additional virus-specific RNA species of unknown function (53). However, it remains clear that group A, group B, and some ungrouped arboviruses replicate via a RF and RI species in infected vertebrate cell culture. Does this also hold true for arbovirus infected invertebrate cell cultures?

Stollar et al. (93) found that SV infected Aal cells exhibit a double-stranded species having a sedimentation constant of 20S, possibly the replicative form. In addition, he found a 32S species of unknown function (possibly the RI) and a 42S species, probably progeny molecules.

On the basis of the above study it appears that arbovirus RNA replication in invertebrate cell culture may parallel the mechanism of arbovirus RNA replication in vertebrate cell culture. The scarcity of information, however, demands further work be done in this area.

Electron Microscopy of the Cytocidal and Noncytocidal Response

In vertebrate cells, arbovirus infection usually culminates in cell death. A comprehensive study by Morgan et al. in 1961 on the development of WEE virus in primary amnionic cells demonstrated marked cytopathology. Morgan found pyknosis of the nucleus, condensation and vacuolization of the cytoplasm, disintegration of mitochondria and rupture of the cell wall (60). The Japanese B encephalitis virus was observed to develop on the cytoplasmic vacuoles in porcine kidney stable cells. The virus matured by "budding" into the vacuole, usually in random arrangement, but occasionally in crystals. The virus packed vacuole then migrated to the cell surface and liberated the virus particles (64). Similar results were obtained with VEE virus in KB cells (61). Acheson and Tamm (1) found similar results in SFV infected chick embryo cells; however, they also demonstrated evidence that the SFV envelope consists of a portion of the plasma membrane. Again condensation and vacuolization of the cytoplasm were observed as predominant cytopathic effects. Finally, a study by Bykovsky et al. on the morphogenesis of VEE virus in chick embryo fibroblasts provided micrographs of each phase of virus development and proposed a model of VEE virus replication (15).

Although arbovirus infection of cultured vertebrate cells is in general cytocidal, arbovirus morphogenesis in invertebrate cells is less well understood. Most light microscopic (49, 50), fluorescent antibody (28) and electron microscopic (40, 51, 104) studies support the view that replication of arboviruses is noncytocidal in the intact insect.

The development of mosquito cell culture provided a means by which comparisons could be made to arbovirus replication in vertebrate cell culture. In 1967 Filshie and Rehacek studied the morphology of Murray Valley encephalitis and Japanese encephalitis viruses in cultured Aedes aegypti cells (30). They found that the group B Japanese encephalitis virus produces cytopathic effects but that Murray Valley encephalitis virus does not. The Japanese B virus, however, is one of only four arboviruses known to cause CPE in insect cell culture. Both viruses were found to be associated with vacuole and endoplasmic reticulum membranes indicating these are the assembly sites.

Finally, a comparative study dealing with the growth of SFV and Kunjin viruses in Aedes albopictus and VERO cells demonstrated that the replication of both viruses in Aal cells is quantitatively similar in all respects to their replication in cells of mammalian origin, except for the induction of cytopathic effects. Thus Davey et al. (25) state:

> "Arbovirus-infected A. albopictus cells therefore offer a useful model system for studies of non-cytopathic infection by this group of viruses."

Volume Distribution Profile Analysis

Subsequent to the development of the Coulter Counter, by Dr. W. H. Coulter in 1953 (23), several studies were undertaken to determine the machine's ability to measure particle or cell volumes accurately (46, 57, 70). The majority of these investigations dealt with RBC volume since the prime application of the machine was clinical in nature. The results of these studies indicated that the Coulter Counter, when calibrated properly and corrected for coincidence (101), provides very accurate data relative to cell numbers and cell volume. This in turn provides very accurate volume distribution profiles.

Following this observation, several attempts were made to employ accurate cell volume measurements in a variety of investigations For example, cell size distribution patterns were employed as a means of early detection of uterine cancer by Ladinsky et al. in 1964 (48). Malignant uterine epithelial cells are considerably larger than normal epithelia allowing rapid detection by this method. A year later G. Haughton et al. at the Karolinska Institutet in Sweden were able to distinguish between normal lymph tissue cells and lymphoma cells, the tumor cells again being larger than normal (37). Cell volume distribution profiles have also been used to count and determine the size distribution of diploid and tetraploid hepatic nuclei (79). Studies of cell growth and division, whether mammalian (2, 8) or bacterial (96), have successfully employed cell volume distribution analysis via Coulter Counter. Indeed, the Coulter Counter has been utilized in several areas of microbiology.

Although investigations aimed at detecting virus induced cell volume changes have been performed in the past (4), most involved separation of different size cells by density gradient centrifugation (73). This technique is time consuming, laborious, and tedious. Previous research by this laboratory (63, 66, 88) demonstrates the rapidity, accuracy, and reproducibility of Coulter Counter volume distribution profile analysis of small volume changes - making detection of noncytocidal virus infections in cell cultures seem within reach.

MATERIALS AND METHODS

TISSUE CULTURE MATERIALS AND PROCEDURES

Two different continuous cell lines were employed in this research; the first being Aedes albopictus mosquito cell culture, the second being VERO cell culture (African Green Monkey kidney cells).

During the course of this study, A. albopictus cultures were obtained from two sources: Dr. Imogene Schneider, Ph.D.
Department of Entomology
Walter Reed Army Institute of Research
Washington, D. C. 20012

Dr. Sonja M. Buckley, M. D.
Yale Arbovirus Research Unit
Department of Epidemiology and Public Health
New Haven, Conneticut 06510

The cells obtained from both sources were virtually identical; however, the majority of the project was carried out with Buckley's cells because of their low passage number. All A. albopictus cells used in this investigation were between passage number 42 to 65.

Since the noncytocidal response to infection of A. albopictus by VEE provided difficulties in assaying virus production in these cells, it was necessary to employ a cell line that does experience visible morphological damage upon VEE infection. The cell line which very nicely replicates most arboviruses and which produces excellent plaque assays is the VERO cell line. These cells were obtained from two sources: Veterinary Science Diagnostic and Research Laboratory
South Dakota State University
Brookings, South Dakota 57006

Dr. A. Machatt, Ph.D.
Veterinary Biologics Division
National Animal Disease Laboratory
Ames, Iowa

Dr. Machatt was the source of cells for the Veterinary Science Laboratory, so both lines were essentially the same except for the passage number. All VERO cells used in this investigation were between passage number 140 to 160.

MATERIALS AND PROCEDURES FOR SUBCULTURING A. ALBOPICTUS CELLS

A. Several items are required for the propagation of A. albopictus cells:

1. Mosquito Culture Medium (MCM). This is purchased commercially from Grand Island Biological Company (GIBCO), 3175 Staley Road, Grand Island, New York 14072. For use, MCM is supplemented with 20% inactivated fetal bovine serum (iFBS).

2. Fetal Bovine Serum (FBS). This item is purchased from GIBCO in dehydrated form. It is simply rehydrated by addition of 100 cc. sterile distilled water and is "inactivated" in a 56°C water bath for 30 minutes. This treatment inactivates any viral inhibitors that may be present in the serum, e.g. antibodies or non-specific inhibitory agents.

3. "TC-30" plastic disposable tissue culture flasks. These sterile flasks hold 30 ml, are pretreated for cell culture, and are purchased from GIBCO ready to use.

4. Trypsin - Versene Solution. A ten-fold concentrated solution is prepared to contain the following:

Trypsin (1:250).	5.0 gm.
Versene (Ethylenediaminetetraacetic Acid Disodium Salt).	2.0 gm.
Double distilled water	900.0 ml.
Phenol Red (0.5%).	4.0 ml.
Penicillin	1.0 gm.
Streptomycin	1.0 gm.
Kanamycin.	0.5 gm.

NaCl	80.0 gm.
KCL	4.0 gm.
$NaHCO_3$	3.5 gm.
Glucose	1.0 gm.

The solution is Millipore* filtered and stored in one milliliter aliquots at -20 C. For use, thaw rapidly and dilute 1:10 in sterile distilled water.

5. Pasteur pipettes. Purchased from any biological supply house and sterilized by autoclaving.
6. Incubator, 27 C.

B. The procedure for cell maintenance is as follows:

1. Upon the arrival of new cell culture flasks, which are commonly shipped completely full of medium, it is necessary to remove all but 2.5 - 3.0 cc. of medium from a 30 cc. flask (or comparable amount per other sized flask). The medium which is removed can be transferred to sterile bottles and used for subsequent transfers.
2. Allow the cells to "recover" for one day.
3. To subculture, pour out the medium from the flask and add 1 cc. trypsin solution.
4. Allow the solution to cover the cell monolayer completely - then invert the flask.
5. Place inverted flasks in a 37 C incubator for 2 minutes.
6. Remove flasks from incubator, pour out trypsin and add 3

---

*Millipore Corporation, Ashby Road, Bedford, Massachusetts 01730; herein referred to as "Millipore".

cc. fresh medium (MCM).

7. Pipette cells free from surface into the fresh medium with a Pasteur pipette.
8. Place six drop aliquots of the cell suspension into new TC-30 subculture flasks - each containing 3 cc. fresh MCM. The A. albopictus cells may be split 1:20 or more.
9. Incubate at 27 C. The cells will have to be transferred approximately every 4 - 6 days at this temperature.

By using six drops cell suspension to "seed" new flasks, confluency is reached in six days. If it is desirable to have confluent monolayers at shorter time intervals, one would simply seed with a larger amount of cell solution.

It is wise to establish an alternate subculture series. This set of flasks is subcultured alternately with the main cell line and serves as a back-up in the event of contamination.

It is important to note that extreme care should be taken to avoid contamination. All subculturing and handling of cells in this project was done in a laminar flow hood (Specialaire Cabinet, Torit Manufacturing Co., St. Paul, Minnesota). This is not absolutely necessary but the hood does a very effective job of holding down contamination problems. Routine precautions regarding sterile technique were observed at all times.

C. Procedure for inoculating A. albopictus cell culture with VEE:

1. Culture flasks to be infected are removed from the 27 C incubator and placed in the alcohol disinfected laminar

flow hood.

2. Discard the old MCM, add 1 cc. Hank's Balanced Salt Solution (HBSS) to control flasks, add 1 cc. HBSS with VEE to infected flasks.
3. Incubate at 37 C for 30 minutes to allow virus adsorption.
4. Pour off HBSS and HBSS with VEE. Rinse the monolayers three times with HBSS.
5. Add 3 cc. fresh MCM supplemented with 20% iFBS. Incubate the cultures at 27 C.

Since these cells do not exhibit CPE, it is necessary to assay the virus production in a lytic cell line; that is, one that does show CPE. The VERO cell culture fits this requirement quite nicely.

MATERIALS AND PROCEDURES FOR SUBCULTURING VERO CELLS

A. The materials required for growth, passage and plaquing VERO cells:

1. Minimum Essential Medium, Eagles (MEM). This medium is purchased commercially from GIBCO in dehydrated form and is prepared by rehydrating, adding sodium bicarbonate to adjust the pH, adding 100 mg/l. Penicillin, Streptomycin, and Kanamycin to control contamination, and is filter sterilized. For growth medium the MEM is supplemented with 20% iFBS; for maintenance medium the MEM is supplemented with 10% iFBS.

2. Fetal Bovine Serum, inactivated (iFBS). Purchased from GIBCO in dehydrated form, this serum is treated exactly as that used on A. albopictus cultures.

3. Calcium and Magnesium Free Saline (GKN). A ten-fold concentrated solution of GKN is composed of the following:

NaCl.	80.0 gm.
KCl	4.0 gm.
Glucose	10.0 gm.
Distilled Water	1000.0 ml.

The solution is sterilized by autoclaving and is diluted 1:10 in distilled sterile water prior to use on cell cultures.

4. Trypsin - Versene Solution. A ten-fold concentrated solution is prepared exactly as that used on A. albopictus cells.

5. Carbon Dioxide Incubator, 37 C. This item is essential for

maintaining the temperature and the 5% CO_2 atmosphere necessary for culture medium pH control.

6. Prescription bottles (glass, 2 oz). These bottles can be purchased at any local drug store and are used as culture flasks. These bottles are inexpensive enough to be considered disposable and are discarded after use.

7. Plaque Medium. For use in plaque overlay agar, this medium is prepared as follows:

MEM.	1 liter pkg.
Distilled Water.	500.0 ml.
$NaHCO_3$	2.2 gm.
Sodium pyruvate (100mM).	10.0 ml.
Lactalbumin hydrolysate.	5.0 gm.
Penicillin	0.2 gm.
Streptomycin	0.2 gm.

Millipore filter, place in stoppered bottles and store at 4 C.

8. Ion Agar (1.45% in sterile water). Purchased from Consolidated Laboratories, Inc., Box 234, Chicago Heights, Illinois.

B. Procedure used to subculture VERO cells:

1. Remove subculture prescription bottle from 37 C incubator and pour off the old medium.
2. Add approximately 5 cc. GKN (1X) to the bottle. Note: the GKN is diluted 1:10 and is thus called 1X as opposed to the concentrated solution designated 10X.
3. Thaw a 1 cc. aliquot of 10X trypsin solution - dilute 1:10 in 9 cc. sterile water for a 1X solution.

4. Pour off GKN, add enough 1X trypsin solution to rinse the cell surface (1-2 cc.), and invert the bottle.
5. Incubate at 37 C for 2-3 minutes
6. Pour off trypsin from bottle - add fresh growth medium. (MEM supplemented with 20% iFBS). The amount of fresh medium added depends on the number of subcultures. For example, one needs 5 cc. of media per 2 oz. prescription bottle; thus, if the subculture is 1:3, one would need to add 15 cc. new media to the flask.
7. Agitate the flask thoroughly to completely suspend the cells in the medium.
8. Dispense 5 cc. aliquots to each of the subculture flasks.
9. Incubate at 37 C and 5% CO_2 atmosphere.

Note: these cells are not usually subcultured more than 1:6.

C. Procedure for plaque assay of VEE in VERO cells:

1. Prepare ten-fold dilutions of stock virus solution (10^{-1} - 10^{-10}) by adding 0.2 cc. virus to 1.8 cc. HBSS.
2. Inoculate two confluent tissue plates of VERO cells with 0.5 cc. of the first dilution; repeat for all dilutions. This step provides two sets of 10 plates each set inoculated with a ten-fold dilution series.
3. Incubate at 37 C for 30 minutes to allow virus adsorption. During this 30 minutes mix (in a 45 C water bath) equal aliquots of Plaque Media and Ion Agar.

4. Pour off virus suspension and rinse monolayers three times with HBSS.
5. Add 5 cc. of plaque agar mixture to each plate and allow to solidify.
6. Invert each plate and incubate at 37 C and 5% CO_2 for 4 - 6 days.
7. Remove agar from plate with spatula.
8. Pour 2 cc. formaldehyde (concentrated) into the plate for 5 minutes or less.
9. Pour off formaldehyde and add enough crystal violet to cover the monolayer for 5 minutes.
10. Observe and determine titer.

The sterility of both cell lines, A. albopictus and VERO, were checked on occasion by various means. Tissue culture fluid was harvested and checked for microbial contamination by inoculating blood agar plates, trypticase soy broth, brain heart infusion broth, tryptose phosphate broth, and nutrient broth (Difco Laboratories, Detroit, Michigan). Aedes albopictus culture fluid was harvested and checked for viral contamination by inoculating VERO cells and suckling Swiss albino mice.

In addition, aliquots of all media, FBS, and buffer solutions were routinely checked for sterility at least one week prior to use. Once every two weeks the shelves and supports in the CO_2 incubator were autoclaved and the water replaced with fresh merthiolate treated water.

Periodically, cells from both lines were placed in frozen storage. The VERO cells were placed in maintenance medium (MEM plus 10% iFBS) containing 10% glycerol, wrapped in cotton, and slowly frozen at -70 C. The A. albopictus cells were placed in medium (MCM plus 10% iFBS) containing 7.5% dimethyl sulfoxide and stored at -70 C. Usually, greater than 70% of the population can be recovered.

VIRUS (VEE) PRODUCTION MATERIALS AND PROCEDURES

The VEE virus used in this study was procurred from the National Communicable Disease Center, Atlanta, Georgia. It is a tissue culture vaccine strain entitled VEE/TC-283.

Stock solutions of virus were prepared in either of two ways, in VERO cell culture or in Swiss albino suckling mice. The suckling mice consistently yielded higher titers and was thus the primary source of virus.

The procedure for infecting VERO with VEE was explained previously; the procedure for suckling mouse inoculation and harvesting is as follows (52):

1. Selecting one to two-day-old suckling mice, inoculate 0.02 cc. stock virus solution intracerebrally using a 1 cc. disposable syringe with a 26 gauge needle.
2. Observe the inoculated litters 12 days for evidence of viral disease.
3. If no symptoms are observed within this period of time, sacrifice the mice and store in a -70 C freezer until the brains are harvested.
4. To harvest infected mouse brain, remove from freezer and allow to thaw.
5. Tape each mouse to a piece of paste board and swab the heads with 1:1000 merthiolate.
6. Remove the viscous brain material with a one cc. syringe equipped with an 18 gauge needle. Approximately 0.1 to

0.2 cc. can be collected from each mouse.

7. Dispense the brain material into centrifuge tubes containing 1 cc. M-199 diluent for each brain harvested. This yields a 10% suckling mouse brain (SMB) solution.
8. Centrifuge the suspension at 1700Xg for 30 minutes at 4 C to remove the cellular debris.
9. The supernatant is then decanted, pooled, and stored at -70 C.

Following the above procedure the pooled supernatant was diluted 1:100 in HBSS, split into several 10 cc. aliquots, stored at -70 C, and used throughout this study as "stock" VEE solution.

Suckling mice were also used to determine virus concentration by performing LD_{50} titrations (74). The titer of the stock VEE suspension employed in this study was 5.0×10^{8} LD_{50}/ 0.2 cc. or 2.5×10^{9} LD_{50}/ 1 cc Following the 1:100 dilution in HBSS, the concentration is 2.5×10^{7} LD_{50}/ 1 cc.

RIBONUCLEIC ACID ANALYSIS MATERIALS AND PROCEDURES

In order to follow the progression of RNA virus replication in tissue culture cells, one may employ several alternative techniques. Of the methods available, those utilized in this research provide for the greatest resolution of RNA species available today. These techniques include: (i) isotope labeling of newly synthesized RNA species, (ii) isolation or extraction of the labeled species, (iii) separation of the isolated species via polyacrylamide gel electrophoresis (PAGE) and (iv) liquid scintillation spectrometer measurement of the separated RNA species.

The methods for labeling and extraction of RNA species were modified from those of Peacock et al. (69). The PAGE and liquid scintillation methods were modified from those of Levine et al. (53).

A. Ribonucleic Acid Analysis Materials and Reagents

Polyacrylamide Gel Electrophoresis Reagents:

1. N, N, N', N'-tetramethylethylenediamine (Eastman Kodak Organic Chemicals, Rochester, New York)
2. Acrylamide (Eastman Kodak Organic Chemicals)
3. N, N'-methylene bisacrylamide (Eastman Kodak Organic Chemicals)
4. Agarose (Seakem) (purchased from Marine Colloids, Inc., Rockland, Maine)
5. Tris-EDTA-Borate Buffer (10X) pH 8.3 (TEB)
6. Ammonium persulfate
7. Trichloroacetic acid, 5.0% in 1X TEB
8. Acetic Acid, 1M
9. Sodium Acetate Buffer, pH 4.7
10. Methylene Blue Staining Solution, 0.2% Methylene Blue in Sodium Acetate Buffer
11. Bromphenol Blue Dye (1% aqueous)
12. Ribonuclease-free Sucrose

RNA Labeling, Extraction, and Scintillation Counting Reagents:

1. Actinomycin D (Nutritional Biochemicals, Cleveland, Ohio)
2. Pancreatic RNase (Nutritional Biochemicals)
3. DNase (Nutritional Biochemicals)
4. Uridine-5-H^3 (ICN Chemical and Radioisotope Division, Irvine, California)
5. Uridine-2-C^{14} (ICN)
6. Triton X-100 (ICN)
7. Tolu-Scint (ICN)
8. Toluene, scintillation grade (ICN)
9. Sodium dodecyl solfate (0.5% in 1X TEB), (SDS)
10. Phenol
11. Hydrogen peroxide, 30%

Note: If source is not listed, the chemical may be commonly found at any chemical supply house.

Equipment Required:

1. Incubator, 45 C
2. Lang-Levy micropipettes
3. Tissue homogenizers
4. Microcentrifuge - Bechman/Spinco 152 Microfuge - and tubes
5. Vibration mixer - Vortex Genie from Scientific Industries
6. Refrigerated centrifuge - International, Inc.
7. Freezer, -20 C
8. Polyacrylamide Gel Electrophoresis Apparatus (Savant, Inc.)
9. Packard Tri-Carb Liquid Scintillation Spectrometer
10. Pasteur pipettes
11. Assorted glassware

B. Preparation of Stock Solutions:

1. Acrylamide - N,N'-Methylenebisacrylamide 19:1, 20%. Acrylamide, 190 g., and N,N'-Methylenebisacrylamide, 10 g., are dissolved together in distilled water over a magnetic stirrer, made up to a volume of one liter, filtered, and stored in a brown bottle. The acrylamide is a neurotoxin and should be handled accordingly. Care must be taken to avoid

skin contact, and mouth pipetting of solutions should be avoided.

2. Tris-EDTA-Borate Buffer, pH 8.3, Peacock's buffer, (TEB). A concentrated stock buffer, ten times the working concentration (hereafter referred to as "10X buffer"), contains:

Tris-(hydroxymethyl)-aminomethane	216.0 g.
Boric Acid.	110.0 g.
Ethylenediaminetetraacetate Disodium Salt (EDTA).	18.6 g.
Distilled Water	2.0 l.

The solution is filtered and stored in a glass bottle.

3. Ammonium Persulfate. Ammonium persulfate, 10% w/v, is dissolved in water, made up to 100 cc. and filtered. It should be prepared fresh every two weeks.

4. Sodium Acetate Buffer, pH 4.7. Combine 134 cc. aqueous 3M sodium acetate and 400 cc. 1M acetic acid and adjust the volume to 2 liters with water.

5. Phenol. The phenol employed in RNA extraction must be redistilled. Place 100 cc. phenol in a distillation flask. Heat the flask in a hood to 181.8 C. Any condensate coming off prior to this temperature is collected and discarded. The first 10 cc. of condensate collected at 181.8 C is discarded; the remainder is collected and saved. This redistilled phenol is mixed 1:1 with sterile distilled water, aliquots are placed in aluminum foil covered 10 cc. serum bottles, and stored at -20 C.

6. Ribonuclease Solution. A solution of 50 mg. RNase in 25 cc.

0.01 M KH_2PO_4 is stored in 0.2 cc. aliquots at -70 C. Thaw a 0.2 cc. aliquot of RNase solution and 0.2 cc. K_2HPO_4, 0.01 M. This is designated a 1X concentration. To prepare a working RNase solution, dilute 0.1 cc. of stock 1X solution in 0.4 cc. K_2HPO_4-KH_2PO_4 buffer, 0.01 M. Do not refreeze leftover enzyme solution.

7. Deoxyribonuclease Solution. A 1X stock solution is prepared by dissolving 10 mg. enzyme in 5 cc. buffer in a small flask. Swirl to dissolve, but do not shake. Stopper and store frozen. The buffer contains 2.5 cc. 0.4 M NaCl, 2.5 cc. 0.01 M K_2HPO_4, 2.5 cc. 0.01 M KH_2PO_4, and 250 microliters 1M $MgCl_2$ in 50 cc. water. To use, dilute the stock 1X solution 1:10.

C. Isotope Labeling of A. albopictus Cell RNA

Labelled cellular RNA was prepared by treating monolayers of A. albopictus with 50 μC/cc. uridine-5-H^3 in MCM for 24 hours. Alternatively, uridine-2-C^{14} (25 μC/cc.) in MCM was employed when double label experiments were performed.

After the appropriate period of time, the RNA was extracted with a modified SDS-phenol method.

D. Isotope Labeling of VEE RNA

To prepare uridine-5-H^3 or uridine-2-C^{14} labeled VEE RNA, monolayers of A. albopictus cells were infected with the virus at a multiplicity of 50:1 for 24 hours. At the end of this period (which

encompasses the virus eclipse phase) the cells were treated with 1 µg/cc. Actinomycin D for one hour to inhibit DNA-dependent RNA polymerase reactions. This media was then replaced with 2 cc. of fresh MCM supplemented with 20% iFBS and containing 50 µC/cc. uridine-5-H^3 or 25 µC/cc. uridine-2-C^{14} for varying periods of time.

The uridine-2-C^{14} employed in all labeling experiments had a specific activity of 50.8 millicuries/millimole (total activity 50 microcuries); the uridine-5-H^3 had a specific activity of 25 millicuries/millimole (total activity 1MC). The tritium half-life is 12.3 years; the carbon half-life is 5.7×10^3 years.

E. Rapid RNA Extraction Method for A. albopictus Cells

1. Decant medium from one TC-30 flask of A. albopictus cells and place cells on ice.
2. Rinse three times with chilled (4 C) phosphate buffered saline (PBS), decant thoroughly and quickly replace the flask on ice.
3. Harvest the cells (via trypsin-pipetting procedure) into 3 cc. of chilled PBS. Place the solution in chilled glass tissue homogenizer tube.
4. Centrifuge 8-10 minutes at 0 C and 1500 rpm. The pellet should contain approximately 3×10^6 cells.
5. Decant supernatant, add 300 µl chilled 0.5% SDS in 1X TEB buffer to the pellet.
6. Homogenize for 10-15 strokes, add 300 µl water-saturated

phenol, mix for 1 minute on Vortex mixer, let stand for 30 seconds.

7. Transfer the solution to plastic Beckman microfuge tubes with a Pasteur pipette. Centrifuge in a Beckman/Spinco 152 Microfuge for 2 minutes.
8. Carefully remove the top aqueous layer and store at -20 C.

   Note: The top layer contains the RNA species; the interface and lower phenol layers contain the denatured protein. Thus, it is necessary to be extremely careful when removing the top layer so as not to disturb the protein fraction, thereby allowing mixing. If one extraction does not successfully remove all protein, it may be necessary to repeat the extraction process 2 or 3 times.

F. Enzymatic Treatment of RNA-containing Aqueous Layers

1. To one volume (be exact - use Lang-Levy micropipettes) of well-mixed aqueous layer, add 1/10 volume of chilled 1.0 M NaCl and mix thoroughly.
2. Add 3 volumes of chilled (4 C) ethanol, mix, and store covered tube at -20 C overnight.
3. Centrifuge the sample in the cold - either in a refrigerated centrifuge (15 minutes at 1500 rpm at 0 C) or in the microfuge for 1 minute in a chilled pan.
4 Carefully remove supernatant, and let the tube drain to remove all the ethanol. A fluffy, white precipitate should

be visible at this point.

5. Redissolve the precipitate in 0.02 M NaCl (chilled at 4 C) by using 1/2 volume of the original aqueous layer, shake gently, and place on ice.
6. Prepare working concentration of enzyme. In this case it may be either DNase or RNase.
7. Place a convenient amount of the redissolved precipitate in a microcentrifuge tube (not less than 20 microliters). Add an equal volume of enzyme and mix well.
8. Incubate at 37 C for 3 minutes in a water bath. Immediately after incubation, place the tube in ice.
9. Add 1 drop of bromphenol blue solution and 1-2 crystals of RNase-free sucrose to the mixture.
10. Electrophorese.

Note: If the aqueous layer does not show a visible precipitate, it may be necessary to add 100 µg of a stock RNA (yeast) to the aqueous layer prior to this procedure. The yeast RNA serves as a carrier to prevent alcohol denaturation of excessively small amounts of RNA in the aqueous layer.

G. Determination of RNA Concentration and Purity in Aqueous Layers

The concentration of RNA found in cell extract samples (aqueous layers) was determined by preparing a standard curve of the optical density versus RNA concentration. Thus, RNA concentration was determined by placing an aliquot of the sample (diluted 1:10) in a

minicuvette and measuring the absorbance at 260 nm. in a 10 cm. light path. The concentration is then read directly off the standard curve graph.

An estimate of the purity of RNA samples was also determined by U.V. absorption. A "clean" preparation should give a 260:230 nm. ratio above 2.3 and a 260:280 nm. ratio above 2.0. If the initial extraction indicated a less than clean preparation, the extraction procedure was repeated.

All absorbance measurements were taken on a Perkin-Elmer Model 124 spectrophotometer.

H. Polyacrylamide Gel Electrophoresis Procedure

1. Preparation of Gels: Composite gels consisting of 2.2% acrylamide and 0.5% agarose are prepared in 10 centimeter glass gel tubes (0.6 mm inside diameter) by combining in a 46 C waterbath the following:

   15 cc. melted 1% (v/v) agarose
   15 µl. N,N,N',N'-tetramethylenediamine
   15 cc. of a solution containing:
      0.72 cc. H_2O
      5.28 cc. acrylamide-N,N'-Methylenebisacrylamide, 19:1
      12.0 cc. Tris-EDTA-Borate buffer (TEB) 10X

   After thoroughly mixing these reagents, 0.3 cc. of 10% (w/v) ammonium persulfate is added as a polymerizing agent. The mixture is then rapidly transferred to the gel tubes with a Pasteur pipette. There should be enough for 14 gel tubes. Allow 30-45 minutes for solidification of the gels.

   Since the solidification of agarose occurs more rapidly

than the polymerization of the acrylamide, the gel forms an uneven surface at both ends. Before use one of the agarose tips is sliced off with a scalpel to provide a flat surface for sample placement. The gels may be stored one week at 4 C in a tightly sealed glass vessel containing a wet piece of cotton.

2. Prerun: A short section of dialysis tubing is soaked in 1X TEB buffer and attached with a rubber band to the bottom of the gel tube (the bottom being the uneven gel surface end) to prevent the gel from slipping out during electrophoresis. Buffer (1X TEB) is placed in the lower buffer chamber, the gels (without sample) are placed in the upper chamber, and the buffer is placed in the upper chamber. The water is turned on to the jacketed buffer chamber to cool the buffer and minimize temperature effects. The temperature stabilizes at 12 C. The power supply is turned on and adjusted to 200 volts. The prerun is completed after 45 minutes. Shut the power off.

3. Run: The RNA sample (10-50 µl.), containing 1-2 crystals of RNase-free sucrose and 1 drop of 1% aqueous bromphenol blue is applied to the surface of the gel (without removing the buffer) with a Lang-Levy micropipette. The dye serves as a marker, migrating slightly faster than 4S RNA. The power is again turned on, adjusted to 200 volts, and the samples are allowed to electrophorese for one hour.

4. Precipitation of RNA: After electrophoresis, the gel tubes are removed from the chamber, the gels extruded from the glass tubes with gentle suction, and placed in 5% trichloroacetic acid (TCA) at 4 C for 45 minutes to precipitate the RNA in the gels. The gels are now ready for analysis by determining isotope content via liquid scintillation spectrometry.

I. Liquid Scintillation Spectrometry

1. Sectioning and preparation of gels for counting. The gels are removed from the 5% TCA and sliced with a razor blade into 2 mm. sections. Each section is placed in a scintillation vial containing 50 µl. of 30% H_2O_2. All vials are placed in a 56 C incubator overnight. This depolymerizes the gels and releases the RNA. The following day 10 cc. of scintillation fluors (625 cc. toluene, 332 cc. Triton X-100, 40 cc. Tolu-Scint, 100 cc. H_2O) is added to each vial. The vials are then placed in a liquid scintillation spectrometer and counted for radioactivity.

2. For maximum counting efficiency of H^3 labelled RNA species, the window settings are adjusted to a ratio of 50/1000 (A/B) the optimum gain 52%. Counting efficiency will usually be less than 50%.

For maximum counting efficiency of C^{14} labelled RNA species, the window settings are adjusted to a ratio of 20/1000 with a gain of 5.95%. Efficiency may be as high

as 80%.

3. The raw scintillation data is then analyzed by plotting counts per minute (CPM) per fraction versus the fraction number.

VOLUME DISTRIBUTION PROFILE ANALYSIS
MATERIALS AND PROCEDURES

To determine the effect of VEE infection on Aal cell culture volume distribution profiles, the experimental design portrayed in Figure 3 was adhered to throughout.

A single flask of Aal cells was subcultured 1:9 and allowed to incubate for six days. On day six, one ml. of HBSS was added to 6 flasks and one ml. HBSS with VEE (stock) was added to the remaining 3 flasks. All 9 were allowed to incubate at 37 C for 30 minutes. Following incubation the HBSS and HBSS with VEE virus were poured off, the cells rinsed three times with HBSS and 2 ml. fresh MCM with 20% iFBS added. Three of the uninfected flasks and the 3 infected flasks were then placed into a 27 C incubator for 2 days. The remaining 3 uninfected flasks were immediately harvested into 3 ml. ISOTON* per flask. One ml was removed for hemacytometer counts, the remaining 8 ml. were diluted in 72 ml. ISOTON (1:10) and counted in a Coulter Counter Model F*. The Coulter Counter determines the number of cells in an electrolytic solution by passing them through a tiny aperture. As the cell passes through the aperture it displaces an amount of solution equivalent to its volume. This displacement results in a change in conductivity which is translated into electrical pulses and displayed on an oscilliscope screen. The number of pulses is equivalent to the number of cells in the volume

*ISOTON and COULTER COUNTER are products of Coulter Electronics, Inc., Hialeah, Florida.

sampled; the height of the pulses is proportional to the cell volume. Pulses below any selected height on the screen can be blocked out by adjustment of a threshold dial. Successive counts at increasing threshold settings (termed "threshold counts") provide a cumulative frequency curve. A frequency distribution curve can be obtained from the differences between successive threshold counts (termed "channel counts"). This curve is termed the "volume profile" curve (24).

The raw Coulter Counter data is stored on magnetic computer tape and analyzed by several BASIC language programs on a Hewlett Packard Model 9830A computer* (Fig. 4).

Six different programs were employed in this study and are listed in the Appendix, Tables I through VI.

The first program entitled "Enter of List Program", takes three counts per threshold (for up to 100 thresholds) and stores the data on a cassette tape file. The program may also be used to list or print out the data found in one or more files. See Appendix, Table I for a listing of this program.

The second program entitled "Coulter Counter Program", is the mainstay of the series. This piece of software calculates basic statistics of raw Coulter Counter data: the mean of the three counts per threshold, the standard deviation, the per-cent standard deviation, the number of cells in each channel (channel counts), and the difference between control and infected channel counts. This program

---

*This computer is a product of Hewlett-Packard, 1501 Page Mill Rd., Palo Alto, California 94304.

also plots (i) a graph of channel counts versus channel and (ii) a graph of channel count differences versus channel. The channel count versus channel graph is referred to as the "volume distribution profile". See a printout in the Appendix, Table II.

The third program, entitled "Prediction Program", is based on the "Coulter Counter Program" but has been modified to perform a different type of analysis. It is used to "predict" the day 8 control volume profile from actual day 6 control volume profile data. The prediction is determined by cell generation time, the number of hours post-infection, and several other factors. Any program of this type is subject to error due to the assumptions made; however, the "predicted" control day 8 volume distribution profiles proved useful in interpretation of the complex experimental volume distribution profiles. See the program printout in the Appendix, Table III.

The fourth program, entitled "Theoretical Coulter Counter Aperture and Attenuation Calculation Program", is a relatively short program but provides a volume of data found to be very useful in Coulter Counter applications This program calculates the aperture and attenuation for a given volume and threshold range - based on the equation B = V*I/K*T where: B is the attenuation, V is the volume, I is the aperture current, K is a constant equal to 0.00053949, and T is the channel number i.e. threshold settings. The output of this program allows one to find the aperture, attenuation, and threshold values providing the greatest resolution for the volume range of the cells in which you are interested. See the program printout

in the Appendix, Table IV.

The fifth program, entitled "Coulter Counter Averaging Program", takes up to twenty separate Coulter Counter experiments and calculates the mean and standard deviation for each channel for control day 6, control day 8, and infected day 8 data. The computer then plots a graph of this data which is the "mean volume distribution profile" for the number of experiments included. See the printout in the Appendix, Table V.

Finally, the sixth program, entitled "Coulter Counter Grouping Program", in effect provides for decreasing resolution by "grouping" data. The degree of resolution is, of course, dependent on the size of the group or the number of channels lumped together. The function of this program is to provide a less complex volume distribution profile. It also performs various calculations on the grouped data and plots a graph of the percentage of the total population versus the channel groups. In addition, this program can take data from up to twenty experiments and calculate the means and standard deviation of the "grouped" data. It then plots a graph of the mean and standard deviation of control day 6, control day 8, and infected day 8 data. See the printout in the Appendix, Table VI.

The respective outputs of the above programs will be displayed and discussed in the results.

RESULTS AND DISCUSSION

Several preliminary experiments were required prior to virus-specific RNA analysis of VEE infected Aal cells. A standard RNA curve (Fig. 5) was prepared to allow determination of RNA concentrations. Following extraction, an aliquot of the cell or virus-specific RNA was measured for U.V. absorbance; the absorbance then being correlated with RNA concentrations via the standard curve. For example, an absorbance of 0.5 units at 260 nm corresponds to an RNA concentration of approximately 300 µg/ml.

An estimate of the sample purity can be determined by a "wavelength scan" of the sample. Figure 6 is a typical RNA sample; the peak being at the expected 260 nm wavelength. Protein contamination of this sample can be seen by the relatively high absorbance at 280 nm.

The liquid scintillation assay of ^{3}H-uridine labelled RNA required a determination of optimum machine parameters. Using a window width of 50/1000, optimum per-cent gain was determined by increasing the per-cent gain while counting a tritium standard. Figure 7 illustrates the per-cent gain versus CPM curve; the optimum being approximately 50%.

A determination of the degree of quenching was made by adding several concentrations of various agents employed in the RNA experiment (H_2O_2, TCA, polyacrylamide, etc.) to scintillation vials containing a known amount of isotope. Several counts were then taken

of the samples at differing window widths (50/1000 and 50/200) to provide channels ratio data for the tritium standard, "unquenched", and quenched samples. It was determined that none of the reagents employed in these experiments contributed, in any great extent, to quenching error. Thus, quench correction was not employed in any subsequent experiments.

An example of the raw data obtained from the liquid scintillation spectrometer is illustrated in Table 1. Digit (a) is the sample number, (b) is the time (in 1/100 minutes), (c) is the CPM in the "red" channel, and (d) is the CPM in the "green" channel. The "red" and "green" simply distinguish two separate channels that may be set to count isotopes requiring different gain and window values.

Machine counting efficiency is determined by counting a tritium standard and performing a series of simple calculations (Fig. 8). The machine counting efficiency for tritium is usually under 30%.

In order to determine the mode of virus-specific RNA replication in a noncytocidal virus infection, it was important to characterize the RNA species found in control, uninfected cells. Thus, Aal cultures were treated with ^{3}H-uridine supplemented MCM, the cellular RNA extracted, and the individual species separated on polyacrylamide gels; Figure 9 illustrates the results. Three cell-specific RNA species, consistent with the findings of Stollar et al. (93) are found: 28S and 18S ribosomal species, and 4S transfer RNA species. These types of RNA are readily isolated due to their abundance. Messenger RNA, however, requires somewhat different techniques

because of its transient nature and minute quantity; hence, the absence of messenger RNA in these analyses.

Having established the species of RNA present in uninfected Aal cells, it was convenient to use these species as "markers" in subsequent experiments. A standard curve depicted in Fig. 10 was prepared by electrophoresing RNA molecules of known Svedberg (S) values. The distance migrated versus "S" value provides a linear curve. Unknown RNA "S" values may then be approximated by the distance of their migration in the acrylamide gels. This type of approximation was used throughout the RNA analysis, supplemented with coelectrophoresis of known molecular weight, ^{14}C labeled cell RNA species.

In order to preclude the possibility of the cellular RNA "covering up" the existence of similar molecular weight virus-specific RNA species, it is necessary to inhibit cell-specific RNA replication. This was done by the addition of the drug Actinomycin D to the culture media. In minute quantities, Actinomycin D inhibits 90% of DNA-dependent-RNA-polymerase reactions in most cell cultures (76). The effect of the drug on the Aal cells employed in this study is depicted in Fig. 11. In this case, RNA was extracted from Actinomycin D treated ^{3}H labeled cultures and coelectrophoresed with control, untreated, ^{14}C labeled cell RNA. The drug very effectively inhibits cell-specific RNA replication.

Having established the effectiveness of Actinomycin D, it then became possible to determine the types of virus-specific RNA species found in VEE infected Aal cells (the type of experiment designed

for this purpose is portrayed in a flow diagram in Fig. 12).

The Aal cells are subcultured 1:6 or whatever split is necessary for the particular experiment. These are allowed to incubate and reach confluency by the sixth day after subculture. The cells are then infected with VEE or remain uninfected controls, treated with Actinomycin D or remain untreated controls, and are labeled with either ^{3}H or ^{14}C. Following incubation for various post-infection times, the virus-specific and/or cell-specific RNA is extracted from the cells and electrophoresed on polyacrylamide gels.

Although post-infection times of 6, 18, 24, and 48 hours were employed, only the 6 and 48 hour data are presented. It appears that all virus-specific RNA species are present in the 6 hour sample and simply increase in amount with increasing post-infection time.

Figure 13 is the 6 hour post-infection curve. By employing ^{14}C labeled cell RNA as a marker, we find that three virus-specific RNA species are present. A small but distinct peak slightly precedes 18S cellular RNA and could correspond to the RF. In addition, there is a large peak immediately following cellular 28S marker RNA; this may be the polydisperse RI RNA species. Finally, after 90 minutes of electrophoresis at 200 volts, one finds a slight peak near the top of the gel (at fraction number 5) which may correspond to the 42S progeny molecules.

Similar results are found at 48 hours post-infection (Fig. 14); however, in this case one simply finds a greater quantity of labeled material of the same species found in the 6 hour post-infection samples.

It was then important to determine whether or not the virus-specific species correspond to the RF, RI, and progeny molecules found in VEE infected vertebrate cells exhibiting a cytocidal response. One means of doing this is by treating the isolated viral RNA with pancreatic ribonuclease (RNase). This enzyme specifically degrades single-strand RNA and leaves double-strand molecules intact. Figure 15 illustrates complete degradation of single-strand cell RNA by Rnase and Fig. 16 illustrates the results of RNase treatment of virus specific RNA. Coelectrophoresis of RNase treated and untreated RNA samples shows degradation of the "26S" and "42S" species but leaves the "20S" peak intact. If one can assume, then, that the "20S" species is double-stranded, it follows that the "42S" and "26S" species are single-stranded. This leaves an interesting question. If the location of the peak near the marker 28S cell RNA approximates the position of 26S RI RNA, it would follow that RNase treatment of this molecular species would degrade the single-strand portion of that molecule. This action could have two effects. First, if the double-strand portion of the molecule were analogous to the double-strand RF with respect to size, one would expect an increase in the "20S" peak height and elimination of the "26S" peak. On the other hand, if the double-strand portion of the RI molecule were not analogous to the RF species, one would expect to find a new peak characteristic of the molecular weight of the double-strand fragment. Although no increase in "20S" peak height is apparent, neither is there formation of a "new" species. Another possibility

exists; that is, the purported "26S" molecule may be single-stranded.

The results presented here are inconclusive with respect to the presence or absence of "26S" RI RNA; however, it is clear that "42S" and "20S" species are detected at six hours post-infection. The action of RNase does not degrade the "20S" RNA suggesting this species is double-stranded. This is consistent with the findings of Stollar et al. (93).

In view of this evidence it is tempting to conclude that the mechanism of VEE replication in Aal cells, exhibiting a noncytocidal response, is analogous to the mechanism of arbovirus replication in vertebrate cells exhibiting a cytocidal response. However, further study is necessary to substantiate these findings.

It is important to note that progeny molecules are detected six hours post-infection indicating replication of the virus is occurring; yet this does not precipitate any pathological changes.

A semi-quantitative view of these molecular events may be obtained by making a few simple calculations For example, each RNA sample was measured for U.V. absorbance to determine the RNA concentration (see standard curve in Fig. 5). Given that the absorbance of the virus-specific RNA sample electrophoresed and depicted in Fig. 22 was 0.78, it follows that the RNA concentration in that sample approximates 1.9 ug/ul. A 50 µl. sample was applied to the gel; this corresponds to 95 µg. RNA. Assuming that no appreciable loss of sample into the buffer occurred, we can then calculate the relative

per cent of the total sample found in each peak and relate that to the concentration. Thus, in Fig. 14, the "42S" peak constitutes 27.4% or 26.0 μg., the "26S" peak constitutes 45.1% or 42.8 μg., and the "20S" peak constitutes 9.8% of the total, hence 9.3 μg.

This is a relatively elementary method and may be refined to provide more detailed information relative to RNA species quantity. It does, however, provide an overview of the types of virus-specific RNA involved in VEE replication in Aal cells.

In addition, the RNA analysis has indicated that progeny RNA molecules are present in a noncytocidal infection, i.e. the virus is replicating. Is it now possible to detect the inapparent virus-induced morphological effects of VEE infection in Aal cells?

The answer to this question was dependent on developing a method of detection that not only was accurate and reproducible but rapid as well. In light of the fact that the method was to be amenable to automation, it was determined that the detection of noncytocidal virus infection would be best suited to physical measurements as opposed to chemical measurements. It appeared virus-induced cell volume changes would be the most suitable parameter; this characteristic being most accurately determined with the Coulter Counter spectrometer.

Several preliminary determinations were necessary before commencing with the actual infected cell volume measurements. First, the volume range encountered in uninfected Aal cells needed to be determined. This was accomplished by optical micrometer measurements

of Aal cell diameters in suspension. The optical micrometer, a product of American Optical Co., Buffalo, N. Y., was calibrated against a Bausch and Lomb graduated slide (Table 2). Following this, diameter measurements of 86 suspended cells were obtained. The mean cell size was found to be 15.67 microns in diameter; the range being 6 microns to 36 microns in diameter. This corresponds to a volume range of 171 cubic microns to 25,440 cubic microns (Fig. 17).

Since this extensive volume range was not logistically possible to monitor and since 10% or less of the total population actively produces virus, a second preliminary study was done to determine that portion of the population most affected by VEE infection. In this case optical micrometer measurements were taken of uninfected and infected cells in suspension. A graph of the data is presented in Fig. 18. Here, we see a considerable percentage change occurring in the 8 to 10 micron diameter range which corresponds to a volume range of 270 to 529 cubic microns. Thus, a look at the 270 to 529 cubic micron volume range considerably reduced the logistical problems and allowed a look at only those cells most affected by the virus.

Prior to counting and sizing the cells, it is necessary to dilute them 1:10 in ISOTON. Thus, the effect of ISOTON on cell volume had to be determined. Three different cells were picked out on a microscope field and their diameter measured five times with the optical micrometer; then, ISOTON was introduced onto the monolayers and the diameters of the same cells again measured five times. The

results of this experiment are depicted in Table 3. The mean cell diameter does not change appreciably with the addition of ISOTON, i.e. the physiological ISOTON apparently has no effect on the cell diameter, hence cell volume as determined optically.

A growth curve experiment was performed in order to determine the optimum post-subculture time at which to measure cell volume. From this curve, illustrated in Fig. 19, we find that confluency is reached in six days and the culture continues in log phase for several days thereafter. From the literature it was determined that VEE would replicate to optimum levels at 2 days post-infection (13). Thus, confluent monolayers 6 days old were infected with VEE until day 8 when control and infected cells were harvested and cell volumes determined.

The next preliminary experiments were designed to determine the reproducibility of Coulter Counter data, i.e. if several flasks of cell cultures of the same age and transfer number were harvested, would one get the same volume profiles each time? Figure 20 illustrates the results of such an experiment. In this case three different flasks of Aal cells were harvested and their cell volumes measured. The data is "grouped" and "normalized" (to be explained later) and plotted as percentage of the total population versus the channel group. The variation from trial to trial amounted to only 2.87%.

Finally, it was necessary to determine the optimum aperture, attenuation, and threshold Coulter Counter settings to obtain the best resolution for the cell volume range of interest. To accomplish

this task a computer program was written; a printout of which can be found in the Appendix, Table IV. This program calculates the attenuation for a given series of apertures, thresholds, and volumes, and prints out the results as seen in Table 4. The left column of figures is the volume in cubic microns; in this case, in increments of 100 cubic microns. The second column of figures refer to threshold dial settings which may range from 1 to 100; and the last column of figures refers to calculated attenuation values. Thus we can say, from the underlined row of data, that a 600 cubic micron cell will be found in threshold 26 at an attenuation setting of 0.500.

Using this type of data, it was determined that the best Coulter Counter settings for the volume range 270 to 529 cubic microns would be an aperture of 512, attenuation of 0.125, and that these size cells would be found between thresholds 47 to 92. These machine settings provide for the best resolution in this volume range.

This data may also be collated in several forms. Table 5 provides the volume ranges that can be measured at all aperture and attenuation combinations. At aperture 512 and attenuation 0.125 the volume range is from 17 to 580 cubic microns. Table 6 provides the resolution obtained by all combinations of aperture and attenuation; at aperture 512 and attenuation of 0.125 we have a resolution of 5.777 cubic microns per channel.

The resolution value is calculated from Table 4 data; for example, since a 600 cubic micron cell is found at threshold 26 at an attenuation of 0.5 and an 800 cubic micron cell is found at threshold 35 at attenuation 0.5, it follows that the increment per

channel (resolution) is 22.2 cubic microns/channel.

To summarize, these preliminary experiments demonstrated the feasibility of using the Coulter Counter for this study and established the parameters by which all subsequent experiments were performed. That is, aperture 512, attenuation 0.125, and thresholds 47 to 92 were used throughout the remainder of the investigation to measure a cell volume range of 270 to 592 cubic microns at a resolution of 5.777 cubic microns per channel.

The effect of VEE infection on Aal cell volume profiles was determined by adhering to the protocol outlined in the materials and methods and depicted in Fig. 3. Cell cultures 6 days old were infected with VEE and harvested after 2 days incubation on day 8. Thus, for each experiment there are volume profiles on day 6 control cells (hereafter referred to as C6), day 8 control cells (C8), and day 8 infected cells (I8). These cells are diluted 1:10 in ISOTON and counted in the Coulter Counter Model F, three counts per threshold. The raw data is input into the "Enter or List" BASIC language program listed in the Appendix, Table I, for storage on magnetic tape. Once all data for each experiment has been collected, all data files may then be employed in the "Coulter Counter Program" listed in the Appendix, Table II. The results of this program are depicted in Table 7. Here we see the three raw counts (b) listed for each threshold (a), the mean of the three counts (c), the standard deviation (d), the percent standard deviation (e), and the channel counts (f). It may be wise at this point to reiterate and to clarify the difference

between "raw threshold counts" and "channel counts". The raw threshold counts are obtained directly from the Coulter Counter and represent all cells found above that particular arbitrary threshold number, i.e. all cells above a given corresponding volume. This volume is dependent entirely on the machine's aperture and attenuation settings as previously discussed. The "channel counts" are obtained by subtracting the mean threshold count from the mean threshold count of the following threshold. This value corresponds to the number of cells of the specific volume found between those particular thresholds. Hence, channel counts are used in the volume profile curves.

Figure 21 is an example of a volume profile obtained from uninfected Aal cells on the sixth day following subculture. Three values of interest are printed on the X axis. The column labeled (a) is the lower limit of the diameter of the cells found in channel (b), column (c) is the lower limit of the volume of the cells found in channel (b). The next higher channel diameter and volume values are then the upper limits of those cells found in channel (b). For example, in channel 47 there are 214 cells between diameters 8.03 to 8.08 microns or between volumes 270.7 to 276.5 cubic microns.

When comparing C6 volume profiles to C8 and I8 or C8 to I8 volume profiles, it becomes an exceedingly difficult task to interpret such complex graphs. In order to better understand the changes occurring in these volume profiles, "trend lines" were employed. That is, the peaks of the volume profiles were connected arbitrarily to smooth the curve and to better portray the trends occurring. The

solid line in Fig. 21 is an example of this process.

An example of an experiment analyzed with this trend-line method can be seen in Figs. 22, 23, and 24. The C6 versus C8 trend curves exhibited in Fig. 22 simply depicts normal cell growth over the 48 hour period. However, since the C8 volume profile peaks do not correspond to the C6 peaks, it became of interest to determine which C6 peaks and C8 peaks correlate. To do this a "Prediction Program" was written to take C6 data and "predict" C8 volume profiles. The basis for this program lies in cell generation time (22 hours), post-infection time (48 hours), volume increase per unit time and resultant location of the predicted-volume-cell in the volume profile. Several assumptions are made and several factors are not dealt with which results in the errors inherent in any prediction situation. For example, cells are assumed to double in volume and divide into equal size daughter cells and cell deaths are not accounted for. The program is, however, useful in interpreting volume profiles. For example, in Fig. 23 we have the actual C8 profile compared to the predicted C8 profile. Although these trend curves do not coincide exactly, we can, with some assurance, correlate the peaks as shown. That is, the actual C8 peak number I corresponds with the predicted C8 peak number I and so forth. Since the predicted C8 profile was derived from the actual C6 data in Fig. 22, these peaks can also be correlated as is shown; peak I of the C6 corresponding to peak I of C8 and so forth. Peak number IV in the C6 profile has moved off scale and is not present in the C8 profile. Now then, what does this mean?

By looking at the normal growth of the Aal cells over a period of two days, i.e. from C6 to C8; and by being able to correlate the resultant peaks, one can make several conclusions regarding the effect of VEE infection on normal cell growth (Fig. 24). There are essentially two changes: (i) a marked suppression of growth indicated by a reduction in peak height, particularly in peak III of C8 and I8, and (ii) a shift occurring in peak III of the I8 volume profile with respect to peak III of the C8 volume profile. This indicates a volume, more specifically, a virus-induced volume change.

Nine repetitions of the initial experiment revealed some difficulty with this type of trend-line analysis. The trend curves were not consistent and at times became very difficult to interpret. Essentially two factors were responsible. First, data obtained from successive experiments showed considerable variation in peak height due to experimental error. That is, the same number of cells could not be harvested from monolayer cultures each time an experiment was performed. Second, a resolution of 5.777 cubic microns per channel would show cell diameter changes as slight as 0.075 microns in an average cell of 400 cubic microns in volume. These difficulties were overcome by "normalizing" and "grouping", respectively (see the programs in the Appendix, Tables V and VI).

The normalizing of data simply consisted of calculating the percentage of the total population found in each channel rather than dealing with actual numbers of cells per channel. All subsequent experiments were analyzed with normalized data. The grouping of data

simply consisted of calculating the actual number of cells found in ten-channel groups. This grouping, in effect, decreased the volume resolution ten-fold to 57.77 cubic microns per channel group.

The grouped data and associated calculations for all nine repetitions are depicted in Figs. 25-33. The 45 channels monitored have been broken into four 10-channel groups; the last 5 channels being discarded since group comparisons would be impossible with a five-membered group. The first three rows of data are the C6, C8, and I8 data, respectively. The top number in each of these rows refers to the channel count in that particular channel group; the bottom number in each of these rows refers to the percentage of the total counts found in that particular channel group. For example, in Fig. 25, in C6 there were 1074 cells found in channels 47 to 56 which constitutes 25% of the total. The last three rows of data are comparative; that is, the top number in each row refers to actual channel count differences, the bottom number refers to the percentage differences. For example, in the fourth row of data a comparison is being made between C6 and C8 data, hence C6:C8. In the channel 47 to 56 group, C8 has 160 more cells than C6, hence a positive value of 160. The percentage of cells in this group decreases 8.8% with respect to C6, hence a negative value of -8.8%. The reference data is always on the left of the colon in this printout, i.e C8:I8 means a comparison of I8 data with respect to C8 data. The percentage values in the totals column in the comparative data rows are calculated with respect to the channel counts rather than the percentages.

These "grouped data" volume profiles may be looked at in two ways. One might compare the profile changes occurring in normal growth (C6:C8) or one might simply compare the C8 to the I8 data.

Close scrutiny of all nine experiments reveals several things. The greatest single difference between C8 and I8 cells in any channel group is 16.5%; the mean difference is 5.15%. The greatest total difference between C8 and I8 volume profiles is 23.1%; the mean difference is 11.53%. These observations reveal that considerable virus-induced volume changes are occurring and are being detected.

Further analysis of this data was attempted by calculating the means of the grouped data for all nine experiment repetitions. Figure 34 is the result of this attempt. In this case the top numbers in each of the first three rows refers to the mean percentage of the total cell population found in that particular channel group or volume range; the bottom numbers are the standard deviations. For example, on the average 27.0 ± 7.0% of the total population in the control day 6 cultures were found in channels 47 to 56. In the comparative data rows the same situation is encountered. For example, in the C6:C8 comparison we find an average of a 6.2% decrease in the C8 data with respect to the C6 data, hence the negative sign; the standard deviation being 9.7%. The totals column deals entirely with channel counts, i.e. the mean total C6 channel count is 4125 ± 1185.

The graph in Fig. 34 is a plot of plus and minus one standard deviation from the mean data. The "envelope" bounded by the solid lines is that area in which one might find the C8 volume profiles;

the envelope bounded by the dotted lines is that area in which one might find the I8 volume profiles. That area cross-hatched is the area in which the I8 envelope lies outside the C8 envelope. This again tells us there is a detectable virus-induced volume change and further limits this change to the 67 to 76 and 77 to 86 channel groups. The mean grouped volume profiles for this data are depicted in Fig. 35.

By calculating and plotting the mean channel counts of the grouped data, one gets a slightly different view of the total picture. Table 8 contains the mean and standard deviations of grouped channel count data; Fig. 36 is the graph of this data. The location and general shape of the C6 volume profile is seen, as is the normal growth of C6 to C8 cell populations; and one sees how the I8 profile differs from the normal C8. Table 9 contains a summary of mean data and volume and diameter ranges for each channel group.

Now that the grouped, normalized, mean data proved somewhat fruitful in more closely delineating the cell volume range most affected by virus infection, it was important to look at normalized, mean data on a channel-by-channel basis. Table 10 contains this information; the digits labeled (a) being the mean percentage, those labeled (b) referring to the standard deviation, i.e. in the C6 cell population one finds $2.13 \pm 2.10\%$ of the population in channel 47. A graph of the mean percentage values versus channel is found in Fig. 37; the C8 data represented by a solid line, and the I8 data represented by a dashed line. This is the mean of all nine volume profiles.

Again, one can see differences between control and infected cultures; many of which would probably be found even in two identical uninfected cultures. The area of tremendous interest, however, is that area between channels 73 to 87. Here there is a considerable fluctuation in the control cell volume profile, but not as much fluctuation in the infected cell volume profile. In addition, there is a considerably higher number of C8 cells in this volume range than I8 cells. This observation could mean one of two things. The virus may be suppressing cell growth and division resulting in a fewer number of cells in this volume range or the virus may be either increasing or decreasing the volume of the cells found in this volume range which would move these cells off the scale into other channels. Whatever the case may be there are sufficient experimental evidences to believe that a closer scrutiny of the 73 to 87 channel, i.e. 155 to 241 cubic micron range is now necessary. It is in this region that one will most likely consistently find virus-induced cell volume changes.

A graph depicting the standard deviation of mean percentage values versus channel is found in Fig. 38. This is simply a plot of plus and minus one standard deviation of both C8 and I8 mean, normalized data. In other words, that area labeled (a) between the upper and lower solid black lines is the "envelope" in which one might find C8 volume profiles The corresponding shaded area labeled (b) is the "envelope" within which one might find the I8 volume profiles. Hence, the shaded areas are those regions in which the I8 "envelope" lies

outside the C8 "envelope". Since these are based on the normalized, grouped data for nine experiments, one can safely assume that these differences are significant.

Here too the region between channels 73 to 87 depicts rather substantial differences between C8 and I8 cells. Indeed, 7 out of 9 experiments show a consistent change in the 77 to 86 channel group.

To summarize, a series of thirty volume displacement profile experiments, nine of which are included in these results, have shown the complexity of monitoring heterogeneous cell volume populations. Virus-induced cell volume changes are detected. The types of data analysis employed in this investigation resolved the cell volume range most affected by VEE, first to the 67 to 86 channel group and subsequently to the 83 to 87 channel group. Seven out of nine experiments reveal a virus-induced volume change in the 77 to 86 channel group. This corresponds to cells having diameters from 6.67 to 7.73 microns and volumes of 155.5 to 241.9 cubic microns. Further study of this volume range may conceivably limit the number of channels to monitor and improve the reliability of the method.

The use of computer analysis of volume profile data proved invaluable with respect to experimental design and time savings. In addition, this type of analysis could easily be entirely automated since the baseline data has been herein described.

Fig. 3. Volume Distribution Profile Analysis Experimental Design.

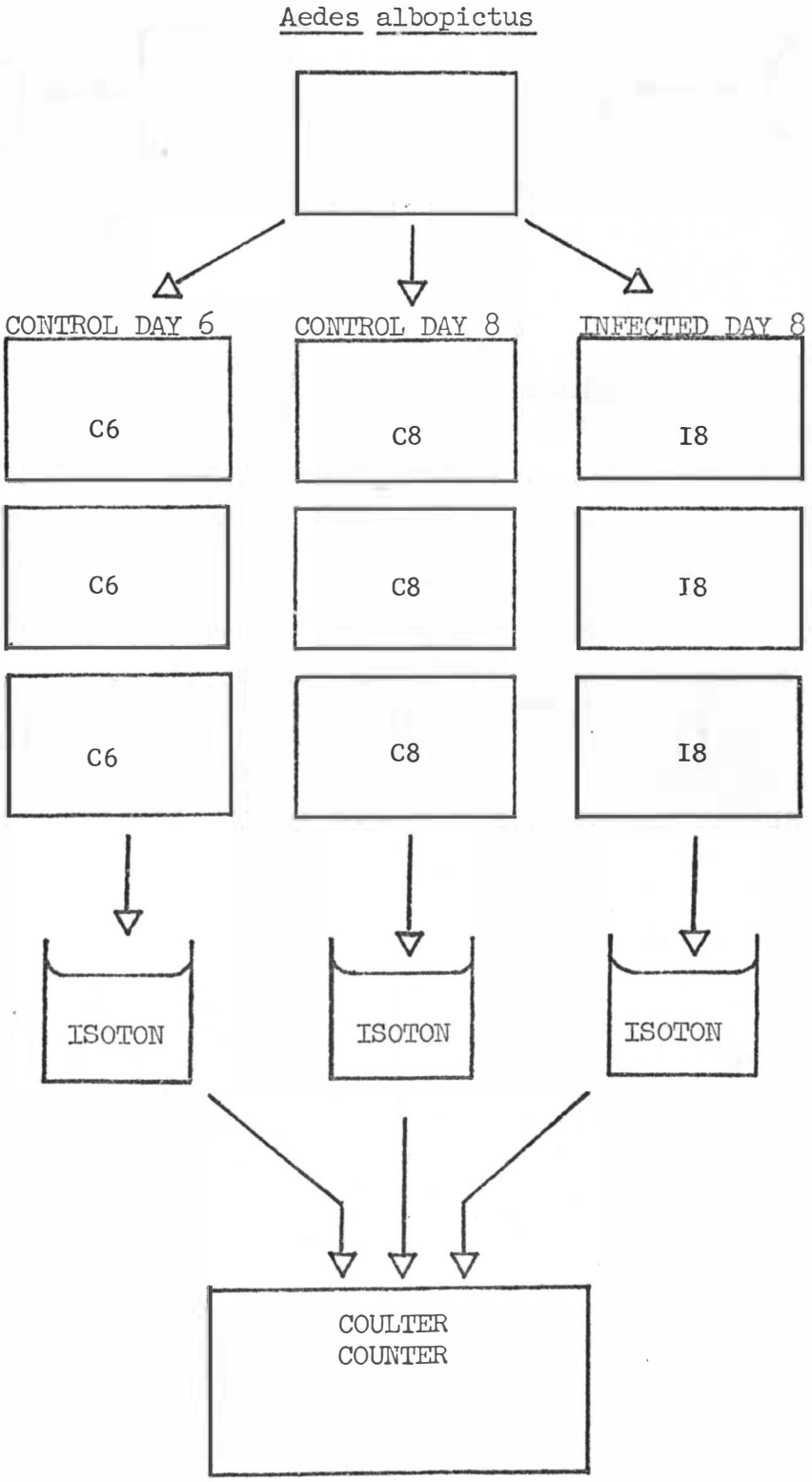

Fig. 4. Computer Assisted Analysis of Coulter Counter Data.

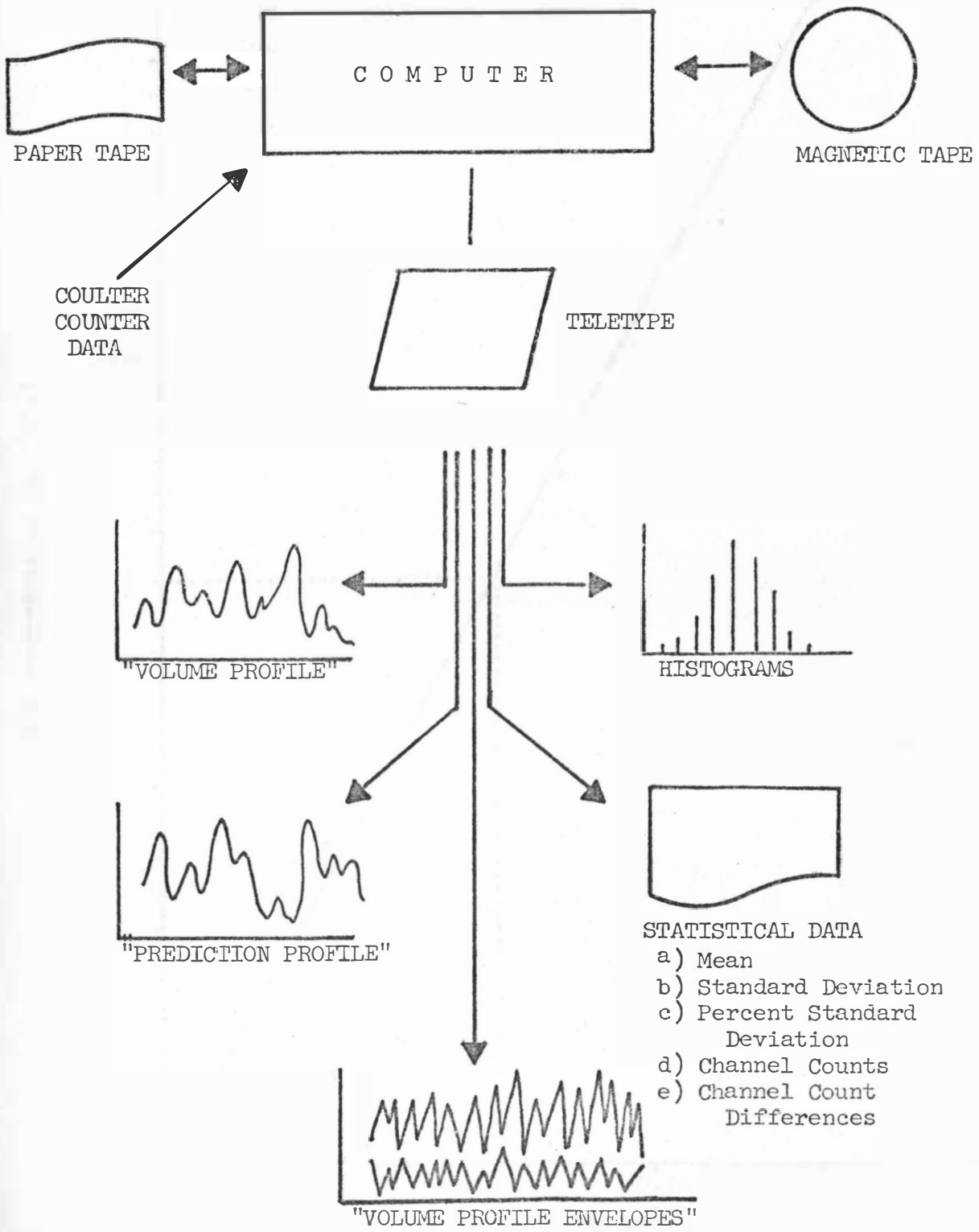

Fig. 5. RNA Concentration versus UV Absorbance Standard Curve.

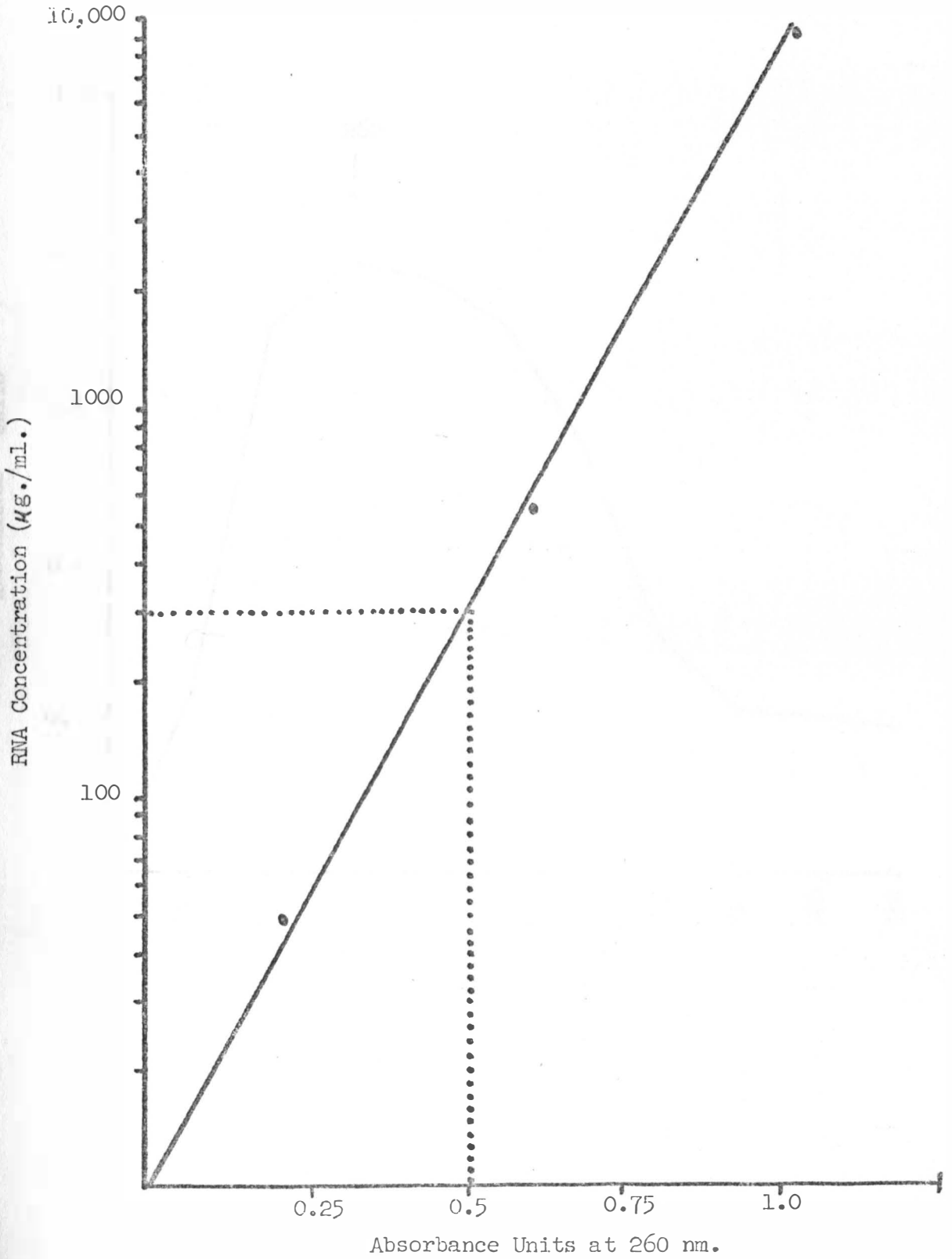

Fig. 6. Wavelength Scan of RNA Sample.

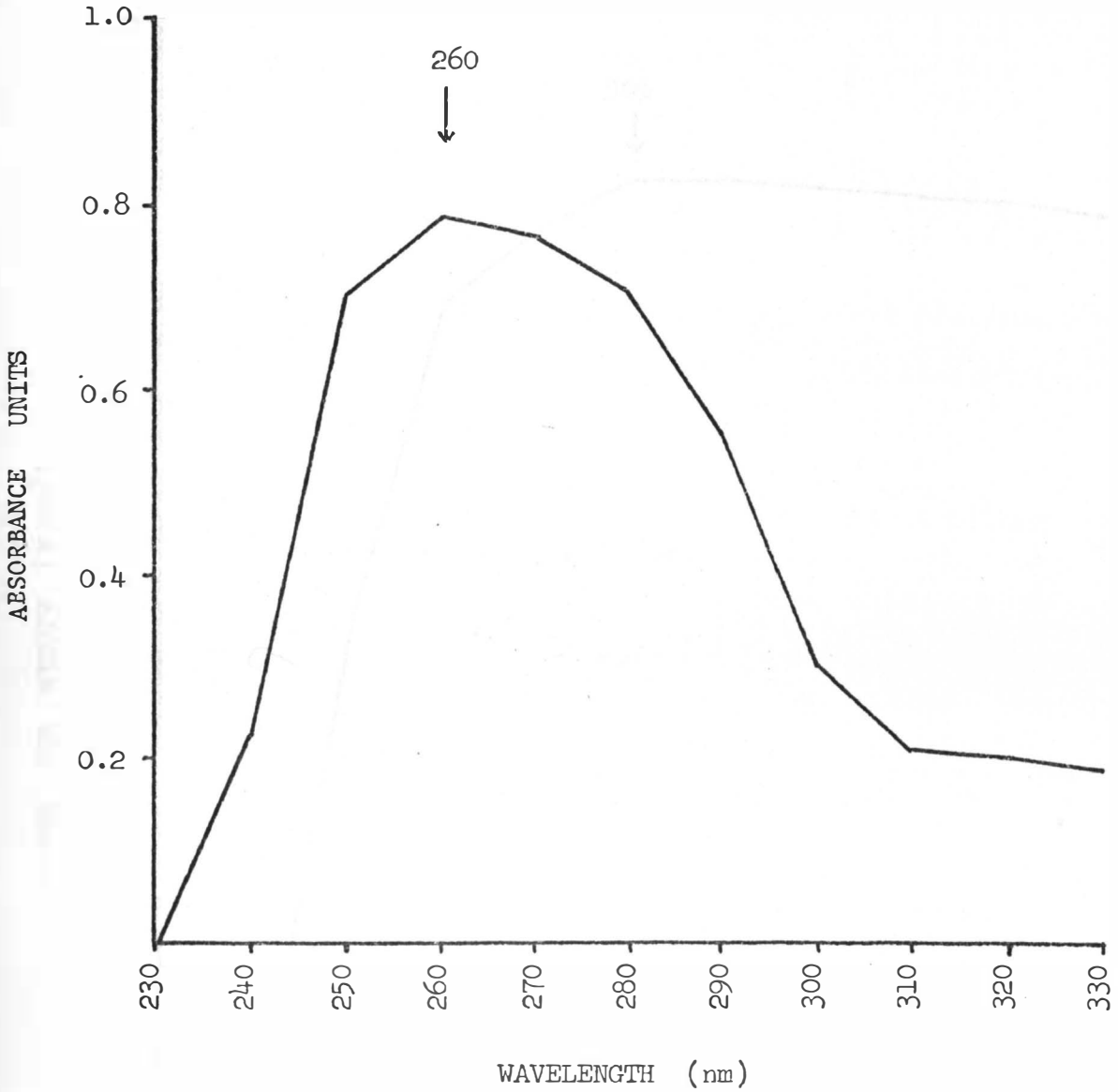

Fig. 7. Optimum Gain Determination.

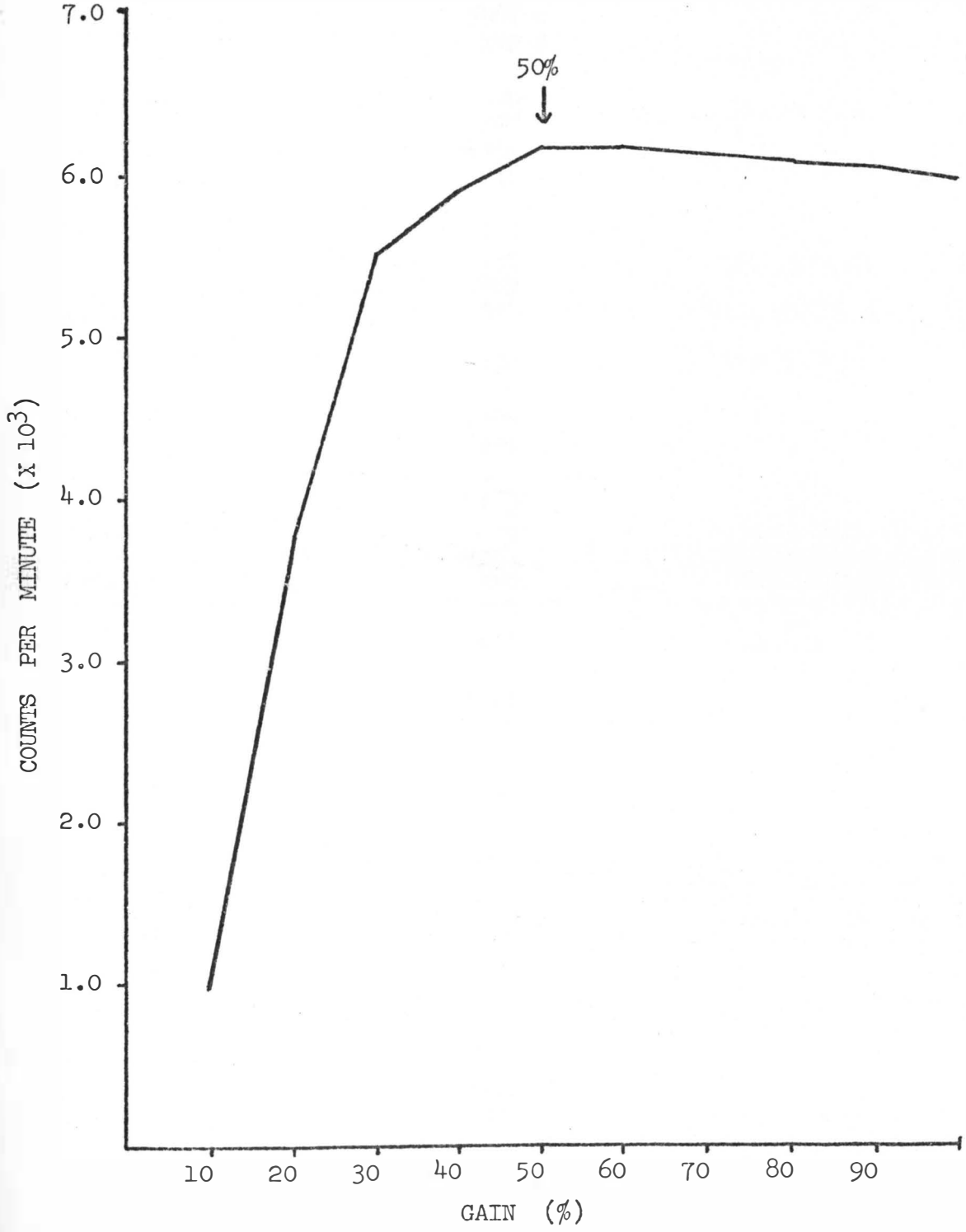

Table 1. Example of Liquid Scintillation Data.

179	a
100	b
3967	c
192	d
180	
100	
4836	
211	
181	
100	
3469	
231	
182	
100	
5503	
230	
183	
100	
4943	
270	
184	
100	
1869	
232	
185	
100	
1021	
201	
186	
100	
874	
182	
187	
100	
721	
148	

Fig. 8. Percent Counting Efficiency Calculations.

^{3}H Standard Data:

1. 153,200 dpm on August 14, 1972.
2. 12.3 year half-life (4489.5 days).
3. 45,200 cpm on August 10, 1974.

Percent Counting Efficiency Calculations:

1. August 14, 1972 to August 10, 1974 = 726 days.
2. 726 days/4489.5 days = 0.1617 half-life elapsed.
3. The first half-life = 76,600 dpm therefore, 76,600 X 0.1617 = 12386 dpm lost. 153,200 original dpm - 12386 lost = 140813 dpm remaining.
4. 45,200/140813 X 100 = 32.1% Counting Efficiency.

Fig. 9. Uninfected A. albopictus RNA Species.

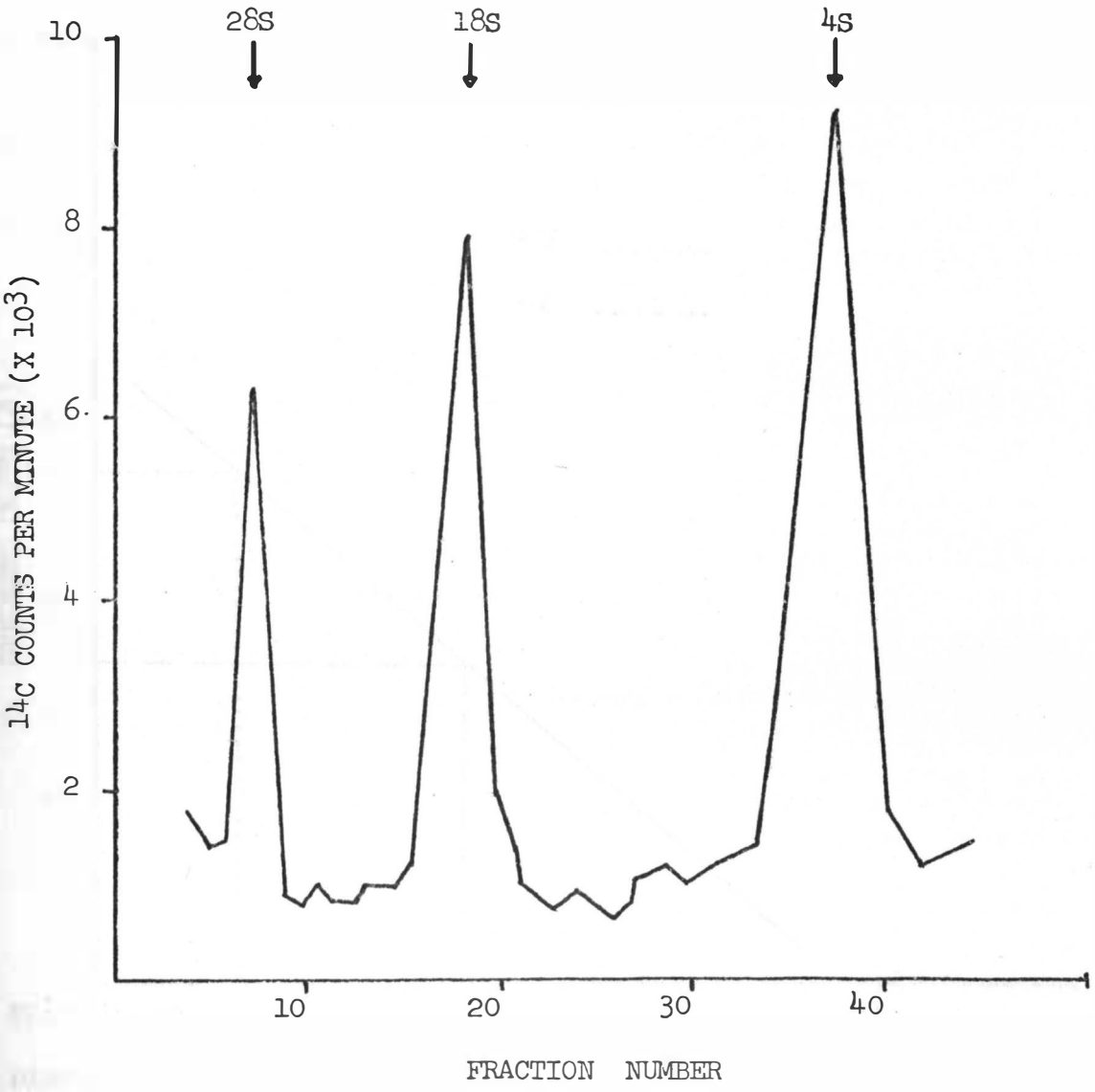

Fig. 10. Svedberg Units versus Migration Distance in Polyacrylamide Gels.

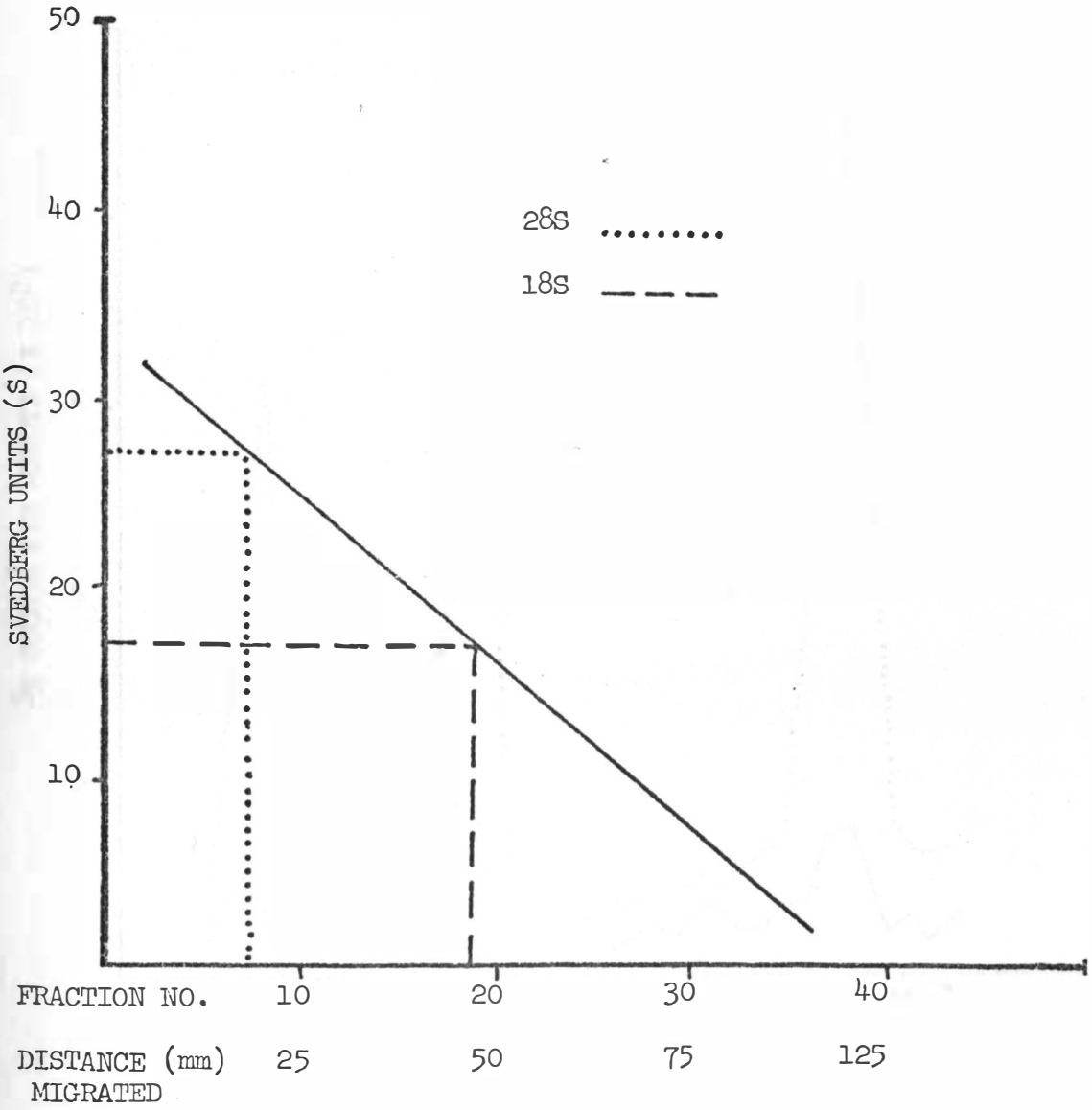

Fig. 11. Actinomycin D Treated A. albopictus RNA.

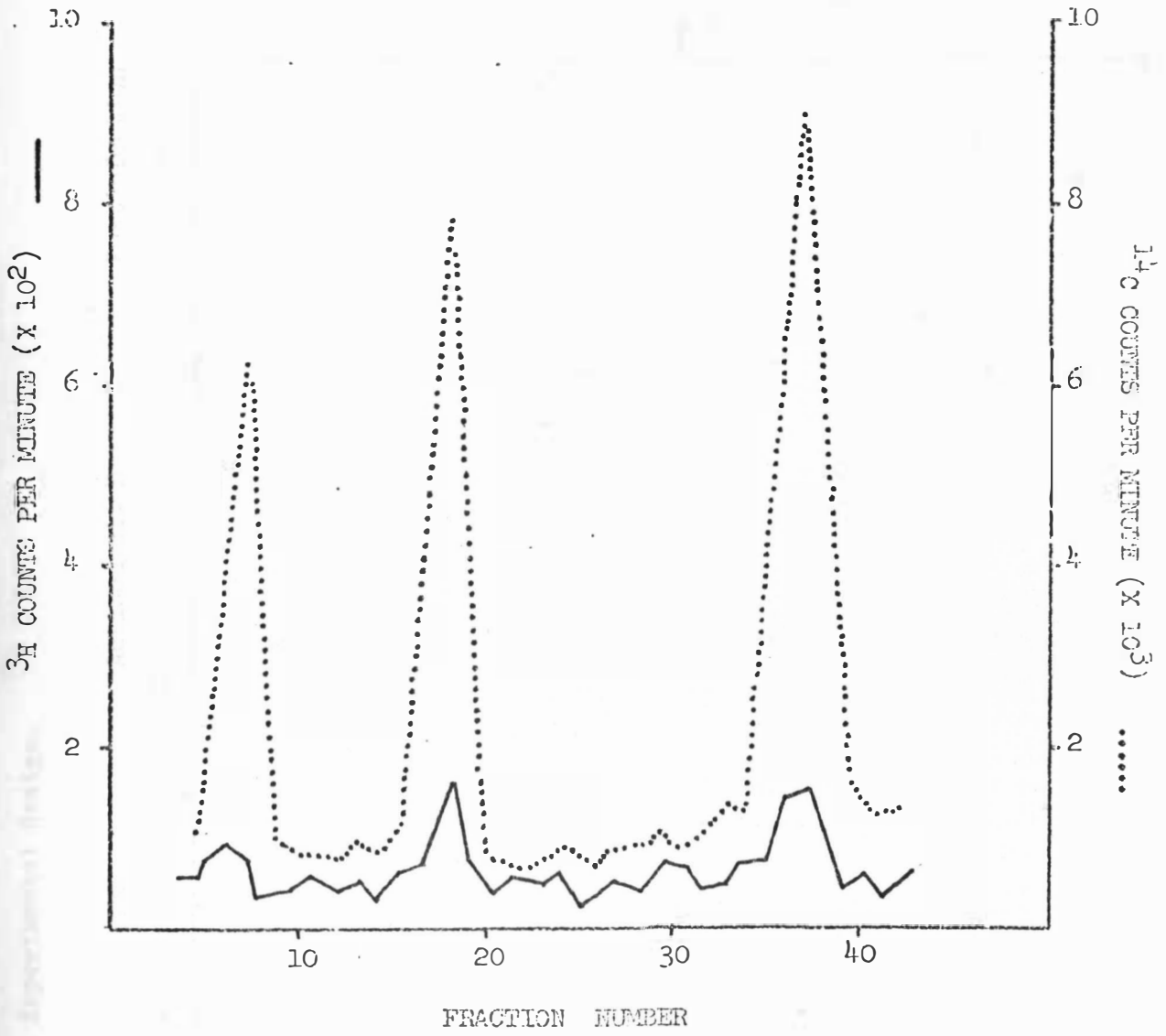

Fig. 12. RNA Analysis Experimental Design.

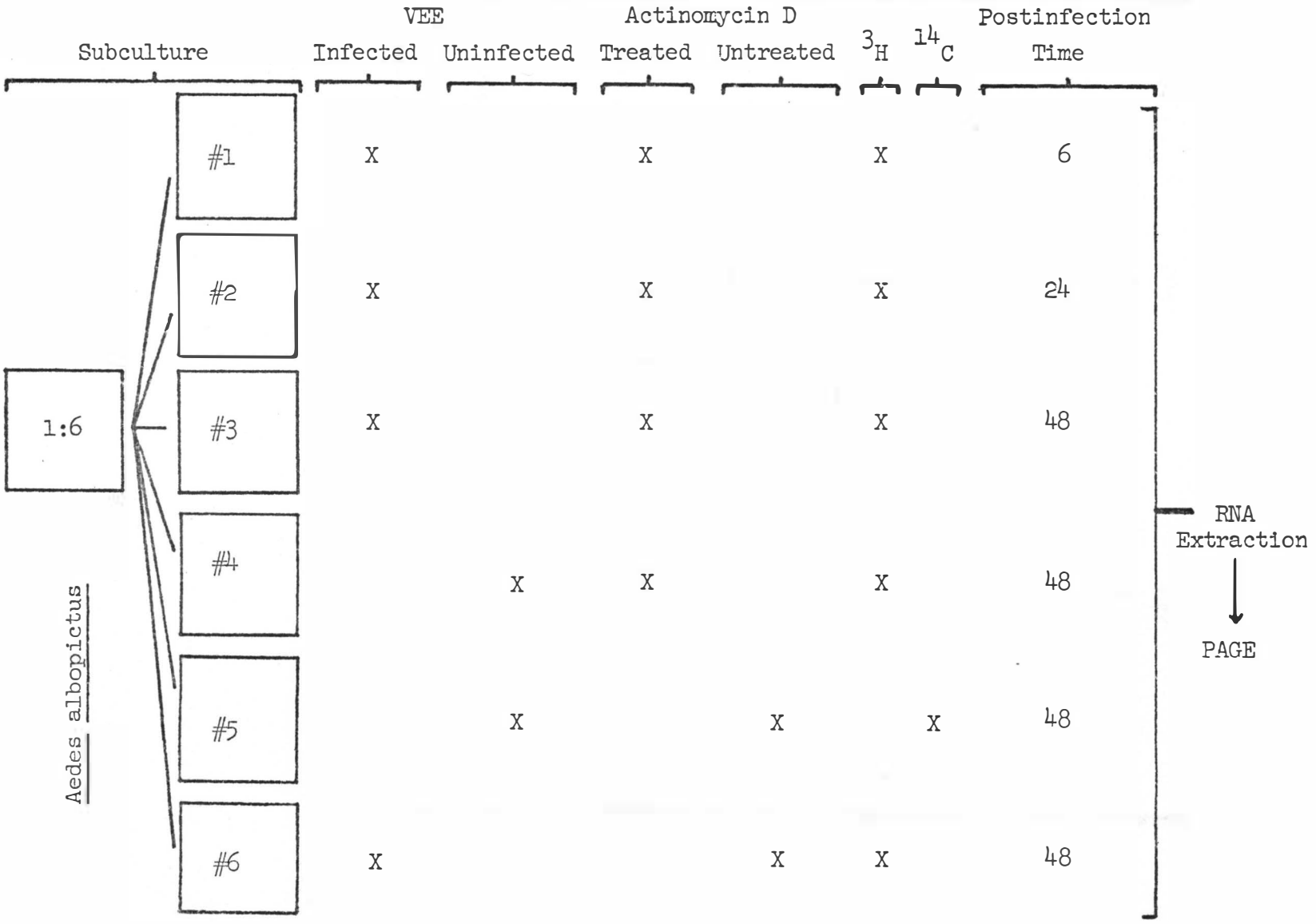

Fig. 13. Vee-specific RNA Species Six Hours Post-infection.

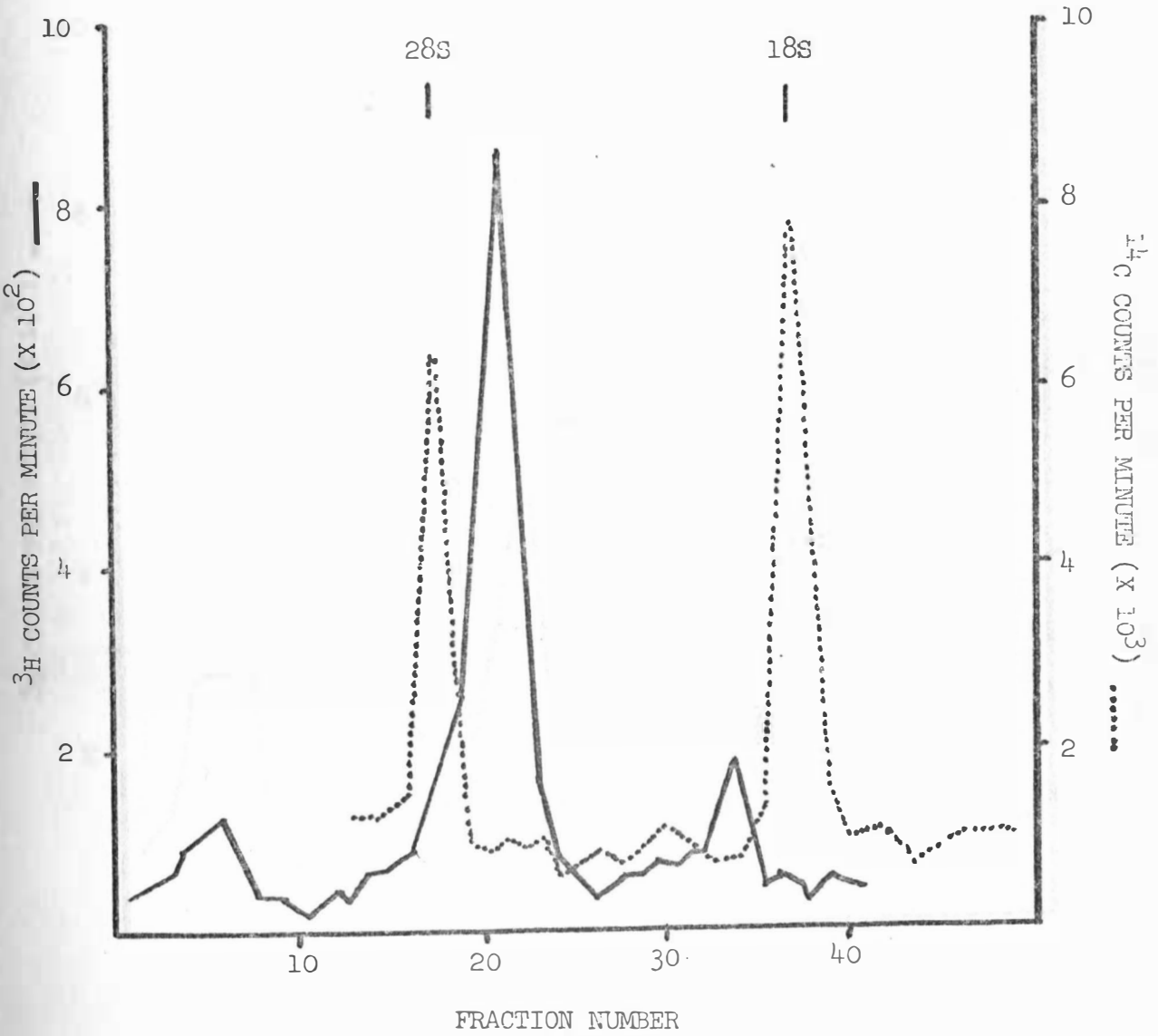

Fig. 14. VEE Specific RNA Forty-eight Hours Post-infection.

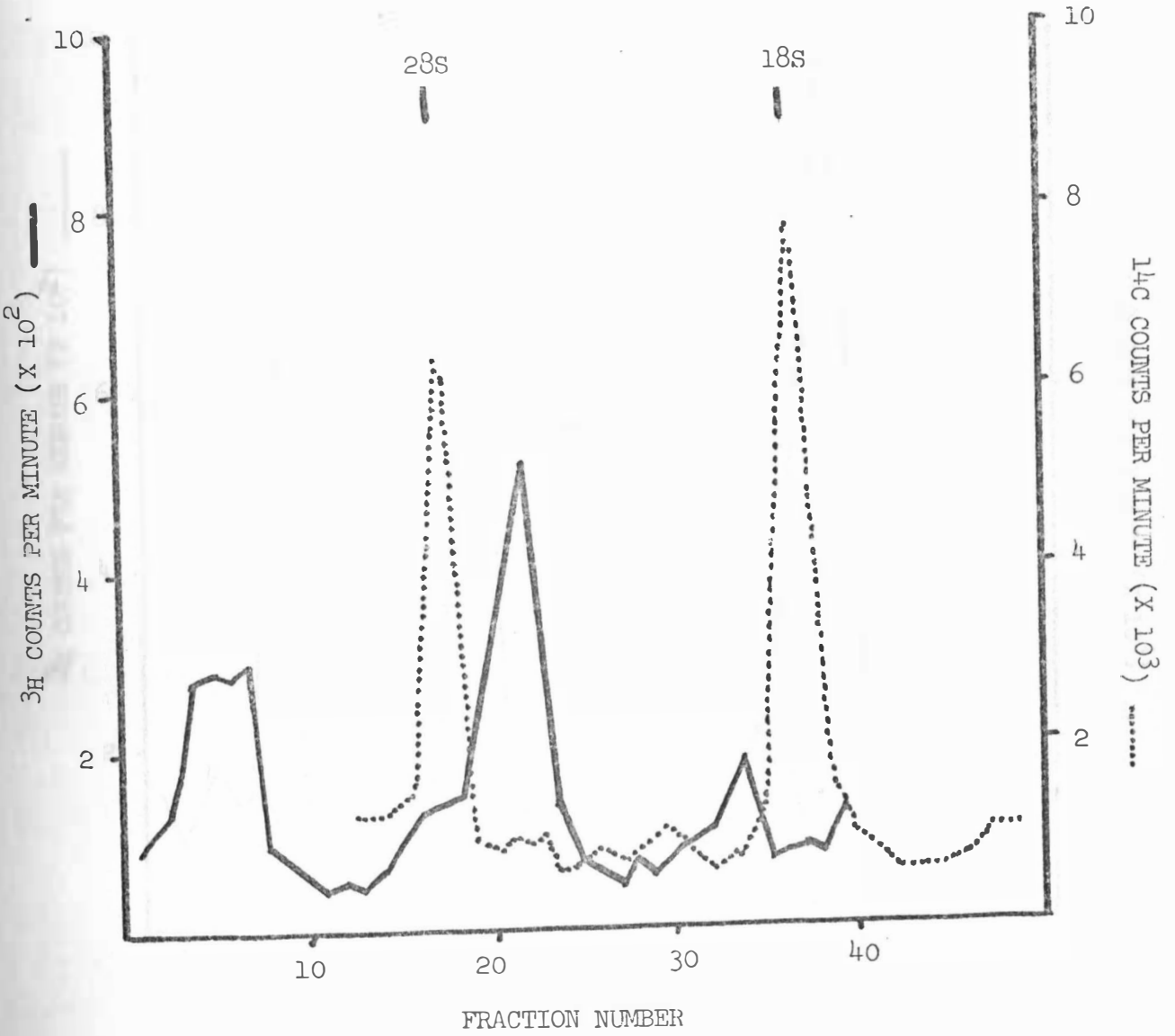

Fig. 15. Ribonuclease Treated A. albopictus RNA.

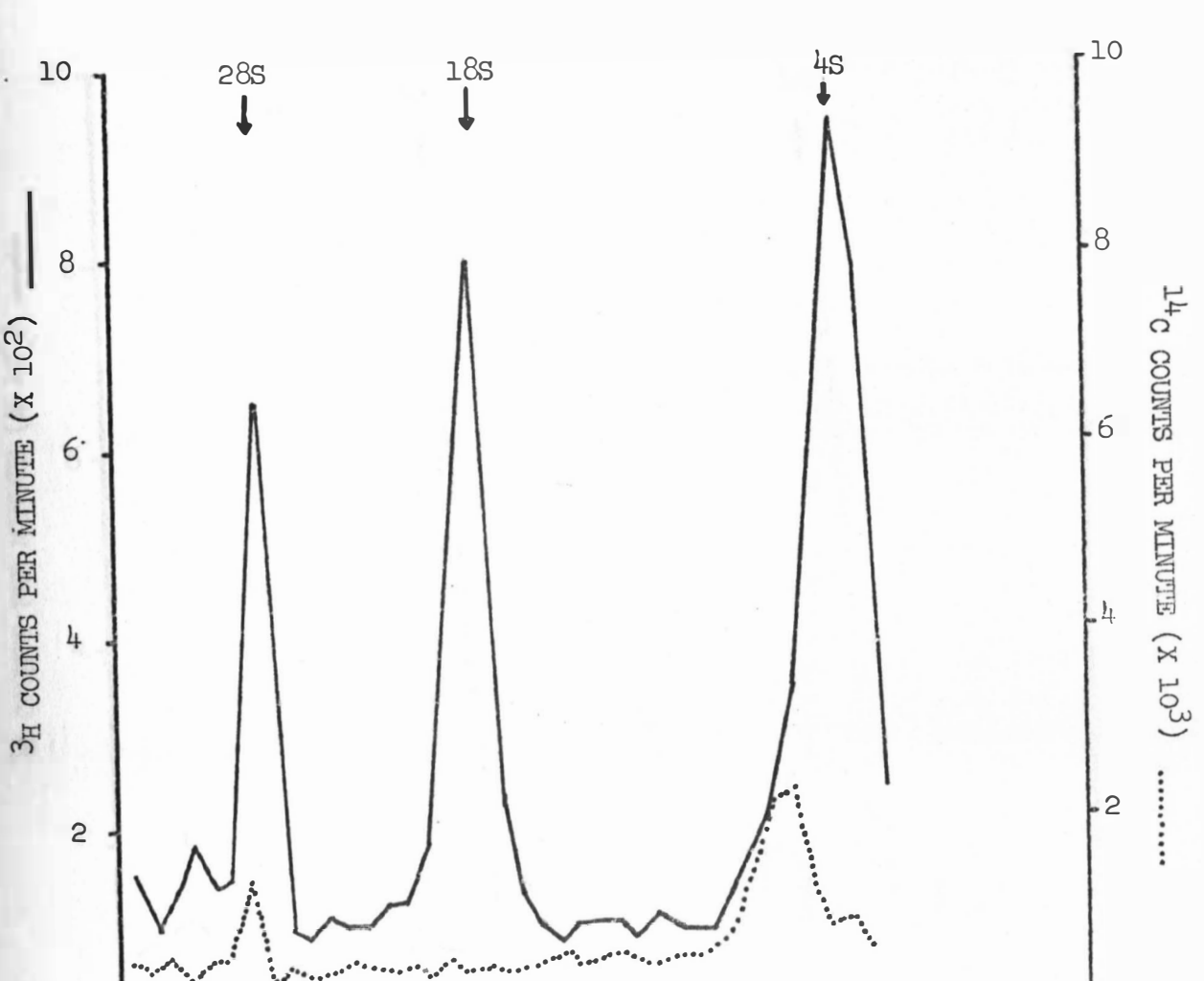

Fig. 16. Ribonuclease Treated VEE-specific RNA.

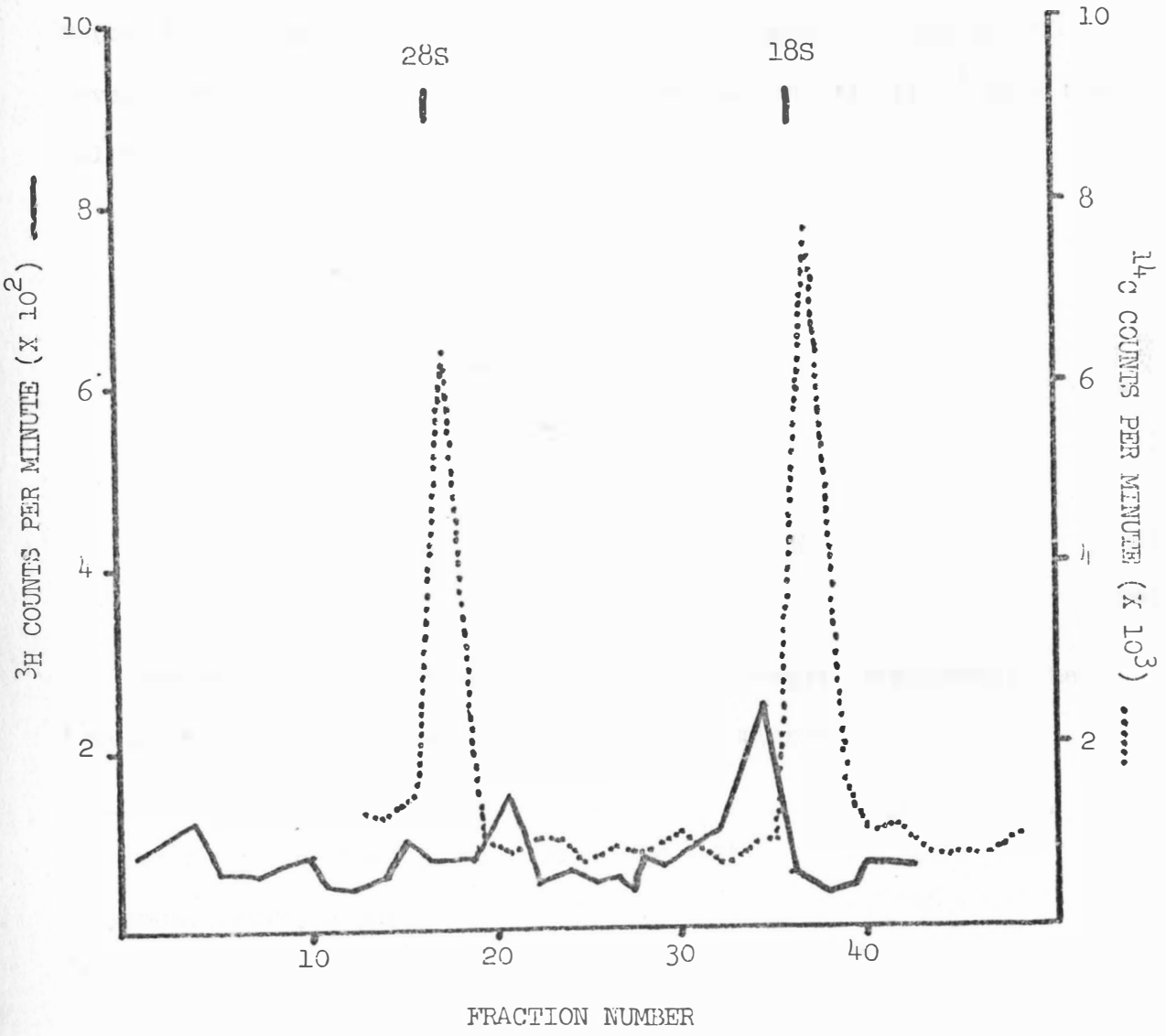

Table 2. Optical Micrometer Calibration.

An American Optical Micrometer[1] was placed on an Olympus Inverted Microscope[2] for calibration. Using a magnification of 200 X, several measurements of a Bausch and Lomb calibrated slide[3] gave the following data:

23.6
22.4
22.3
22.0
22.5
24.1
22.4
23.8
23.7
23.4
22.0
22.6
274.8

The mean (22.9) micrometer graduations equals 10 microns; therefore, 1 micrometer graduation equals 0.4366 micron.

---

[1] American Optical Company, Buffalo, New York

[2] Olympus, Tokyo, Japan

[3] Bausch and Lomb, Rochester, New York

Fig. 17. Diameter (Volume) Range of Aedes albopictus.

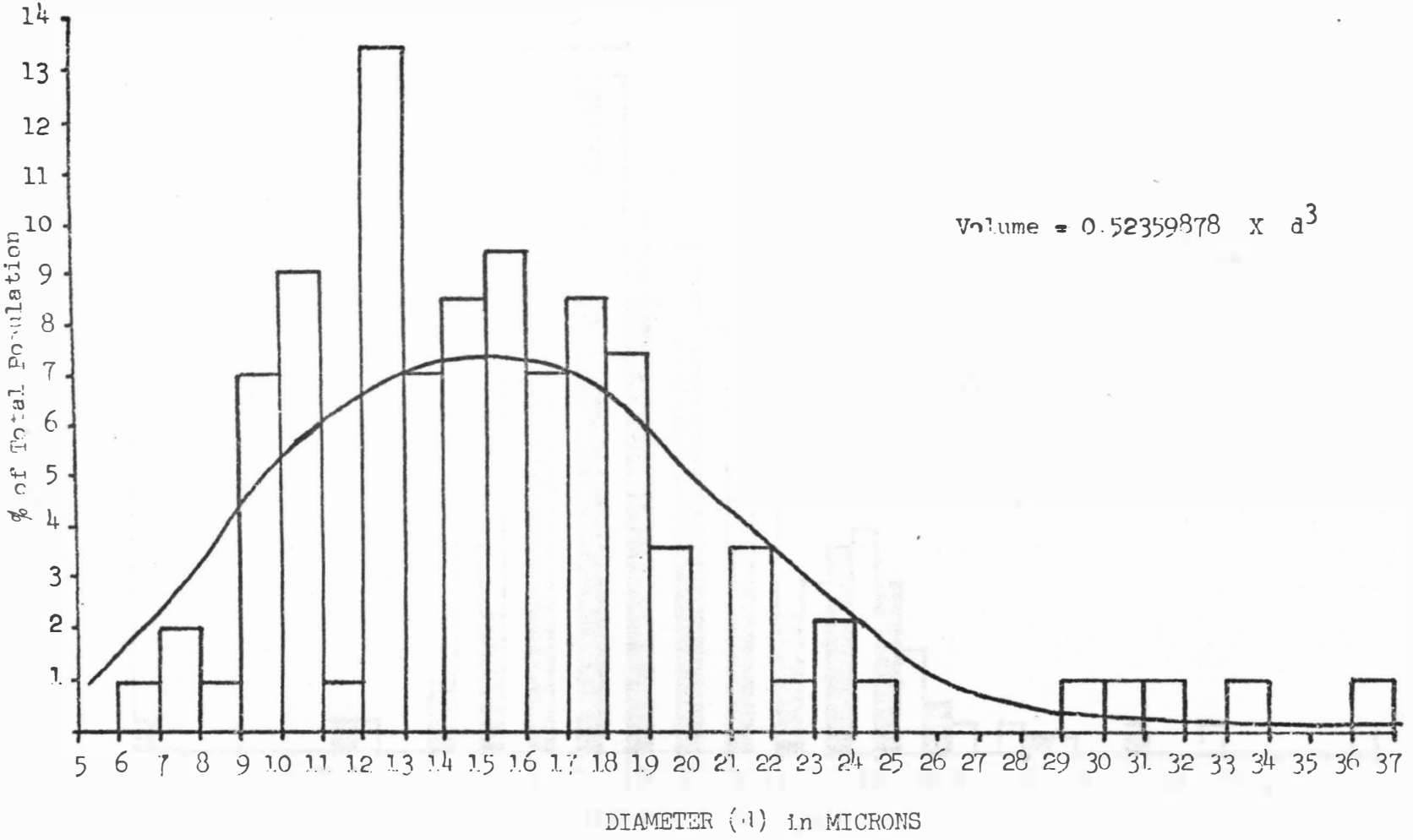

Fig. 18. Diameter (Volume) Range of Uninfected and VEE Infected A. albopictus.

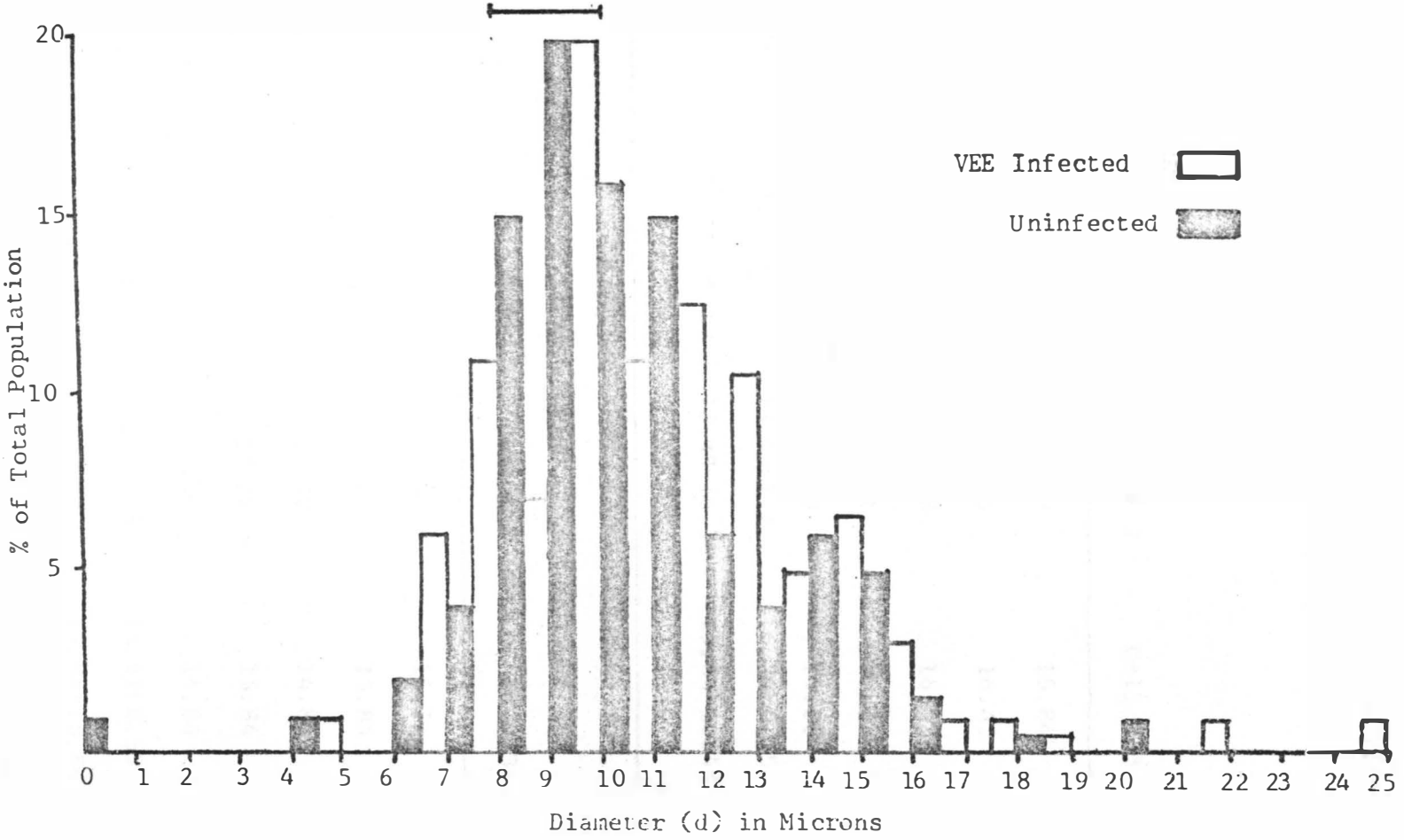

Table 3. Effect of Isoton on A. albopictus Cell Diameter (Volume).

BEFORE ISOTON

Measurement	Cell # 1	Cell # 2	Cell # 3
1	14.4	16.59	15.84
2	12.66	12.96	16.45
3	12.87	12.48	16.45
4	13.0	12.61	16.19
5	12.92	12.53	16.28
X,S.D.	13.17±0.7	13.43±1.77	16.24±0.25
Range	12.66-14.4	12.48-16.59	15.84-16.45

AFTER ISOTON

Measurement	Cell # 1	Cell # 2	Cell # 3
1	12.83	13.97	15.71
2	13.14	13.88	15.84
3	12.83	13.70	14.84
4	13.09	13.22	15.84
5	13.22	13.97	14.84
X,S.D.	13.02±0.18	13.74±0.31	15.41±0.53
Range	12.83-13.22	13.22-13.97	14.84-15.84

Fig. 19. Growth Curve of A. albopictus Cells.

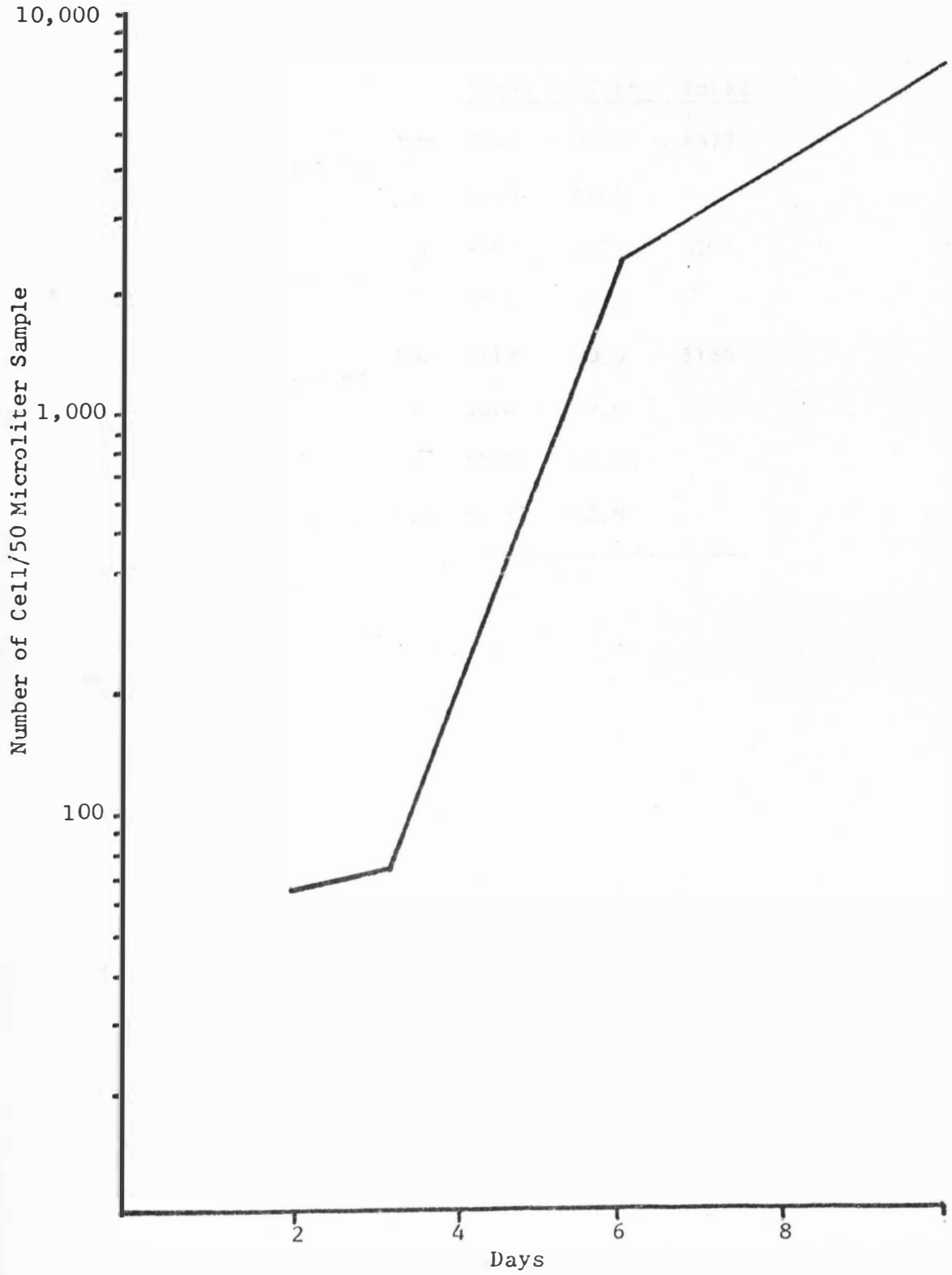

Fig. 20. Precision of Coulter Counter Volume Profiles Among Cells of the Same Age and Transfer Number.

		Channel Groups		
		47-56	57-66	Total
Trial #1	Sum	3302	3075	6377
	%	51.8	48.2	
Trial #2	Sum	2769	2472	5241
	%	52.8	47.2	
Trial #3	Sum	3119	3065	6184
	%	50.4	49.6	
	X	53.66	46.34	
	S.D.	±2.87	±2.87	

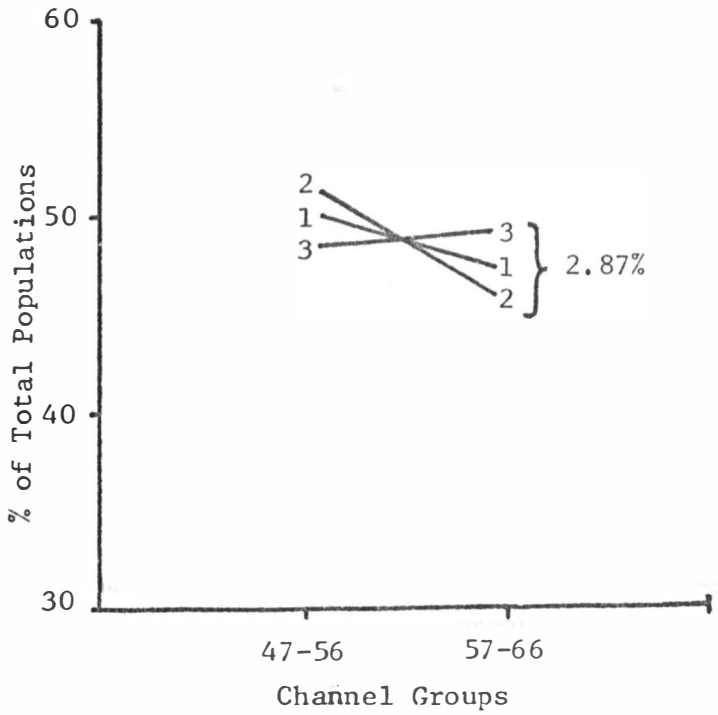

Table 4. Example of Computer Calculated Coulter Counter Parameters at Aperture 512.

Volume: (μ^3)	Threshold:	Attenuation:
500	11	0.93662
500	31	0.35009
500	43	0.25239
500	44	0.24666
500	60	0.13033
500	61	0.17792
500	62	0.17505
500	63	0.17227
500	64	0.12920
500	65	0.12763
500	66	0.12620
500	67	0.12475
500	68	0.12333
500	69	0.12194
500	90	0.12059
600	13	1.00130
600	26	0.50090
600	37	0.35193
600	52	0.25045
600	53	0.24572
600	72	0.13053
600	73	0.17340
600	74	0.17509
600	75	0.17365
700	15	1.01293
700	43	0.35335
700	60	0.25323
700	61	0.24903
700	62	0.24506
700	84	0.13085
700	85	0.17375
700	86	0.17667
700	87	0.17464
700	88	0.17265
800	17	1.02144
800	18	0.96470
800	35	0.49613
800	49	0.35436
800	59	0.25166
800	70	0.24806
800	96	0.13036
800	97	0.17942
800	98	0.17719
800	99	0.17540
800	100	0.17365

Table 5. Volume Range for All Aperture and Attenuation Combinations.

Ap.[1]	Attn.[2]	Vol. Range[3]	Ap.[1]	Attn.[2]	Vol. Range[3]
	0.125	0 - 1		0.125	0 - 9
	0.177	0 - 1		0.177	0 - 12
	0.250	0 - 2		0.250	2 - 18
	0.354	0 - 3		0.354	8 - 25
	0.500	0 - 4		0.500	5 - 36
	0.707	3 - 6		0.707	22 - 51
1	1.0	0 - 9	8	1.0	5 - 75
	2.0	2 - 18		2.0	10 -140
	4.0	4 - 36		4.0	20 -290
	8.0	18 - 72		8.0	23 -570
	0.125	0 - 2		0.125	2 - 18
	0.177	0 - 3		0.177	0 - 26
	0.250	0 - 4		0.250	4 - 36
	0.354	0 - 6		0.354	16 - 51
	0.500	5 - 9		0.500	5 - 72
	0.707	6 - 12		0.707	43 -100
2	1.0	2 - 18	16	1.0	9 -150
	2.0	4 - 36		2.0	17 -290
	4.0	5 - 72		4.0	23 -580
	8.0	23 - 99		8.0	23 -1159
	0.125	0 - 4		0.125	4 - 37
	0.177	0 - 6		0.177	0 - 52
	0.250	0 - 9		0.250	5 - 73
	0.354	4 - 12		0.354	32 -100
	0.707	11 - 25		0.500	20 -140
4	1.0	4 - 37	32	1.0	3 -300
	2.0	5 - 73		2.0	17 -580
	4.0	10 -140		4.0	23 -1156
	8.0	26 -280		8.0	23 -2302

Table 5 (Con't.)

Ap.[1]	Attn.[2]	Vol. Range[3]	Ap.[1]	Attn.[2]	Vol. Range[3]
	0.125	7 - 73		0.125	5 - 290
	0.177	0 - 100		0.177	4 - 410
	0.250	10 - 140		0.250	17 - 580
	0.354	33 - 200		0.354	33 - 820
	0.500	20 - 290		0.500	23 - 1152
	0.707	45 - 400		0.707	24 - 1625
64	1.0	6 - 600	256	1.0	49 - 2307
	2.0	23 - 1153		2.0	24 - 4625
	4.0	23 - 2300		4.0	92 - 9227
	8.0	46 - 4600		8.0	530 -18400
	0.125	12 - 140		0.125	17 - 580
	0.177	2 - 200		0.177	8 - 820
	0.250	20 - 290		0.250	23 - 1161
	0.354	33 - 410		0.354	33 - 1625
	0.500	23 - 580		0.500	23 - 2300
	0.707	57 - 790		0.707	65 - 3250
128	1.0	12 - 1153	512	1.0	44 - 4636
	2.0	23 - 2307		2.0	93 - 9258
	4.0	46 - 4625		4.0	370 -18500
	8.0	92 - 9200		8.0	370 -37000

[1]Aperture

[2]Attenuation

[3]Volume Range in Cubic Microns

Table 6. Resolution (μ^3/channel) at All Aperture and Attenuation Combinations

	Aperture									
	1	2	4	8	16	32	64	128	256	512
0.125	0.0112	0.0225	0.0448	0.0896	0.1792	0.359	0.718	1.436	2.872	5.777
0.177	0.0159	0.0319	0.0638	0.1273	0.254	0.509	1.018	2.036	4.072	8.144
0.250	0.0225	0.0448	0.0897	0.1795	0.3590	0.7184	1.436	2.873	5.777	11.55
0.354	0.0317	0.0638	0.1273	0.2545	0.5090	1.0180	2.036	4.072	8.144	16.28
0.500	0.0449	0.0899	0.180	0.360	0.720	1.444	2.888	5.777	11.55	23.10
0.707	0.0635	0.1273	0.2545	0.500	1.0180	2.036	4.072	8.144	16.288	32.56
1.0	0.0909	0.1803	0.360	0.722	1.444	2.888	5.777	11.55	23.10	46.36
2.0	0.1818	0.3600	0.7200	1.444	2.888	5.777	11.55	23.10	46.20	92.40
4.0	0.360	0.820	1.4545	2.8750	5.777	11.55	23.10	46.25	92.92	185.00
8.0	0.720	1.444	2.888	5.777	11.55	23.10	46.00	92.00	184.00	368.10

Table 7. Example of "Coulter Counter Program" Printout.

CONTROL DAY 4	CONTROL DAY 6	INFECTED DAY 6
a 71 b 9144 9909 c	71 24596 24207	71 26306 26552
9796 903.6 d	24242 259.6	26955 351.8
9767 2.1% e	24022 1.2%	26392 1.3%
f 234	20 -213	-61 -294
72 9521 9673	72 24423 24266	72 26874 26612
9894 194.6	23923 297.7	26352 261.0
9611 2.0%	24453 1.2%	26611 1.0%
-121	346 467	248 366
73 9779 9797	73 23771 23921	73 26222 26367
9555 251.0	24225 263.6	26703 291.6
10056 2.6%	23766 1.1%	26177 1.1%
223	-100 -323	387 164
74 9464 9574	74 24112 24021	74 26077 25901
9628 221.0	23905 103.7	26163 245.1
9429 2.3%	24046 0.4%	25702 0.9%
-45	201 246	-146 -101
75 9789 9619	75 24143 23820	75 26285 26126
9423 184.3	23397 363.1	25765 313.7
9644 1.9%	23921 1.6%	26329 1.2%
26	168 136	339 328
76 9554 9592	76 23772 23658	76 25688 25872
9843 233.9	23908 321.9	26196 261.7
9390 2.4%	23295 1.4%	25731 1.1%
29	106 77	-2 -31
77 9755 9563	77 23796 23532	77 26000 25674
9401 178.8	23114 379.6	25594 242.3
9534 1.9%	23756 1.6%	26019 0.9%
252	342 90	230 -14
78 9306 9311	78 22999 23210	78 25427 25635
9391 67.6	23464 235.8	26097 410.4
9246 0.7%	23166 1.0%	25362 1.6%
-95	-57 37	102 197
79 9589 9406	79 23452 23267	79 25725 25533
9848 309.8	23035 212.5	25237 230.8
9520 3.3%	23315 0.9%	25535 1.0%
203	450 247	213 10
80 9091 9203	80 22661 22818	80 25149 25320
8979 295.8	23228 358.7	25789 406.5
9538 3.2%	22564 1.5%	25042 1.6%
85	-200 -267	313 227
81 9019 9116	81 23301 23012	81 24832 25007
9290 150.5	22516 435.9	25370 321.8
9040 1.7%	23237 1.9%	24810 1.3%
-25	466 491	-69 -44

Fig. 21. Vol

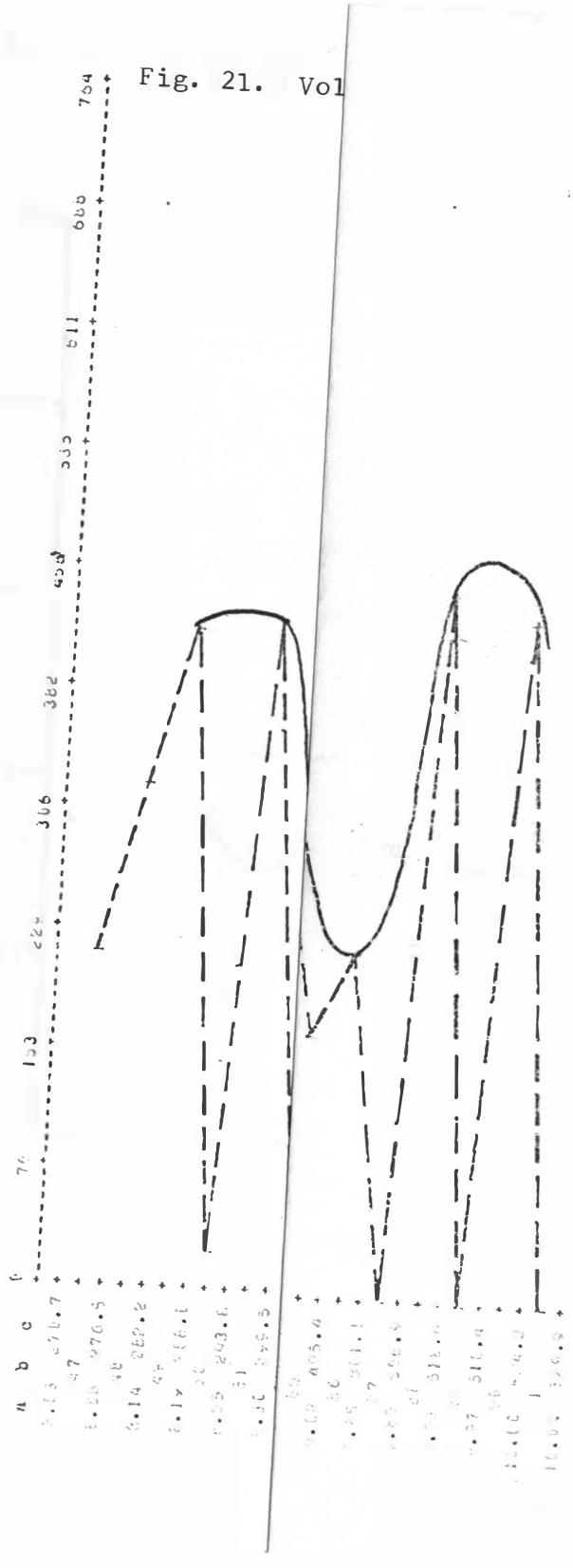

lls

Fig. 22. "Trend Line" Analysis of Uninfected A. albopictus Cells (C6 vs C8).

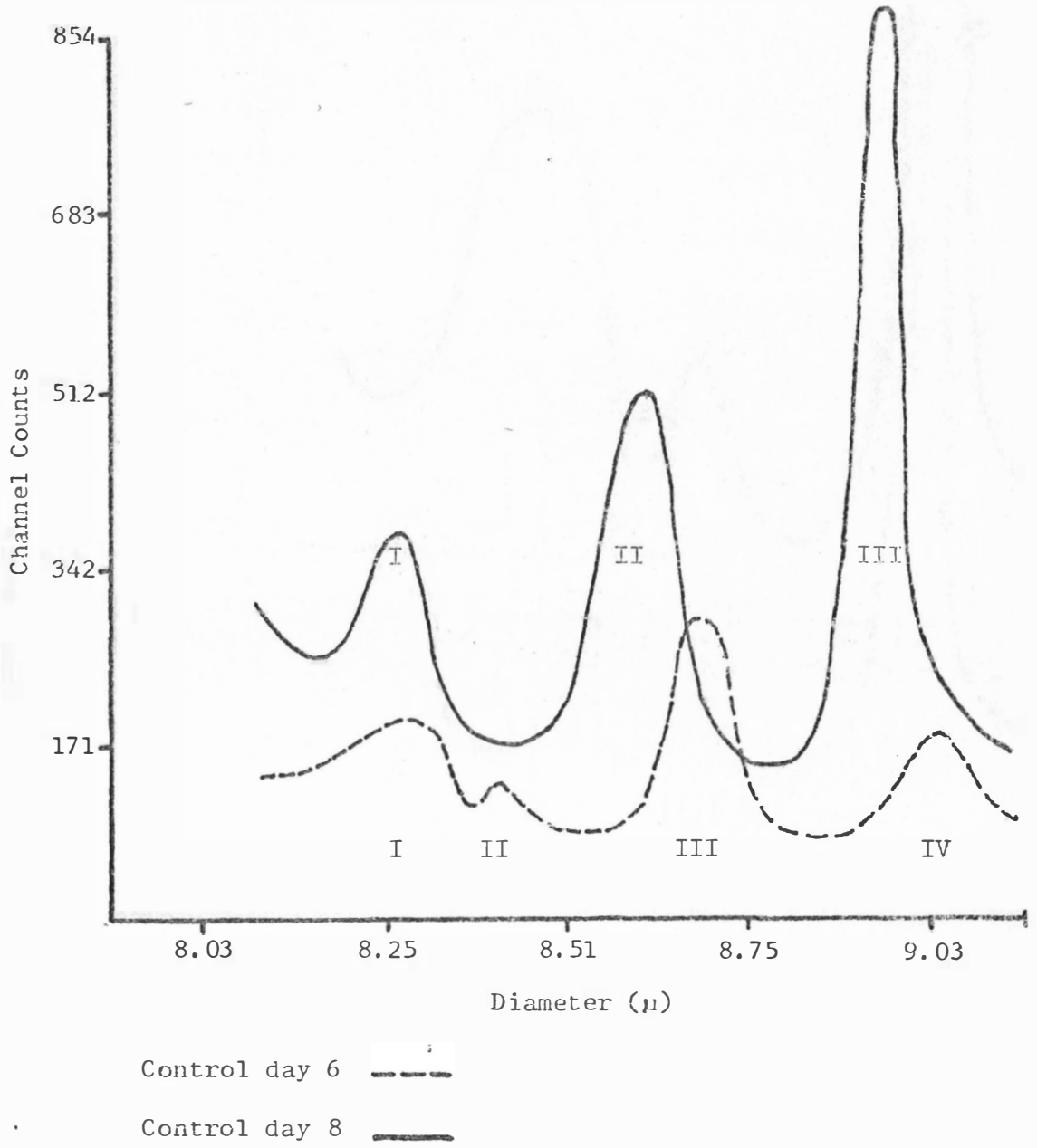

Fig. 23. "Trend Line" Analysis of Uninfected and Predicted Volume Profiles (C6 vs Predicted C8).

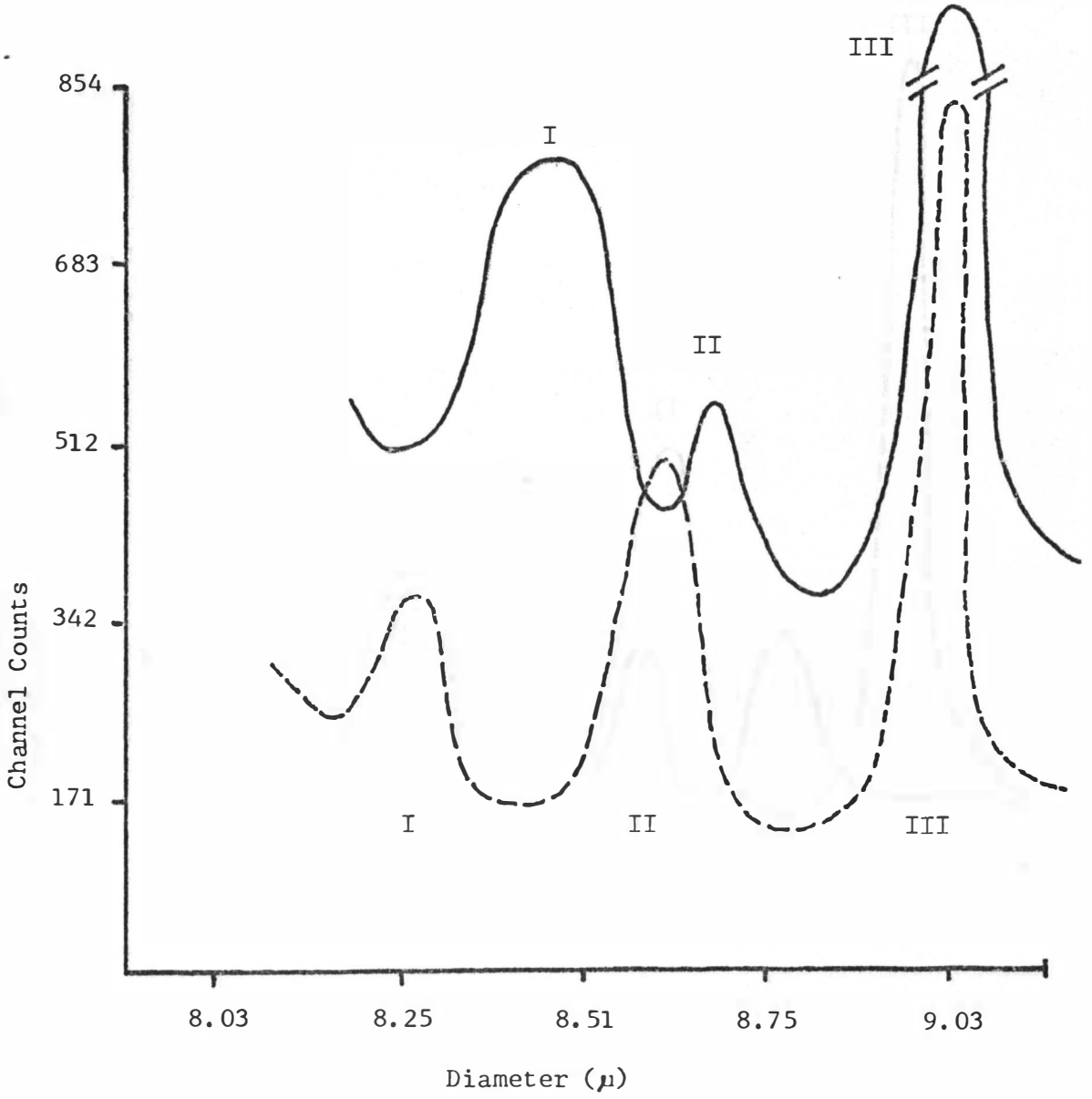

Fig. 24. "Trend Line" Analysis of Uninfected and Infected A. albopictus Cells (C8 vs I8).

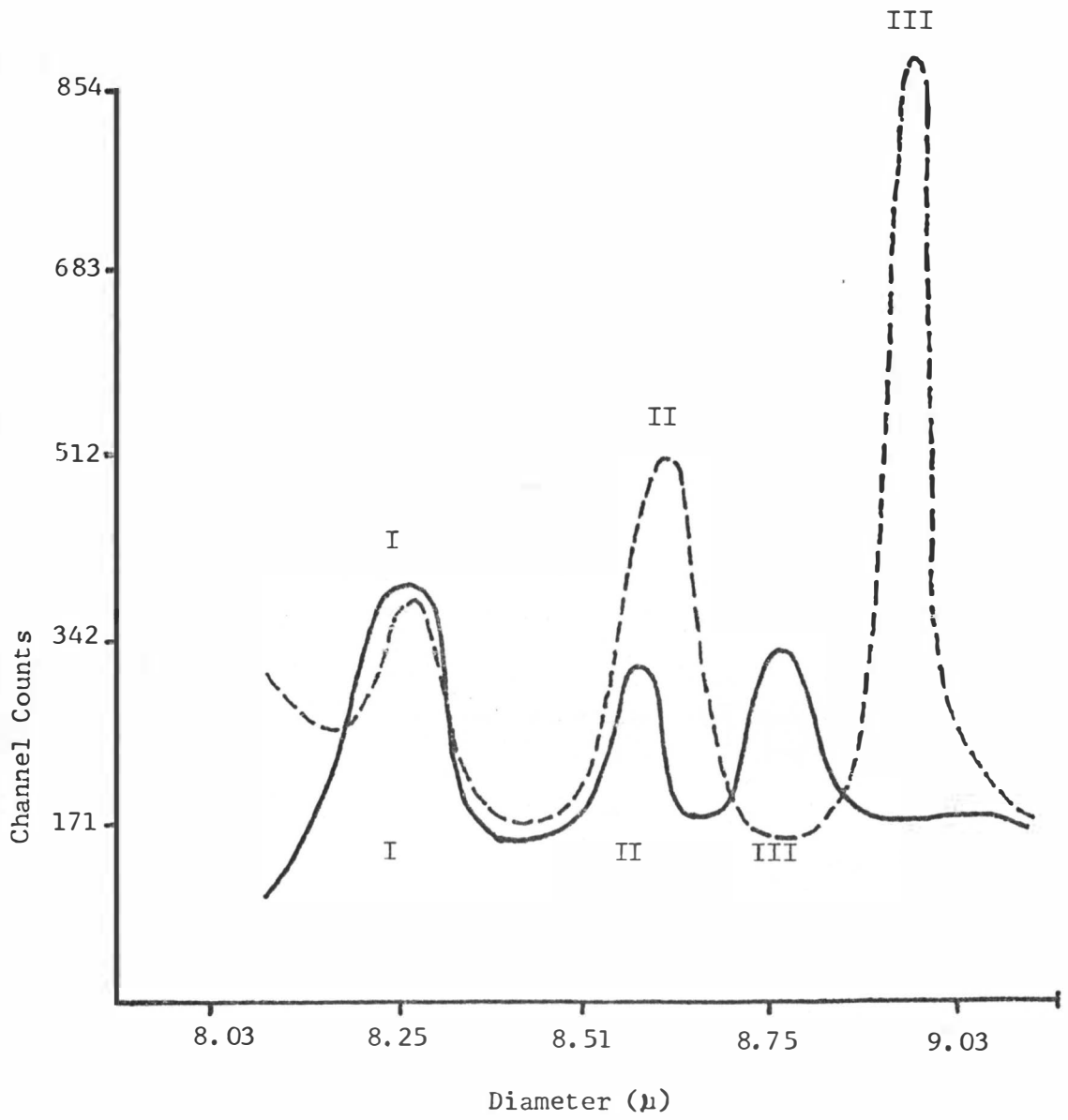

Fig. 25. Experiment 17 Grouped Data Analysis.

CHANNEL	47-56	57-66	67-76	77-86	TOTAL
1 CONTROL	1074	1113	1245	855	4292
DAY 6	25.0%	26.1%	29.0%	19.9%	100.0%
2 CONTROL	1234	2593	1307	2469	7603
DAY 6	16.2%	34.1%	17.2%	32.5%	100.0%
3 INFECTED	1184	1768	2073	2137	7163
DAY 6	16.5%	24.7%	28.9%	29.8%	100.0%
C6:C6	160	1475	62	1614	3311
	-8.3%	8.1%	-11.8%	12.6%	43.6%
C6:I6	110	650	829	1282	2871
	-8.5%	-1.4%	-0.1%	9.9%	40.1%
C6:I6	-50	-825	766	-332	-440
	0.3%	-9.4%	11.8%	-2.6%	-6.1%

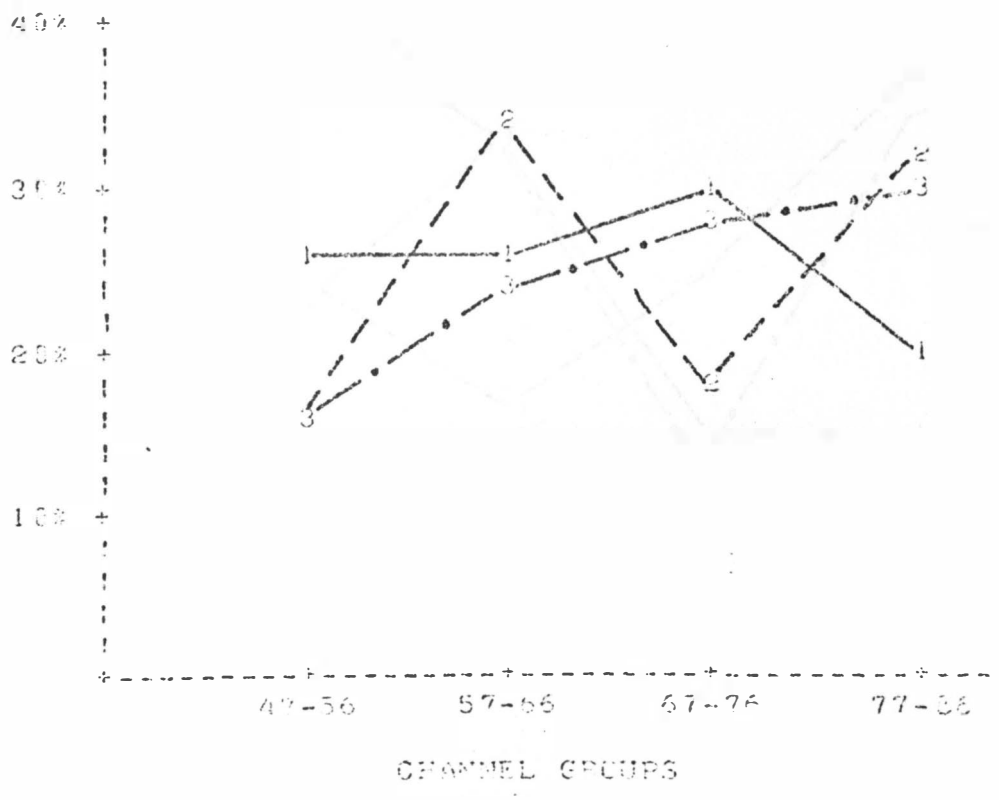

Fig. 26. Experiment 18 Grouped Data Analysis.

CHANNEL	47-56	57-66	67-76	77-86	TOTAL
1 CONTROL	982	778	366	362	2487
DAY 6	39.5%	31.3%	14.7%	14.6%	100.0%
2 CONTROL	1709	1148	1725	2540	7120
DAY 8	24.0%	16.1%	24.2%	35.7%	100.0%
3 INFECTED	1254	1667	721	1921	5763
DAY 8	21.7%	32.6%	12.5%	33.2%	100.0%
C6:C8	726	370	1359	2178	4633
	-15.5%	-15.2%	9.5%	21.1%	65.1%
C6:I8	272	1110	355	1559	3296
	-17.8%	1.4%	-2.2%	18.7%	57.0%
C8:I8	-454	740	-1004	-618	-1337
	-2.3%	16.5%	-11.9%	-2.4%	-23.1%

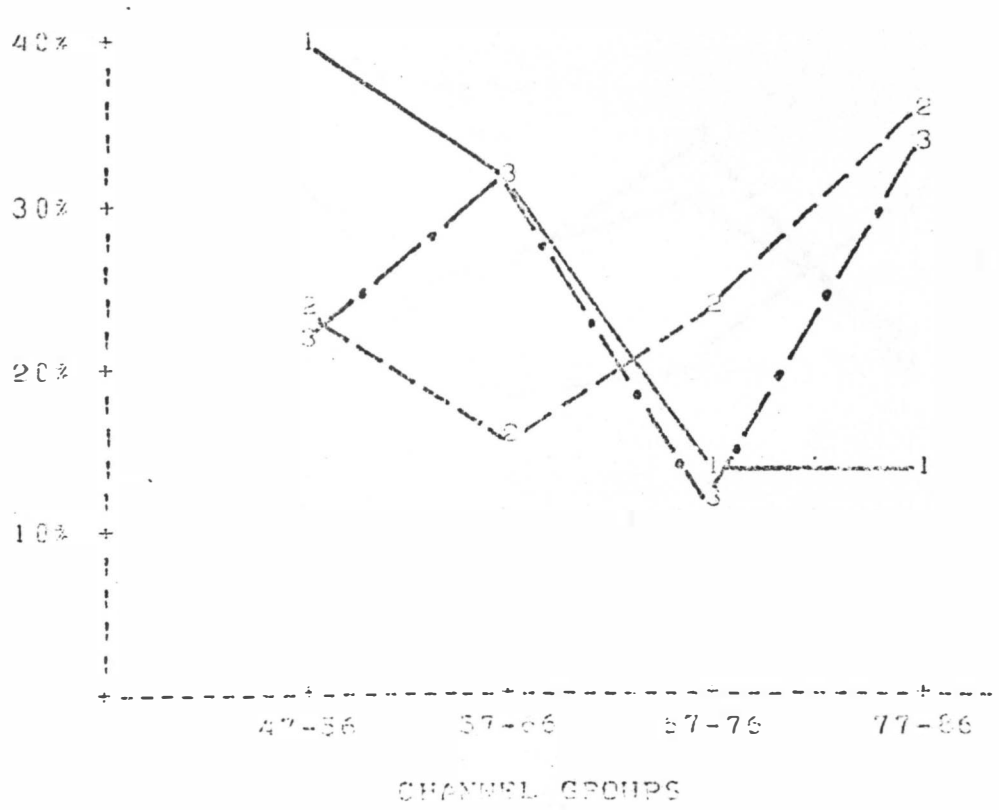

Fig. 27. Experiment 20 Grouped Data Analysis.

CHANNEL	47-56	57-66	67-76	77-86	TOTAL
1 CONTROL	612	757	839	606	2814
DAY 6	21.8%	26.9%	29.8%	21.5%	100.0%
2 CONTROL	1760	952	1097	1585	5394
DAY 6	32.6%	17.6%	20.3%	29.4%	100.0%
3 INFECTED	1077	1420	1917	1116	5530
DAY 6	19.5%	25.7%	34.7%	20.2%	100.0%
C6:C6	1146	195	258	980	2581
	10.9%	-9.3%	-9.5%	7.9%	47.8%
C6:I6	464	663	1079	511	2717
	-2.3%	-1.2%	4.9%	-1.3%	49.1%
C6:I6	-684	466	821	-469	136
	-13.2%	8.6%	14.3%	-9.2%	2.5%

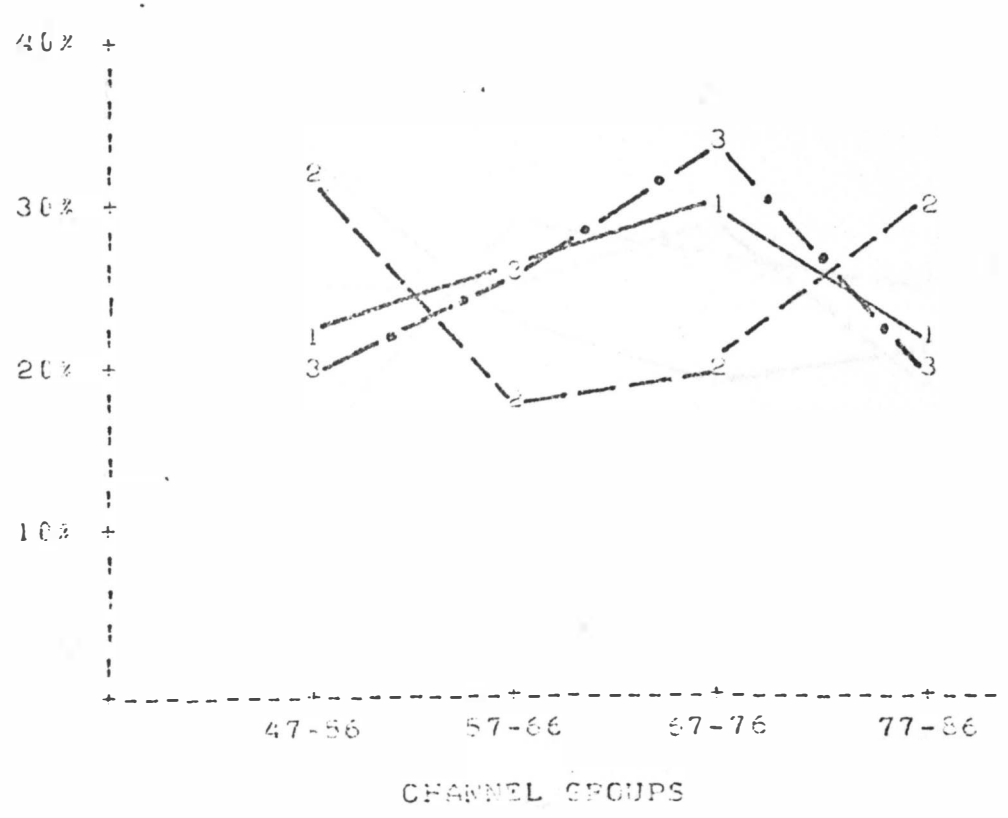

Fig. 28. Experiment 23 Grouped Data Analysis.

CHANNEL	47-56	57-66	67-76	77-86	TOTAL
[1]CONTROL DAY 6	1720 33.2%	1225 23.7%	1083 20.9%	1146 22.1%	5174 100.0%
[2]CONTROL DAY 6	837 15.7%	1610 30.2%	1495 28.1%	1387 26.0%	5329 100.0%
[3]INFECTED DAY 6	1729 25.9%	1721 25.8%	1948 29.2%	1277 19.1%	6675 100.0%
C6:C6	-883 -17.5%	354 6.5%	412 7.1%	241 3.9%	155 2.9%
C6:I6	9 -7.3%	496 2.1%	865 8.3%	131 -3.0%	1501 22.5%
C6:I6	892 16.2%	111 -4.4%	453 1.1%	-110 -6.9%	1346 20.2%

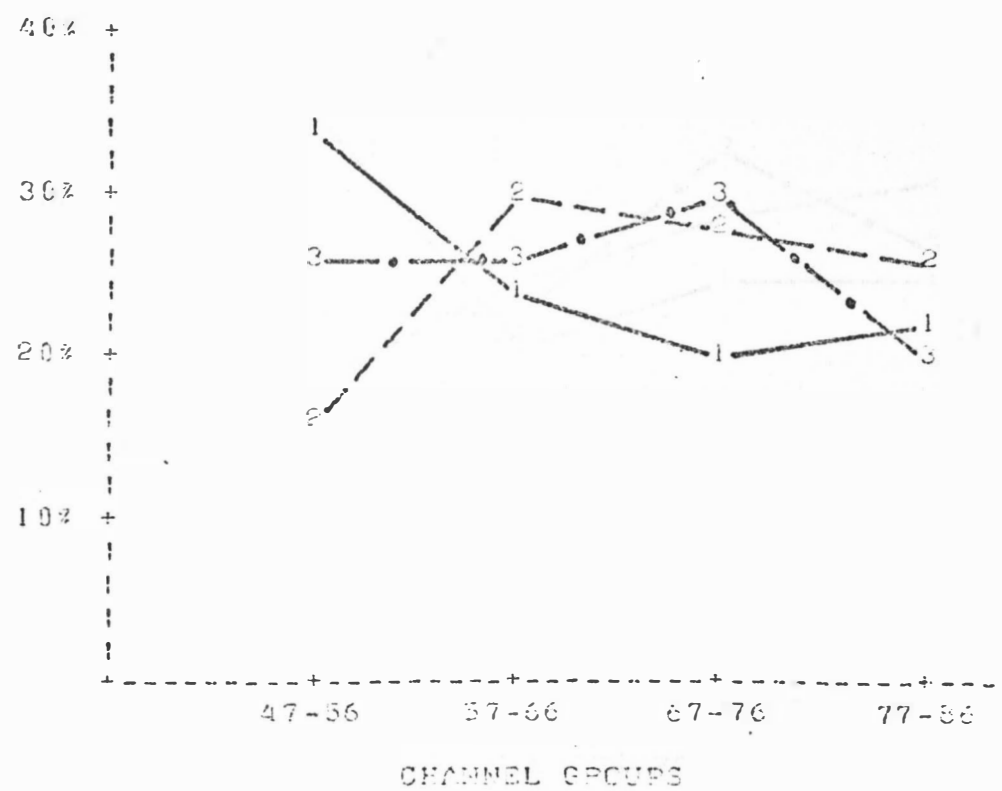

Fig. 29. Experiment 24 Grouped Data Analysis.

CHANNEL	47-56	57-66	67-76	77-86	TOTAL
1CONTROL	2109	1212	1539	1482	6342
DAY 6	33.3%	19.1%	24.3%	23.4%	100.0%
2CONTROL	1292	1836	2101	2158	7387
DAY 6	17.5%	24.9%	28.4%	29.2%	100.0%
3INFECTED	1545	1446	2142	1737	6870
DAY 6	22.5%	21.0%	31.2%	25.3%	100.0%
C6:C6	-817	624	562	676	1045
	-15.8%	5.7%	4.2%	5.8%	14.1%
C6:I6	-564	234	603	255	528
	-10.9%	1.9%	6.9%	1.9%	7.7%
C6:I6	253	-390	41	-421	-517
	5.0%	-3.6%	2.7%	-3.9%	-7.5%

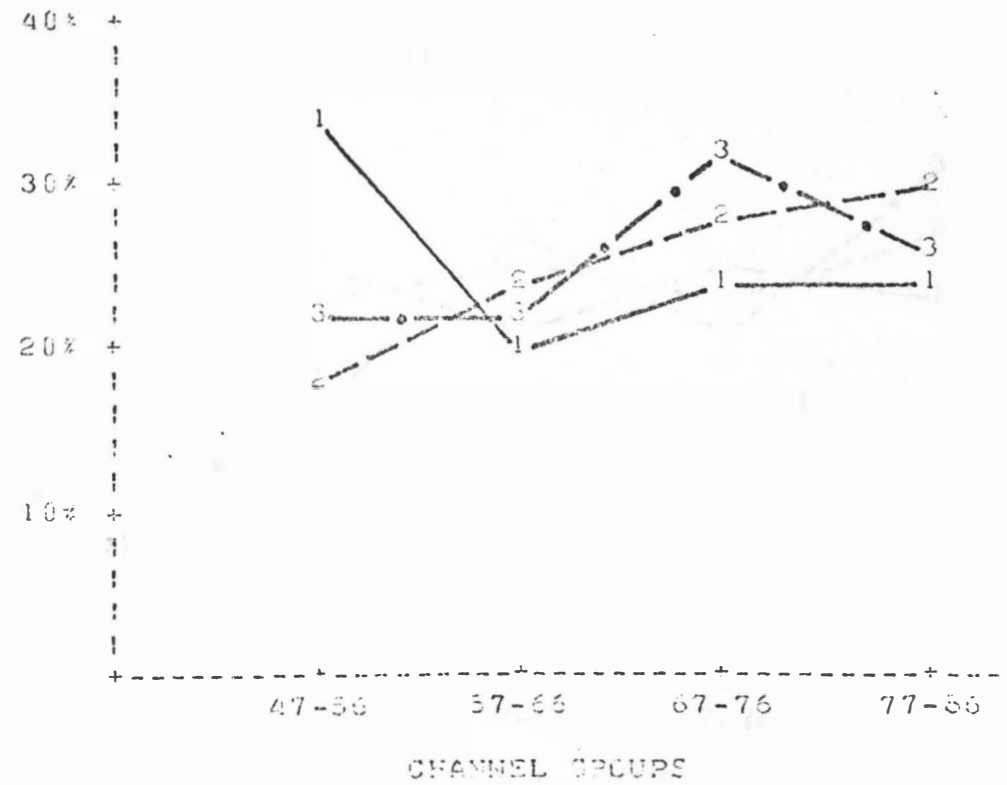

Fig. 30. Experiment 25 Grouped Data Analysis.

CHANNEL	47-56	57-66	67-76	77-86	TOTAL
1 CONTROL	1016	850	959	936	3771
DAY 6	26.9%	22.5%	25.4%	24.8%	100.0%
2 CONTROL	1437	1617	1427	1688	6169
DAY 8	23.3%	26.2%	23.1%	27.4%	100.0%
3 INFECTED	1226	1977	1554	2155	6912
DAY 8	17.7%	28.6%	22.5%	31.2%	100.0%
C6:C8	421	756	468	752	2397
	-3.6%	3.4%	-2.3%	2.6%	38.9%
C6:I8	210	1117	594	1219	3140
	-9.2%	5.8%	-3.0%	6.4%	45.4%
C8:I8	-211	361	127	466	743
	-5.6%	2.4%	-0.7%	3.8%	10.7%

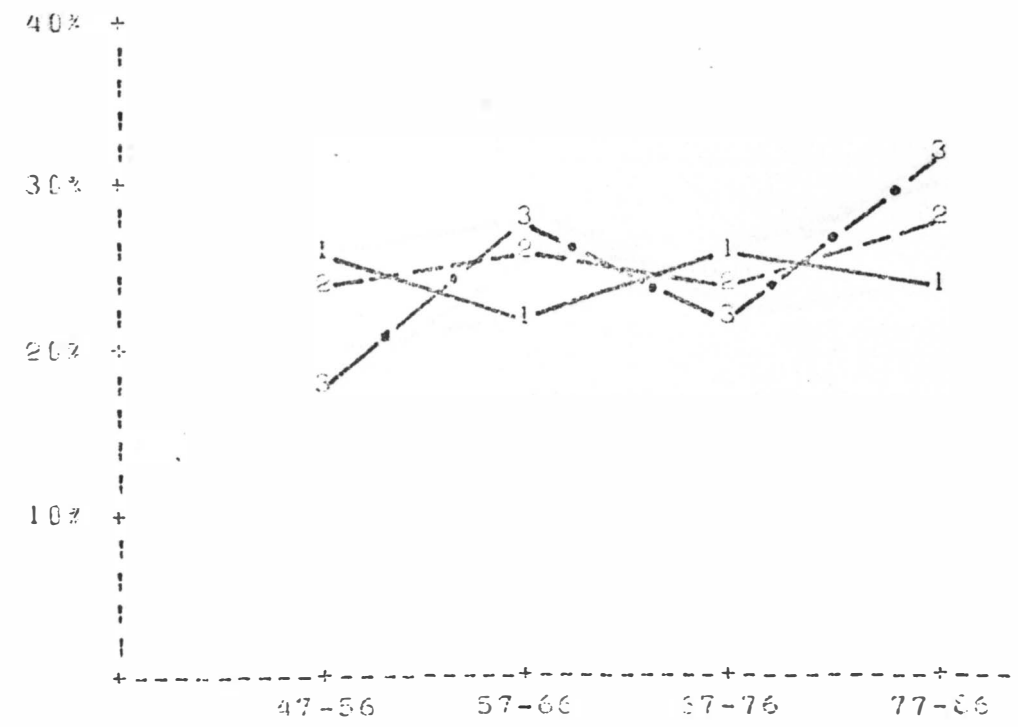

Fig. 31. Experiment 26 Grouped Data Analysis.

CHANNEL	47-56	57-66	67-76	77-86	TOTAL
1 CONTROL	1053	1172	901	989	4116
DAY 6	25.6%	28.5%	21.9%	24.0%	100.0%
2 CONTROL	961	1463	1326	1745	5494
DAY 8	17.5%	26.6%	24.1%	31.8%	100.0%
3 INFECTED	1338	1463	1722	1949	6472
DAY 8	20.7%	22.6%	26.6%	30.1%	100.0%
C6:C8	-92	291	425	756	1379
	-3.1%	-1.9%	2.2%	7.7%	25.1%
C6:I8	284	291	821	950	2346
	-4.9%	-5.9%	4.7%	6.1%	36.4%
C8:I8	377	0	396	204	977
	3.2%	-4.0%	2.5%	-1.6%	15.1%

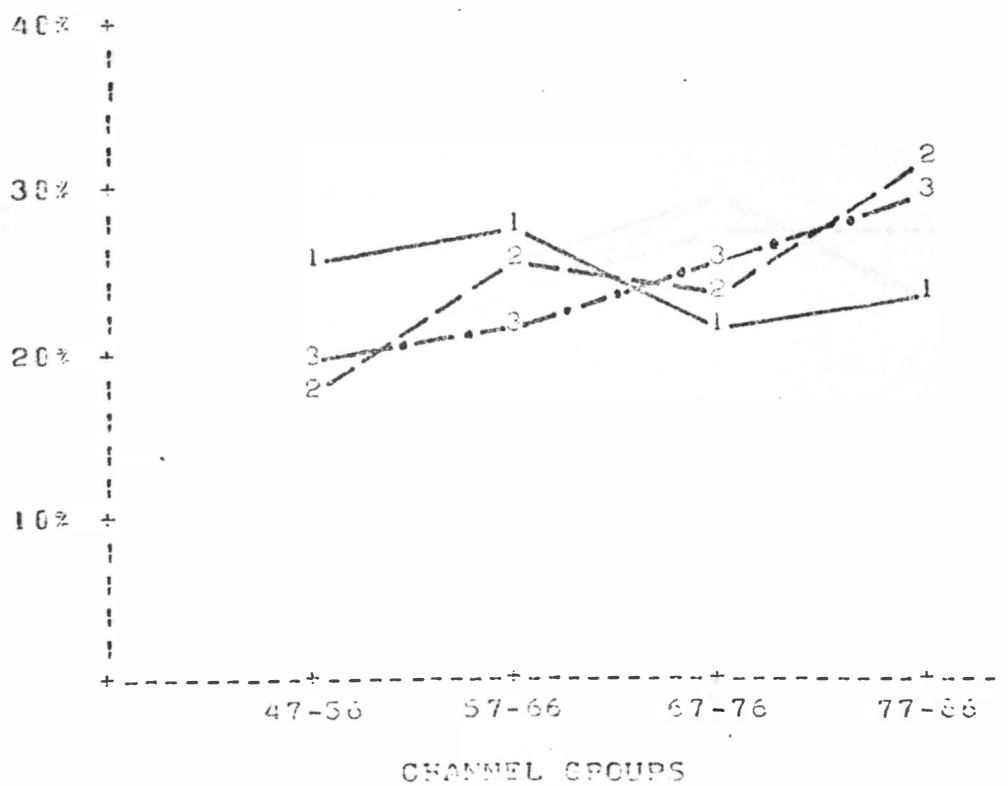

Fig. 32. Experiment 27 Grouped Data Analysis.

CHANNEL	47-56	57-66	67-76	77-86	TOTAL
1 CONTROL	828	1237	1415	1156	4635
DAY 6	17.9%	26.7%	30.5%	24.9%	100.0%
2 CONTROL	1493	1535	1900	1504	6532
DAY 8	22.9%	23.5%	29.1%	24.6%	100.0%
3 INFECTED	1519	1721	2117	1992	7349
DAY 8	20.7%	23.4%	28.8%	27.1%	100.0%
C6:C8	665	298	486	448	1897
	5.0%	-3.2%	-1.4%	-0.4%	29.0%
C6:I8	691	484	702	836	2714
	2.8%	-3.3%	-1.7%	2.2%	36.9%
C8:I8	26	186	217	388	817
	-2.2%	-0.1%	-0.3%	2.5%	11.1%

Fig. 33. Experiment 29 Grouped Data Analysis.

CHANNEL	47-56	57-66	67-76	77-86	TOTAL
1 CONTROL	704	777	942	1067	3490
DAY 6	20.2%	22.3%	27.0%	30.6%	100.0%
2 CONTROL	854	871	1366	1749	4841
DAY 8	17.6%	18.0%	28.3%	36.1%	100.0%
3 INFECTED	689	1377	1463	1684	5234
DAY 8	13.2%	26.3%	28.3%	32.2%	100.0%
C6:C8	150	94	426	682	1351
	-2.5%	-4.3%	1.3%	5.5%	27.9%
C6:I8	-15	600	541	617	1743
	-7.0%	4.1%	1.3%	1.6%	33.3%
C8:I8	-165	507	115	-65	392
	-4.5%	8.3%	0.1%	-3.9%	7.5%

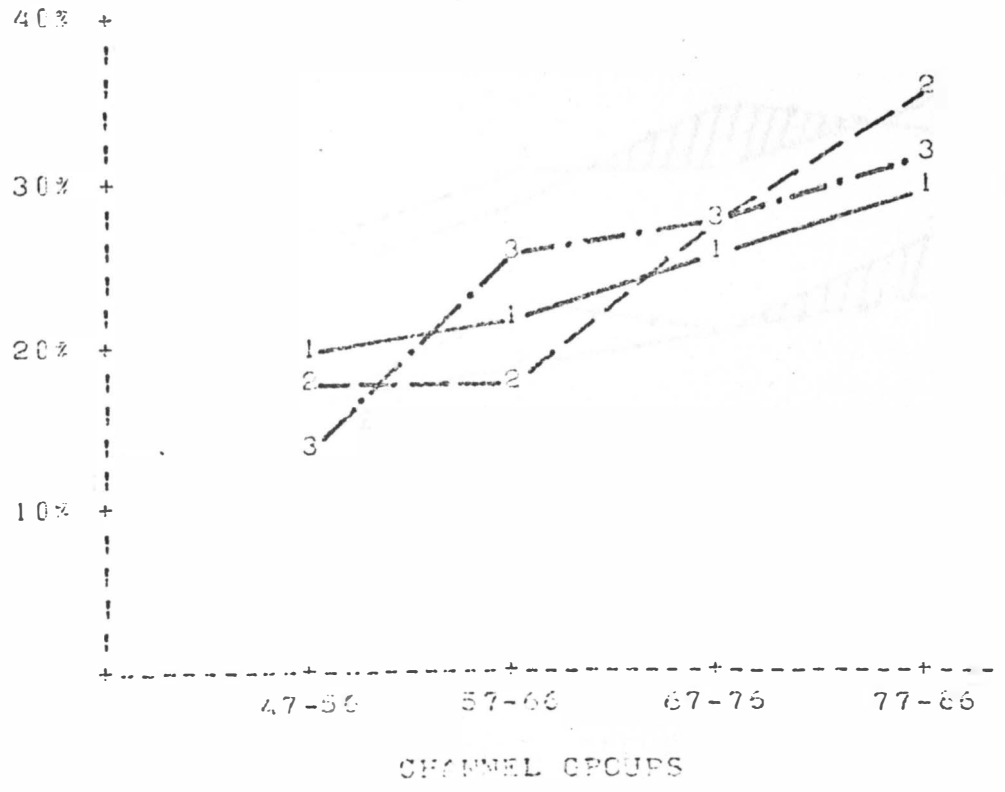

Fig. 34. Mean Grouped Data.

CHANNEL	47-56	57-66	67-76	77-86	TOTAL
1 CONTROL	27.0%	25.3%	24.6%	22.9%	4125
DAY 6	7.0%	3.7%	5.1%	4.3%	1165
2 CONTROL	20.8%	24.1%	24.6%	30.3%	6206
DAY 6	5.5%	6.0%	4.1%	4.1%	1065
3 INFECTED	19.6%	25.4%	27.1%	27.6%	6266
DAY 6	3.7%	3.3%	6.2%	5.2%	789
C6:C8	-6.2%	-1.1%	-0.1%	7.4%	2093
	9.7%	7.8%	7.1%	6.3%	1333
C6:I6	-7.2%	0.2%	2.3%	4.8%	2161
	5.7%	3.3%	4.0%	6.6%	860
C8:I8	-1.0%	1.3%	2.4%	-2.6%	78
	6.8%	6.1%	7.5%	4.2%	804

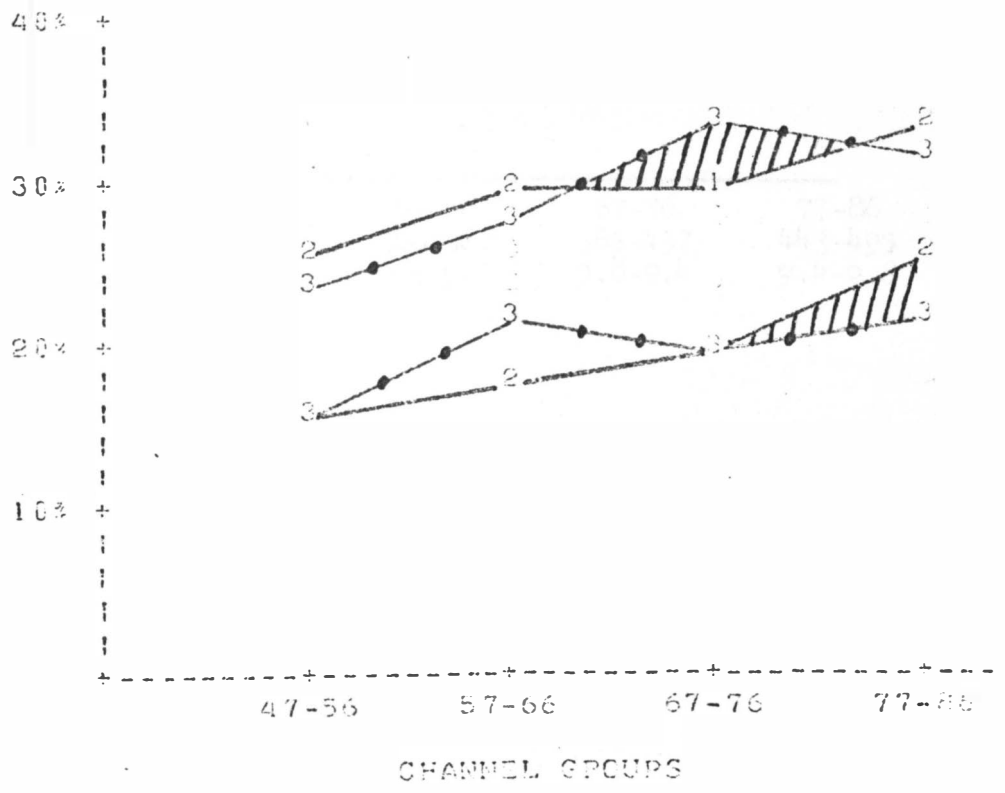

Fig. 35. Mean, Normalized Volume Profile.

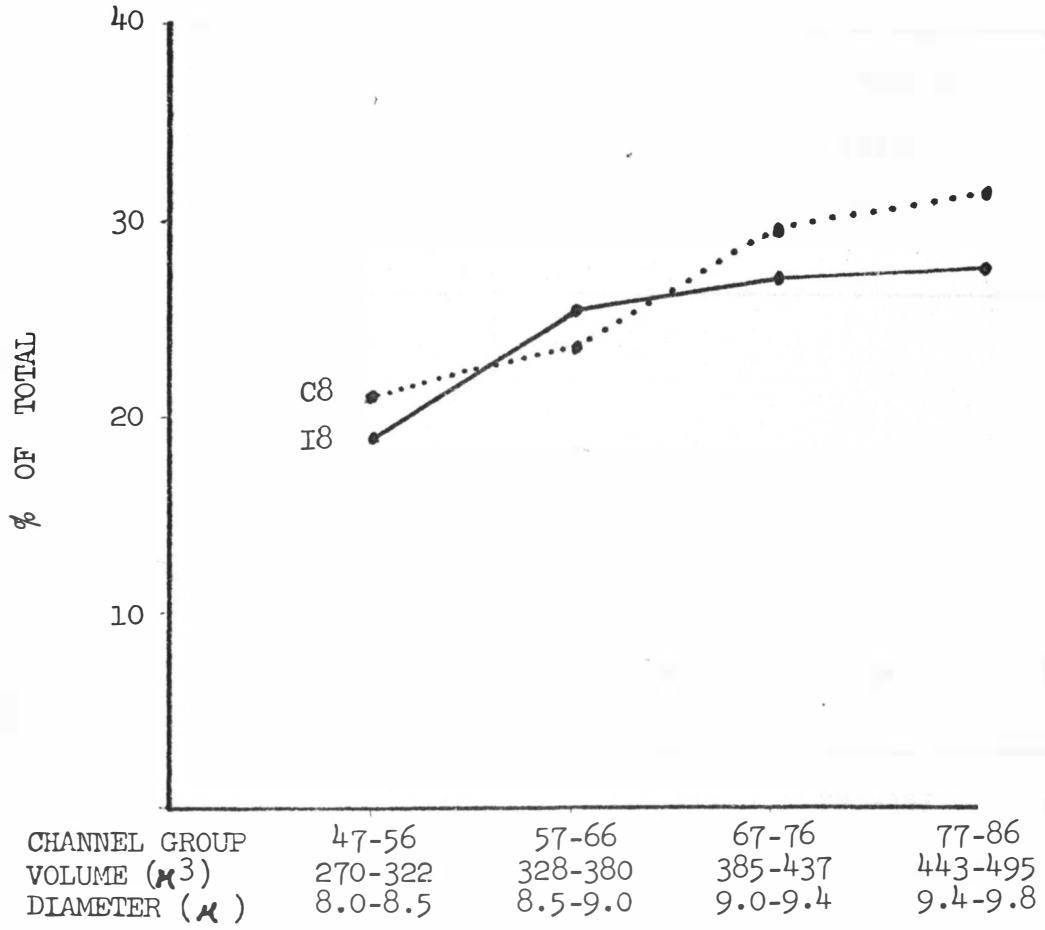

Table 8. Mean Channel Counts from Grouped Data.

	47-56	57-66	67-76	77-86	Total
C6	1122±486	1015±215	1032±346	955±326	4124
C8	1286±347	1440±375	1527±319	1880±404	6133
I8	1284±303	1642±220	1741±451	1774±365	6441

Table 9. Summary of Grouped Data Parameters.

	47-56	57-66	67-76	77-86
(μ^3) Volume	270-322	328-380	385-437	443-495
(μ) Diam.	8.0-8.5	8.56-8.99	9.0-9.42	9.46-9.82
$\bar{X}$ %C8	20.8±5.5	24.1±6.0	24.8±4.1	30.3±4.1
$\bar{X}$ %I8	19.8±3.7	25.4±3.3	27.1±6.2	27.6±5.2

Fig. 36. Volume Profile of Mean Channel Counts.

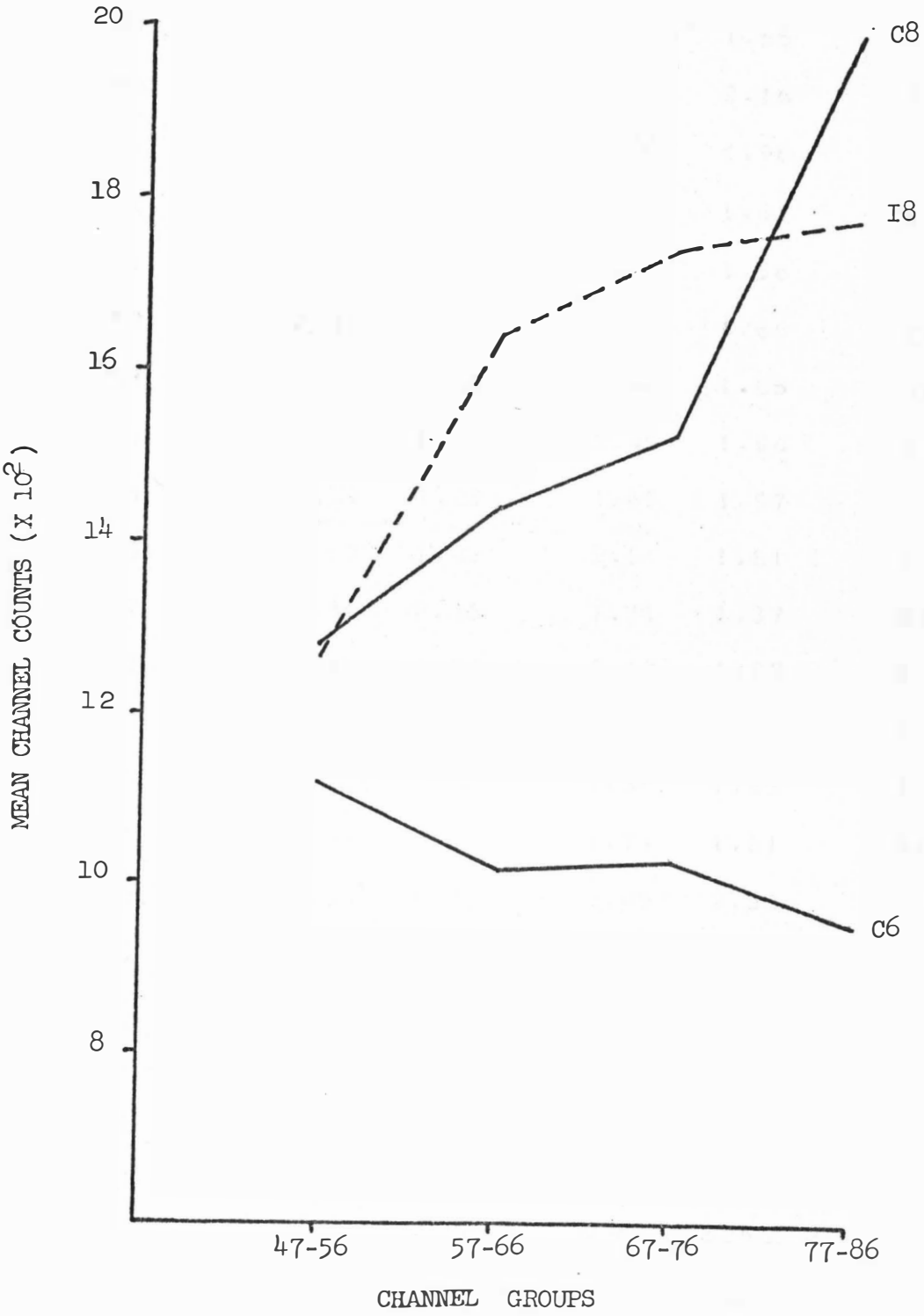

Table 10. Mean, Normalized Channel-by-Channel Data.

CHANNEL #	CONTROL DAYS		CONTROL DAYS		INFECTED DAYS	
	a	b				
47	2.13	2.10	1.25	1.55	0.19	0.32
48	4.35	2.95	2.52	2.16	3.60	3.08
49	2.41	1.90	1.32	0.98	1.23	1.33
50	1.36	2.29	1.53	1.51	2.37	1.98
51	3.28	2.33	1.59	1.56	2.51	2.25
52	2.14	2.38	2.14	1.66	1.47	1.81
53	1.95	1.40	1.14	1.65	2.05	1.49
54	3.04	1.71	2.45	1.94	0.90	0.90
55	1.59	1.68	1.65	1.97	2.17	1.16
56	0.97	1.42	2.64	1.81	1.40	1.50
57	3.34	2.86	1.71	1.37	2.31	1.83
58	1.45	1.53	2.13	1.97	2.09	2.15
59	2.40	1.93	2.26	1.44	2.73	1.94
60	0.80	1.54	1.34	1.63	1.93	1.34
61	3.97	2.88	1.79	1.81	0.86	1.10
62	0.98	1.77	2.45	2.53	2.14	1.74
63	2.64	2.40	1.76	1.55	2.16	2.44
64	1.32	1.23	1.62	2.05	2.89	2.48
65	2.92	2.01	2.67	2.05	2.67	2.41
66	1.69	1.82	1.71	1.65	1.95	2.61
67	2.56	2.32	2.70	2.45	2.43	2.39
68	2.51	2.51	2.01	2.34	3.22	1.93
69	1.92	1.55	2.00	1.87	2.57	2.31

Fig. 37. Mea

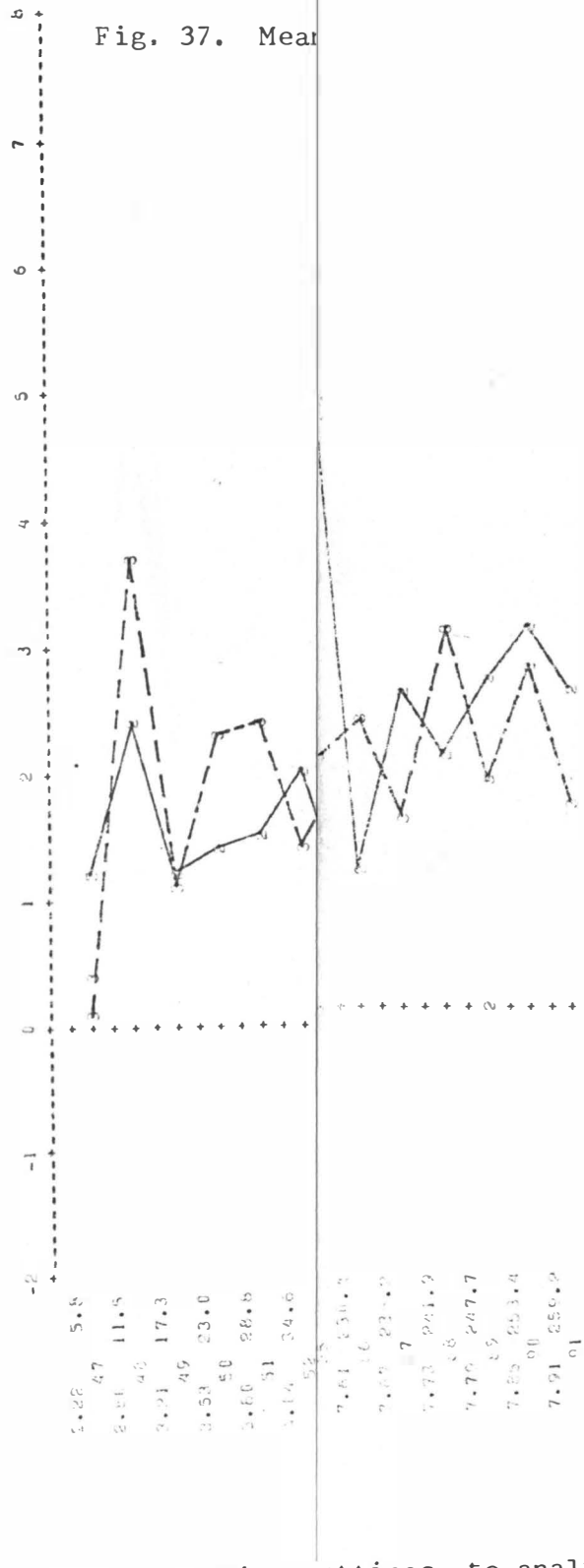

28S

ction

lls:

; RNase

iles.

are

ion

.on.

RNA

l.

ell

nined.

er

Counter machine settings, to analyze Coulter Counter data, and to plot volume profiles.

CONCLUSIONS

1. Aedes albopictus cell-specific RNA species were isolated; 28S 18S and 4S. All are single-stranded as determined by the action of RNase.
2. VEE-specific RNA species were isolated from infected Aal cells: "42S", "26S", and "20S".
3. The 20S species is RNase-resistant indicating its double-strandedness. This is possibly the RF. The 42S species is RNase sensitive, i.e. is single-stranded, probably progeny molecules. The data relative to the strandedness of the "26S" species are inconclusive.
4. A standard curve relating known Svedberg unit versus migration distance was determined.
5. Actinomycin D inhibits all A. albopictus cell RNA replication.
6. Both 6 and 48 hour post-infection samples contain the same RNA species. There is an increase in the amount of RNA labeled.
7. The volume range of A. albopictus was determined.
8. ISOTON was determined to have no effect on A. albopictus cell volume.
9. A growth curve of A. albopictus was prepared.
10. The precision of Coulter Counter volume profiles was determined. The variation is under 3%.
11. Computer programs were written to assist in choosing Coulter Counter machine settings, to analyze Coulter Counter data, and to plot volume profiles.

12. The volume range and resolution at all Coulter Counter machine settings were determined.

13. Various types of data analysis were developed to interpret volume profiles. These include profile prediction, channel-by-channel analysis, trend line analysis, normalized and grouped data analysis.

14. The volume range of cells most affected by VEE was reduced to 155.5 cubic microns to 241.9 cubic microns. In this range seven out of nine experiments show a consistent volume difference between control and infected cells.

APPENDIX

Table I. Enter or List Program.

```
10  COM A,Z,S,D$(32),DS(3,50)
20  DIM A$(5)
30  DISP     ENTER OR LIST:
40  INPUT A$
50  IF AS="ENTER" THEN 80
60  IF A$="LIST" THEN 340
70  GOTO 30
80  MAT D=ZER
90  DISP  "ENTER FILE FOR DATA STORAGE";
100 INPUT F
110 DISP "ENTER DATA DESCRIPTION <= 32CHAR";
120 INPUT D$
130 DISP "ENTER FIRST AND LAST THRESHOLD";
140 INPUT A,Z
150 DISP "ENTER THRESHOLD STEP ";
160 INPUT S
170 TO=1
180 FOR T=A  TO Z STEP S
190 DISP  "ENTER 3 COUNTS FOR T#";T;
200 INPUT D(1, TO),D(2, TO),D(3,TO)
210 TO=TO+1
220 NEXT T
230 DISP  "ENTER # OF CORRECTIONS";
240 INPUT C
250 FOR I=1 TO C
260 DISP "INPUT T#, READING#, & COUNT";
270 INPUT T,C,D(C,T/S)
280 NEXT I
290 STORE  DATA F
300 END
310 REM
320 REM:  LISTING SECTION
330 REM
340 DISP "LIST DATA ALSO";
350 INPUT A$
360 C1=0
370 IF A$="NO" THEN 390
380 C1=1
390 DISP "ENTER FIRST & LAST FILE FOR LIST";
400 INPUT FO,F9
410 L=60
420 FOR I+FO TO F9
430 LOAD  DATA I
440 LO=5+C1*(1+4*(INT((Z-A-1)/10)+1))
450 L=L+LO
460 IF L 60 THEN 510
470 L=LO
```

```
480 PRINT WBYTE12
490 WAIT 1234
500 PRINT LIN2
510 PRINT LIN2,SPA5,"FILE #";I
520 PRINT SPA5,DS
530 WRITE (15,540)A,Z
540 FORMAT 5X,"THRESHOLD",F3.0," TO",F3.0
550 IF C1=0 THEN 760
560 PRINT
570 T=A
580 PRINT TAB7;
590 FOR K=T TO T+10
600 WRITE (15,610)K;
610 FORMAT F6.0
620 IF K=Z THEN 640
630 NEXT K
640 PRINT
650 FOR J=1 TO 3
660 PRINT TAB7;
670 FOR K=T TO T+ 10
680 WRITE (15,690)D(J,K);
690 FORMAT F6.0
700 IF K=Z THEN 720
710 NEXT K
720 PRINT
730 NEXT J
740 T=T+11
750 IF T <=Z THEN 580
760 NEXT I
770 END
```

Table II. Coulter Counter Program.

```
10  COM A,Z,S,D$(32),DS(3,50)
20  REM:  COULTER COUNTER PROGRAM
30  DIM TS(9,50),CS(3,50),MS(3),SS(3)
40  DIM A$(5),C$(5),QS(110),PS(110)
50  DIM T$(160),H$(100),B$(3)
60  REM:  RUN SECTION
70  REM
80  X=0
90 C$= 12345
100 FOR I=1 TO 110
110 Q$(I,I)=
120 NEXT I
130 QS(1,1)="+"
140 DISP "ENTER TITLE: 5 LINES <=32 SPACES";
150 FOR I=1 TO 5
160 INPUT TX(I*32-31,I*32)
170 NEXT I
180 DISP "ENTER # OF DATA SETS: <=3";
190 INPUT N
200 DISP "DO YOU WANT CHANNEL DIFFERENCES";
210 INPUT B$
220 DISP "ENTER HEADINGS: <=20 SPACES";
230 FOR I=1 TO N
240 INPUT T$(L*20-19,I*20)
250 NEXT I
260 DISP "ENTER FIRST AND LAST THRESHOLD #";
270 INPUT A0,Z0
280 DISP "ENTER APERTURE SETTING ";
290 INPUT A8
300 DISP "ENTER ATTENUATION SETTING ";
310 INPUT A9
320 C4=0
330 DISP "DO YOU WISH TO SET THE SCALE ";
340 INPUT A$
350 IF A$="NO" THEN 420
360 C4=1
370 DISP "ENTER YMAX FOR CHANNEL PLOT ";
380 INPUT Y
390 IF B$="NO" THEN 420
400 DISP "ENTER YMIN,YMAX FOR DIFF. PLOT ";
410 INPUT Y0,Y9
420 FOR I=1 TO N
430 DISP "ENTER FILE # FOR DATA SET #";I;
440 INPUT S(I)
450 NEXT I
460 FOR I=1 TO N
470 LOAD  DATA S(I)
```

```
480 J=0
490 J9=(A0-A)/S
500 FOR J0=A0 TO Z0 STEP S
510 J=J+1
520 J9=(A0-A)/S
530 FOR K=1 TO 3
540 T(3*I-3+K,J)=D(K,J9)
550 NEXT K
560 NEXT J0
570 NEXT I
580 REM
590 REM COMPUTE CHANNEL COUNTS
600 REM
610 A=A0
620 Z=Z0
630 X=0
640 FOR I=1 TO N
650 T=0
660 FOR T0=A TO Z-1 STEP S
670 T=T+1
680 M1=(T(3*I-2,T)+T(3*I-1,T+T)3*I,T)/3
690 M2=(T(3*I-2,T+1)+T(3*I-1,T+1)+T(3*I,T+1))/3
700 C(I,T)=M1-M2
710 IF X >= C(I,T)  THEN730
720 X=C(I,T)
730 NEXT T0
740 NEXT I
750 REM
760 REM PRINT DATA
770 C=0
780 FOR C0=A TO Z STEP S
790 C=C+1
800 IF (C-1)/12=INT((C-1)/12) THEN 820
810 GOTO 840
820 GOSUB 2360
830 PRINT H$,LIN1
840 K=1
850 FOR I=1 TO N
860 C1=T(K,C)
870 C2=T(K+1,C)
880 C3=T(K+2,C)
890 M(I)=(C1+C2+C3)/3
900 S(I)=(((C1-M(I))↑2+(C2-M(I))↑2+(C3-M(I))↑2)/2)↑0.5
910 K=K+3
920 NEXT I
930 FOR I=1 TO N
940 WRITE (15,950)C0,T(3*I-2,C),M(I);
950 FORMAT F4.0,1X,2F6.0,3X
```

```
960 NEXT I
970 PRINT
980 FOR I=1 TO N
990 WRITE (15,1000)T(3*I-1,C),S(I);
1000 FORMAT 5X,F6.0,F6.1,3X
1010 NEXT I
1020 PRINT
1030 FOR I=1 TO N
1040 IF M(I)=0 THEN 1070
1050 S1=100*S(I)/M(I)
1060 GOTO 1080
1070 S1=0
1080 WRITE (15,1090)T(3*I,C),S1;
1090 FORMAT 5X,F6.0,F5.1,"%",3X
1100 NEXT I
1110 PRINT
1120 IF CO=Z THEN 1230
1130 FOR I=1 TO N
1140 IF I=1 TO N
1150 IF D$="NO" THEN 1190
1160 WRITE (15,1170)C(I,C),C(I,C)-C(1,C);
1170 FORMAT 2X,2Ft.0,6X
1180 GOTO 1210
1190 WRITE (15,1200)C(I,C);
1200 FORMAT 2X,F6.0,12X
1210 NEXT I
1220 PRINT
1230 NEXT CO
1230 REM
1250 REM PLOT CHANNEL COUNTS
1260 REM
1270 GOSUB 2360
1280 PRINT LIN3
1290 IF C4=1 THEN 1310
1300 Y=X
1310 Y=Y/100
1320 PRINT TAB15,"O";
1330 FOR J-1 TO 10
1340 WRITE (15,1350)J*Y*10;
1350 FORMAT 2X,F8.0
1360 NEXT J
1370 PRINT
1380 WAIT 333
1390 PRINT TAB15,"+";
1400 FOR I=1 TO 10
1410 WRITE (15,1420)"---------+";
1420 FORMAT F1.0
1430 NEXT I
1440 PRINT
1450 C=0
```

```
1460 FOR CO=A TO (Z-1) STEP S
1470 C=C+1
1480 P$=QS
1490 M=0
1500 FOR I=1 TO N
1510 P=C(I,C)/Y+1
1520 IF P >= 1 THEN 1540
1530 P=1
1540 PS(P,P)=C$(I,I)
1550 IF M>P THEN 1570
1560 M=P
1570 NEXT I
1580 V=CO*A8*A9*0.09
1590 D=((6*V)/PI)↑(1/3)
1600 WRITE (15,1610)D,V
1610 FORMAT F7.2,F7 1,1X,"+"
1620 WRITE (15,1630)CO,PS(1,M)
1630 FORMAT 6X,F3.0,6X,F1.0
1640 NEXT CO
1650 V=CO*A8*A9*0.09
1660 D=((6*V)/PI)↑(1/3)
1670 WRITE (15,1610)D,V
1680 IF BS="NO" THEN 2350
1690 REM
1700 REM FIND DIFFERENCES FROM CONTROL
1710 X=Y=0
1720 FOR I=2 TO N
1730 C=0
1740 FOR CO=A TO (Z-1) STEP S
1750 C=C+1
1760 C(I,C)=C(I,C)=C(1,C)
1770 NEXT CO
1780 NEXT I
1790 FOR I=1 TO (N-1)
1800 C=0
1810 FOR CO=A TO (Z-1) STEP S
1820 C=C+1
1830 C(I,C)=C(I+1,C)
1840 IF X >= C(I,C) THEN 1860
1850 X=C(I,C)
1860 IF Y <= C(I,C)  THEN 1880
1870 Y=C(I,C)
1880 NEXT CO
1890 NEXT I
1900 IF C4=1 THEN 1930
1910 YO=Y
1920 Y9=X
1930 S1=(Y9-YO)/100
1940 REM
1950 REM PLOT DATA
```

```
1960 REM
1970 GOSUB 2360
1980 PRINT LIN3
1990 Q=ABS(YO/S1)+1
2000 Q$(1,1)="+"
2010 Q$(Q,Q)="+"
2020 PRINT TAB6;
2030 FOR J=0 TO 100 STEP 10
2040 WRITE (15,2050)YO+J*S1;
2050 FORMAT 2X,F8.0
2060 NEXT J
2070 PRINT
2080 PRINT TAB14,"+";
2090 FOR I=1 TO 10
2100 WRITE (15,2110)"--------+";
2110 FORMAT F1.0
2120 NEXT I
2130 PRINT
2140 C=0
2150 FOR CO=A TO (Z-1) STEP S
2160 C=C+1
2170 P$=Q$
2180 M=Q
2190 FOR I=1 TO (N-1)
2200 P=(C(I,C)/S1)+Q
2210 P$(P,P)=C$(I,I)
2220 IF M>P THEN 2240
2230 M=P
2240 NEXT I
2250 V=CO*A8*A9*0.09
2260 D=((6*V)/PI)↑(1/3)
2270 WRITE (15,2280)D,V
2280 FORMAT F7.2,F7.1,1X"+"
2290 WRITE (15,2300)CO,P$(1,M)
2300 FORMAT 6X,F3.0,6X,F1.0
2310 NEXT CO
2320 V=CO*A8*A9*0.09
2330 D=((6*V)/PI)↑(1/3)
2340 WRITE (15,2280)D,V
2350 END
2360 PRINT WBYTE12
2370 WAIT 3333
2380 PRINT LIN3
2390 FOR I=1 TO 5
2400 PRINT SPA5,T$(I*32-31,I*32)
2410 NEXT I
2420 PRINT
2430 RETURN
```

Table III. Prediction Program.

```
10 COM A,Z,S,D$(32),DS(3,50)
20 REM: PREDICTION PROGRAM
30 DIM TS(6,50),CS(2,50),MS(2),SS(2)
40 DIM A$(5),C$(5),Q$(105),P$(105)
50 DIM T$(160),H$(100),B$(3)
60 DIM E$(5),F$(5)
70 MAT C=ZER
80 REM:  RUN SECTION
90 REM
100 X=0
110 C$="12345"
120 FOR I=1 TO 105
130 Q$(I,I )=
140 NEXT I
150 Q$(1,1)="+"
160 DISP  ENTER TITLE:  5 LINES < =32 SPACES";
170 FOR I=1 TO 5
180 INPUT T$(I*32-31,I*32)
190 NEXT I
200 DISP "ENTER # OF DATA SETS: < =5 ";
210 INPUT N
220 DISP "ENTER HEADINGS: < =20 SPACES ";
230 FOR I=1 TO N
240 INPUT H$(I*20-19,I*20)
250 NEXT I
260 DISP "ENTER FIRST AND LAST THRESHOLD # ";
270 INPUT A0,Z0
280 DISP "ENTER APERTURE SETTING ";
290 INPUT A8
300 DISP "ENTER ATTENUATION SETTING";
310 INPUT A9
320 DISP "DO YOU WISH DATA PRINTOUT ";
330 INPUT F$
340 DISP "DO YOU WISH A PREDICTION PLOT";
350 INPUT E$
360 IF E$="NO" THEN 410
370 DISP "INPUT P.I. TIME";
380 INPUT P1
390 DISP "INPUT GENERATION TIME (HRS.)";
400 INPUT G1
410 C4=0
420 DISP "DO YOU WISH TO SET THE SCALE";
430 INPUT A$
440 IF A$="NO" THEN 480
450 C4=L
460 DISP "ENTER YMAX FOR CHANNEL PLOT";
```

```
470 INPUT Y
480 FOR I=1 TO N
490 DISP "ENTER FILE # FOR DATA SET #";I;
500 INPUT S(I)
510 NEXT I
520 FOR I=1 TO N
530 LOAD  DATA S(I)
540 J=0
550 J9=(A0-A)/S
560 FOR J0=A= TO Z0 STEP S
570 J=J+1
580 J9=J9+1
590 FOR K=1 TO 3
600 T(3*L-3+K,J)=D(K,J9)
610 NEXT K
620 NEXT J0
630 NEXT I
640 REM
650 REM COMPUTE CHANNEL COUNTS
660 REM
670 A=A0
680 Z=Z0
690 X=0
700 FOR I=1 TO N
710 T=0
720 FOR T0=A TO Z-1 STEP S
730 T=T+1
740 M1=(T(3*I-2,T)+T(3*I-1,T)+T(3*I,T))/3
750 M2=(T(3*I-2,T+1)+T(3*I-1,T+1)+T(3*I,T+1))/3
760 C(I,T)=M1-M2
770 IF X >=C(I,T)THEN 790
780 X=C(I,T)
790 NEXT T0
800 NEXT I
810 REM
820 IF F$="NO" THEN 1330
830 REM PRINT DATA
840 C=0
850 FOR C0=A TO Z STEP S
860 C=C+1
870 IF (C-1)/12=INT((C-1)/12) THEN 890
880 GOTO 910
890 GOSUB 1950
900 PRINT H$,LIN1
910 K=1
920 FOR I=1 TO N
930 C1=T(K,C)
940 C2=T(K+1,C)
950 C3=T(K+2,C)
```

```
960 M(I)=(C1+C2+C3)/3
970 S(I)=(((C1-M(I))↑2+(C2-M(I))↑2+(C3-M(I))↑2)/2)↑0.5
980 K=K+3
990 NEXT I
1000 FOR I=1 TO N
1010 WRITE (15,1020)CO,T(3*I-2,C),M(I);
1020 FORMAT F4.0,1X,2F6.0,3X
1030 NEXT I
1040 PRINT
1050 FOR I=1 TO N
1060 WRITE (15,1070)T(3*I-1,C),S(I);
1070 FORMAT 5X,F6 0,F6.1,3X
1080 NEXT I
1090 PRINT
1100 FOR I=1 TO N
1110 IF M(I)=0 THEN 1140
1120 S1=100*S(I)/M(I)
1130 GOTO 1150
1140 S1=0
1150 WRITE (1r,1160)T(3*I,C),S1;
1160 FORMAT 5X,F6.0,F5.1,"%",3X
1170 NEXT I
1180 PRINT
1190 IF CO=Z THEN 1300
1200 FOR I=1 TO N
1210 IF I=1 THEN 1260
1220 IF D$="NO" THEN 1260
1230 WRITE (15,1240)C(I,C),C(I,C)=C(1,C);
1240 FORMAT 2X,2F6.0,6X
1250 GOTO 1280
1260 WRITE (15,1270)C(I,C);
1270 FORMAT 2X,F6.0,12X
1280 NEXT I
1290 PRINT
1300 NEXT CO
1310 IF D$="NO" THEN 1490
1320 REM PREDICTION CALCULATIONS
1330 C=0
1340 FOR CO=A TO Z-1 STEP S
1350 C=C+1
1360 NO=C(1,C)*2↑(INT(L/G1))
1370 IF X>NO THEN 1390
1380 X=NO
1390 V=(CO+0.5)*A8*A9*0.09
1400 V2=(V/G1)*((P1/G1)-(INT(PL/GL)))*(G1)/(2↑INT(P1/G1))+V
1410 C1=S*INT(((V2/(A8*A9*0.09)+0.5)/S))-AO+1
1420 IF C1 50 THEN 1450
1430 C(2,C1)= C(2,C1 +NO)
1440 NEXT CO
```

```
1450 N=N+1
1460 REM
1470 REM PLOT CHANNEL COUNTS
1480 REM
1490 GOSUB 1950
1500 PRINT LIN3
1510 IF C4=1 THEN 1530
1520 Y=X
1530 Y=Y/100
1540 PRINT TAB15,")";
1550 FOR J=1 TO 10
1560 WRITE (15,1570)J*Y*10;
1570 FORMAT 2X,F8.0
1580 NEXT J
1590 PRINT
1600 WAIT 333
1610 PRINT TAB15,"+";
1620 FOR I=1 TO 10
1630 WRITE (15,1640)"--------+";
1640 FORMAT F1.0
1650 NEXT I
1660 PRINT
1670 C=0
1680 FOR CO=A TO (Z-1) STEP S
1690 C=C+1
1700 P$=Q$
1710 M=0
1720 FOR I=1 TO N
1730 P=C(I,C)/Y+1
1740 IF P <= 1 THEN 1760
1750 P=1
1760 IF P <= 100 THEN 1790
1770 P$(102,102)="$"
1780 P=103
1790 P$(P,P)=C$(I,I)
1800 IF M>P THEN 1820
1810 M=P
1820 NEXT I
1830 V=CO*A8*A9*0.09
1840 D=((6*V)/PI)↑(1/3)
1850 WRITE (15,1860)D,V
1860 FORMAT F7.2,F7.1,1X,"+"
1870 WRITE (15,1880)CO,P$(1,M)
1880 FORMAT 6X,F3.0,6X,F1.0
1890 NEXT CO
1900 V=CO*A8*A9*0.09
1910 D=((6*V)/PI)↑(1/3)
1920 WRITE (15,1860)D,V
1930 REM
```

```
1940 END
1950 PRINT WBYTE12
1960 WAIT 3333
1970 PRINT LIN3
1980 FOR I=1 TO 5
1990 PRINT SPA5,T$( I*32-31,I*32 )
2000 NEXT I
2010 PRINT
2020 RETURN
```

Table IV. Theoretical Coulter Counter Aperture and Attenuation Calculation Program.

```
10 DIM Q(1,10)
20 DISP "INPUT ATTENUATION VALUES";
30 INPUT Q(1,1),Q(1,2),Q(1,3),Q(1,4),Q(1,5),Q(1,6),Q(1,7),Q(1,8),
     Q(1,9),Q(1,10)
40 PRINT "THEORETICAL CALCULATIONS OF BEST ATTENUATION AND THRESHOLD
     SETTINGS ..
45 PRINT "ON THE COULTER MODEL F FOR A 70 MICRON NOSEPIECE..."
50 PRINT "BASED ON THE EQUATION B=V*I/K*T WHERE:"
60 PRINT "     B=ATTENUATION"
70 PRINT "     K=A CALCULATED CONSTANT (5.3949E-4)"
80 PRINT "     V=VOLUME(0-20000u3 IN INCREMENTS OF 1000)"
90 PRINT "     T=CHANNEL NO. i. e THRESHOLD SETTING(0-100)"
100 PRINT"     I=APERTURE CURRENT(FOR SETTINGS 1,2,4,8,16,32,64,128,
          256,512)"
110 PRINT
120 PRINT
130 PRINT TAB5"NOTE: TO LIST ALL POSSIBLE VALUES OF B WOULD TAKE
          SEVERAL DAYS.."
140 PRINT TAB5"THEREFORE ONLY THOSE VALUES AVAILABLE ON THE COULTER
          COUNTER."
150 PRINT TAB5"ARE LISTED ie ONLY THOSE CORRESPONDING TO 0.12500+-
          0.00500"
160 PRINT TAB5"0.17700+-0.00500,0.250+-0.00500,0.354+-0.005000,0.500+
          -0.00500"
170 PRINT TAB5"0.70700+-0.00500,1.00000+-0.05000,2.00000+-0.05000,
          4.00000+-0.05"
180 PRINT TAB5"8.00000+-0.050000"
190 FOR A=0 TO 512 STEP A*2
200 PRINT
210 PRINT
220 PRINT
230 PRINT "APERTURE="A"
240 PRINT
250 PRINT
260 PRINT
270 WRITE (15,280)
280 FORMAT 3X,"VOL.",7X,"T(0-100)",8X,"ATT."
290 PRINT
300 PRINT
310 DATA 6E-03,3E-03,1.5E-03,7.5E-04,3.75E-04,1.875E-04,9.375E-05,
     4.687E-05
320 DATA 2.343E-05,1.171E-05
330 READ I
340 K=5.3949E-04
350 FOR V=100 TO 1000 STEP 10
```

```
360 FOR T=1 TO 100
370 B=(V*I)/(K**T)
380 IF B>Q(1,1)-0.005 AND B<Q(1,1)+0.005 THEN 490
390 IF B>Q(1,2)-0.005 AND B<Q(1,2)+0.005 THEN 490
400 IF B>Q(1,3)-0.005 AND B<Q(1,3)+0.005 THEN 490
410 IF B>Q(1,4)-0.005 AND B<Q(1,4)+0.005 THEN 490
420 IF B>Q(1,5)-0.005 AND B<Q(1,5)+0.005 THEN 490
430 IF B>Q(1,6)-0.005 AND B<Q(1,6)+0.005 THEN 490
440 IF B>Q(1,7)-0.05 AND B<Q(1,7)+0.05 THEN 490
450 IF B>Q(1,8)-0.05 AND B<Q(1,8)+0.05 THEN 490
460 IF B>Q(1,9)-0.05 AND B<Q(1,9)+0.05 THEN 490
470 IF B>Q(1,10)-0.05 AND B<Q(1,10)+ 0.05 THEN 490
480 GOTO 510
490 WRITE (15,500)V,T,B
500 FORMAT F7.0,3X,F10.0,8X,F10.5
510 NEXT T
520 NEXT V
530 NEXT A
540 END
```

Table V. Coulter Counter Averaging Program.

```
10 COM A,Z,S,D$(32),DS(3,50)
20 REM:  C.C. AVERAGING
30 DIM CS(9,50),T$(160),C$(5)
40 DIM Q$(101),P$(101),FI(20,3)
50 REM:  RUN SECTION
60 REM
70 C$="12345"
80 MAT C=ZER
90 FOR I=1 TO 101
100 Q$(I,I)=" "
110 NEXT I
120 Q$(21,21)="+"
130 DISP "ENTER TITLE: 5 LINES   =32 SPACES";
140 FOR I=1 TO 5
150 INPUT T$(I*32-31,I*32)
160 NEXT I
170 DISP "ENTER # OF DATA SETS:  =3  ";
180 INPUT N
190 DISP "ENTERAPERTURE SETTING ";
200 INPUT A 8
210 DISP "ENTER ATTENUATION SETTING";
220 INPUT A9
230 FOR I=1 TO N
240 DISP "ENTER FILE #'S FOR DATA SET #";I;
250 INPUT F(I,1),F(I,2),F(I,3)
260 NEXT I
270 FOR I=1 TO N
280 FOR J=1 TO 3
290 LOAD  DATA F(I,J)
300 DISP F(I,J)
310 WAIT 3000
320 S=0
330 M1=(D(1,1)+D(2,1)+D(3,1))/3
340 FOR T=1 TO 45
350 M2=(D(1,T+1)+D(2,T+1)+D(3,T+1))/3
360 M=M1-M2
370 IF M<0 THEN 410
380 D(1,T)=M
390 S=S+M
400 GOTO 420
410 D(1,T)=0
420 M1=M2
430 NEXT T
440 FOR T=1 TO 45
450 C(J,T)=C(J,T)+100*D(1,T)/S
```

```
460 C(J+3,T)=C(J+3,T)+((100*D(1,T))/S)↑2
470 NEXT T
480 NEXT J
490 NEXT I
500 REM: CALCUIATE MEANS
510 FOR T=1 TO 46
520 FOR A=1 TO 3
530 C(A,T)=C(A,T)/N
540 C(A+3,T)=((C(A+3,T)/N-C(A,T)↑2)*(N/(N-1)))↑0.5
550 NEXT A
560 NEXT T
570 REM
580 REM PRINT DATA
590 GOSUB 1150
600 PRINT "CHANNEL #   CONTROL DAY6   CONTROL DAY8   INFECTED DAY8",
      LIN2
610 FOR C=1 TO 45
620 WRITE (15,630)C+46;
630 FORMAT F6.0,2X
640 FOR I=1 TO 3
650 WRITE (15,660)C(I,C),C(I+3,C);
660 FORMAT F10.2,F7.2
670 NEXT I
680 PRINT LIN1
690 NEXT C
700 REM
710 REM PLOT CHANNEL COUNTS
720 REM
730 GOSUB 1150
740 PRINT LIN3
750 PRINT TAB6;
760 FOR J=-2 TO 8
770 WRITE (15,780)J;
780 FORMAT 2X,F8.0
790 NEXT J
800 PRINT
810 WAIT 333
820 PRINT TAB15,"+";
830 FOR I=1 TO 10
840 WRITE (15,850)"---------+";
850 FORMAT F1.0
860 NEXT I
870 PRINT
880 FOR C=1 TO 45
890 P$=Q$
900 M=0
910 FOR I=2 TO 3
920 FOR J=-1 TO 1
930 P=(C(I,C)+J*C(I+3,C)+C)*10
```

```
940 IF P>= 1 THEN 970
950 P=1
960 GOTO 990
970 IF P<= 100 THEN 990
980 P=100
990 P$(P,P)=C$(I,I)
1000 IF M>P THEN 1020
1010 M=P
1020 NEXT J
1030 NEXT I
1040 V=C*A8*A90.09
1050 D=((6*V)/PI)↑(1/3)
1060 WRITE (15,1070)D,V
1070 FORMAT F7.2,F7.1,21X,"+"
1080 WRITE (15,1090)C+46,P$(1,M)
1090 FORMAT 6X,F3.0,6X,F1.0
1100 NEXT C
1110 V=CO*A8*A9)0.09
1120 D=((6*V)/PI)↑(1/3)
1130 WRITE (15,1070)D,V
1140 END
1150 PRINT WBYTE12
1160 WAIT 3333
1170 PRINT LIN3
1180 FOR I=1 TO 5
1190 PRINT SPA5,T$(I*32-31,I*32)
1200 NEXT L
1210 PRINT
1220 RETURN
```

Table VI. Coulter Counter Grouping Program.

```
10 COM A,Z,S,D$(32),DS(3,50)
20 REM:  C.C. GROUPING PGM
30 DIM T(12,5),F(10,5),M(5),S(12,5)
40 DIM T$(60),C$(6),A$(40),B$(40)
50 DIM P$(120),Q$(96)
60 MAT S=ZER
70 C$=" 1 2 3"
80 FOR I=1 TO 40
90 B$(I,I)=" "
100 NEXT L
110 Q$="AVERAGED DATA AFTER GROUPING AND NORMALIZATION FOR EXPERI-
      MENT #'S"
120 T$="    CHANNEL    47-56    57-66    67-76    77-86    TOTAL"
130 P$="    CONTROL    DAY 6    CONTROL    DAY 8"
140 P$(41)="  INFECTED    DAY 8    C6:C8"
150 P$(81)="     C6:I8          C8:I8"
160 DISP "DO YOU WISH AVERAGED DATA (OCR1)";
170 INPUT F1
180 IF F1=0 THEN 210
190 DISP "ENTER EXPERIMENT#'S";
200 INPUT Q$(65)
210 DISP "ENTER # OF DATA SETS";
220 INPUT NO
230 FOR N=1 TO NO
240 DISP "ENTER DATA FILE #'S";
250 INPUT F(N,1),F(N,3),F(N,5)
260 NEXT N
270 FOR N=1 TO NO
280 MAT T=ZER
290 FOR I=1 TO 5 STEP 2
300 LOAD  DATA F(N,I)
310 IF F1=1 THEN 330
320 Q$((I-1)*16+1,I*16+16)=D$
330 M=-9
340 FOR J=1 TO 5
350 M=M+10
360 M(J)=(D(1,M)+D(2,M)+D(3,M))/3
370 NEXT J
380 FOR J=1 TO 4
390 T(I,J)=M(J)-M(J+1)
400 NEXT J
410 T(I,5)=M(1)-M(5)
420 NEXT I
430 FOR I=2 TO 6 STEP 2
440 FOR J=1 TO 5
450 T(I,J)=T(I-1,J)/T(I-1,5)*100
```

```
460 NEXT J
470 NEXT I
480 FOR I=1 TO 5
490 T(7,I)=T(3,I)-T(1,I)
500 T(8,I)=(T(4,I)-T(2,I))
510 T(9,I)=T(5,I)-T(1,I)
520 T(10,I)=(T(6,I)-T(2,I))
530 T(11,I)=T(5,I)-T(3,I)
540 T(12,I)=(T(6,I)-T(4,I))
550 NEXT I
560 T(8,5)=(T(3,5)-T(1,5))/T(3,5)*100
570 T(10,5)=(T(5,5)-T(1,5))/T(5,5)*100
580 T(12,5)=(T(5,5)-T(3,5))/T(5,5)*100
590 IF F1=0 THEN 750
600 FOR I=2 TO 12 STEP 2
610 FOR J=1 TO 4
620 S(I-1,J)=S(I-1,J)+T(I,J)
630 S(I,J)=S(I,J)+T(I,J)↑2
640 NEXT J
650 S(I-1,5)=S(I-1,5)+T(I-1,5)
660 S(I,5)=S(I,5)+T(I-1,5) 2
670 NEXT I
680 IF N<NO THEN 1460
690 FOR I=1 TO 11 STEP 2
700 FOR J=1 TO 5
710 T(I,J)=S(I,J)/N
720 T(I+1,J)=((S(I+1,J)/N-T(I,J)↑2)*(N/(N-1)))↑0.5
730 NEXT J
740 NEXT I
750 PRINT WBYTE12
760 WAIT 1234
770 PRINT LIN3
780 FOR I=1 TO 3
790 PRINT Q$(32*I-31,32*I)
800 NEXT I
810 PRINT LIN2,T$,LIN1
820 WAIT 333
830 FOR R=1 TO 12
840 WRITE (15,850)P$(R*10-9,R*10);
850 FORMAT F1.0
860 FOR C=1 TO 5
870 IF F1=1 AND C<5 THEN 910
880 WRITE (15,890)T(R,C);
890 FORMAT F10.0
900 GOTO 930
910 WRITE (15,920)T(R,C),"%";
920 FORMAT F9.1,F1.0
930 NEXT C
940 PRINT
950 WAIT 333
```

```
960 R=R+1
970 WRITE (15,850)P$( R*10-9,R*10);
980 FOR C=1 TO 5
990 IF F1=1 AND C=5 THEN 1030
1000 WRITE (15,1010)T(R,C),"%";
1010 FORMAT F9.1,F1.0
1020 GOTO 1040
1030 WRITE (15,890)T(R,C);
1040 NEXT C
1050 PRINT LIN1
1060 NEXT R
1070 PRINT LIN1
1080 FOR CO=40 TO 2 STEP -10
1090 FOR C=CO TO CO-8 STEP -2
1100 M=L
1110 A$=B$
1120 FOR I=2 TO 6 STEP 2
1130 FOR J=1 TO 4
1140 IF F1=1 THEN 1170
1150 IF T(I,J) <= C+1 AND T(I,J)>C-1 THEN 1210
1160 GOTO 1250
1170 IF T(I-1,J)+T(I,J) <= C+1 AND T(I-1,J)+T(I,J)>C-1 THEN 1210
1180 IF T(I-1,J) <=C+1 AND T(I-1,J)>C-1 THEN 1210
1190 IF T(I-1,J)-T(I,J) <= C+1  AND T(I-1,J)-T(I,J)>C-1 THEN 1210
1200 GOTO 1250
1210 M1=10*J
1220 IF M>M1 THEN 1240
1230 M=M1
1240 A$(M1,M1)=C$(I,I)
1250 NEXT J
1260 NEXT I
1270 IF C=CO THEN 1300
1280 PRINT TAB10,NBYTE124;
1290 GOTO 1320
1300 WRITE (15,1310)C;
1310 FORMAT 5X,F3.0"% +"
1320 PRINT A$(1,M)
1330 NEXT C
1340 NEXT CO
1350 PRINT TAB10,"+";
1360 FOR I=1 TO 4
1370 FOR J=1 TO 9
1380 PRINT "-";
1390 NEXT J
1400 PRINT "+";
1410 NEXT I
1420 PRINT "---"
1430 WAIT 333
1440 PRINT TAB14,T$(12,51)
```

```
1450 PRINT LIN1,TAB25,"CHANNEL GROUPS"
1460 NEXT N
1470 END
```

LITERATURE CITED

1. Acheson, N. H., and I. Tamm. 1967. Replication of Simliki Forest virus: An electron microscopic study. Virology 32: 128-143.

2. Anderson, E. C., and D. F. Peterson. 1967. Cell growth and division. II. Experimental studies of cell volume distributions in mammalian suspension cultures. Biophys. J. 7: 353-364.

3. Arif, B. M., and P. Faulkner. 1972. Genome of Sindbis virus. J. Virol. 9: 102-109.

4. Ball, F. R., and E. L. Medzon. 1973. Sedimentation changes of L cells in a density gradient early after infection with Vaccinia virus. J. Virol. 12: 588-593.

5. Baltimore, D., and R. M. Franklin. 1962. Preliminary data on a virus-specific enzyme system responsible for the synthesis of viral RNA. Biochem. Biophys. Res. Commun. 9: 388-392.

6. Baltimore, D., and M. Girard. 1966. An intermediate in the synthesis of poliovirus RNA. Proc. Nat. Acad. Sci. U. S. A. 56: 741-748.

7. Beck, C. E., and R. W. G. Wyckoff. 1938. Venezuelan equine encephalomyelitis. Science 88: 530.

8. Bell, G. I., and E. C. Anderson. 1967. Cell growth and division. I. A mathematical model with applications to cell volume distribution in mammalian suspension cultures. Biophys. J. 7: 329-351.

9. Bhat, U. K. M., and K. R. P. Singh. 1969. Structure and development of vesicles in larval tissue culture of *Aedes aegypti* (L.). J. Med. Entomol. 6: 71-74.

10. Bishop, D. H. J., J. R. Claybrook, and S. Spiegelman. 1967. Electrophoretic separation of viral nucleic acids on polyacrylamide gels. J. Mol. Biol. 26: 373-387.

11. Bishop, M. J., D. F. Summers, and L. Levintow. 1965. Characterization of ribonuclease-resistant RNA from poliovirus-infected HeLa cells. Proc. Nat. Acad. Sci. U. S. A. 54: 1273-1281.

12. Borst, P., and C. Weissmann. 1965. Replication of viral RNA. VIII. Studies on the enzymatic mechanism of replication of MS2 RNA. Proc. Nat. Acad. Sci. U.S.A. 54:982-987.

13. Buckley, S. M. 1969. Susceptibility of the Aedes albopictus and A. aegypti cell lines to infection with arboviruses. Proc. Soc. Exp. Biol. Med. 131: 625-630.

14. Burrell, C. J., E. M. Martin, and P. D. Cooper. 1970. Post-translational cleavage of virus polypeptides in arbovirus-infected cells. J. Gen. Virol. 6: 319-323.

15. Bykovsky, A. F., F. I. Yershov, and V. M. Zhdanov. 1969. Morphogenesis of Venezuelan equine encephalomyelitis virus. J. Virol. 4: 496-504.

16. Cartwright, K. L., and D. C. Burke. 1970. Virus nucleic acids formed in chick embryo cells infected with Semliki Forest virus. J. Gen. Virol. 6: 231-248.

17. Casals, J. 1957. The arthropod-borne group of animal viruses. Trans. N. Y. Acad. Sci. Ser. 2. 19: 219-235.

18. Casals, J., and L. V. Brown. 1954. Hemagglutination with arthropod-borne viruses. J. Exp. Med. 99:429-449.

19. Casals, J., and D. H. Clarke. 1965. Arboviruses: Group A, p. 583. In F. L. Horsfall, and I. Tamm (eds.). Viral and rickettsial infections of man. J. B. Lippincott Company, Philadelphia, Montreal.

20. Chappell, W. A., C. H. Calisher, R. F. Toole, K. C. Maness, D. R. Sasso, and B. E. Henderson. 1971. Comparison of three methods to isolate Dengue virus type 2. Appl. Microbiol. 22: 1100-1103.

21. Converse, J. L., and S. C. Nagle. 1967. Multiplication of yellow fever virus in insect tissue cell cultures. J. Virol. 1:1096-1097.

22. Cook, J. S. 1967. Size determination of human erythrocytes with an electronic counter. J. Lab. and Clin. Med. 70: 849-856.

23. Coulter, W. H. 1953. U. S. Patent No. 2,656,508.

24. Coulter Counter instruction and service manual for the Coulter Counter Model F. 1970. Coulter Electronics, Inc. Hialeah, Florida 33010.

25. Davey, M. W., D. P. Dennett, and L. Dalgarno. 1973. The growth of two Togaviruses in cultured mosquito and vertebrate cells. J. Gen. Virol. 20: 225-232.

26. Dobos, P., and P. Faulkner. 1969. Properties of 42S and 26S Sindbis viral ribonucleic acid species. J. Virol. 4: 429-438.

27. Dobos, P., and P. Faulkner. 1970. Molecular weight of Sindbis virus ribonucleic acid as measured by polyacrylamide gel electrophoresis. J. Virol. 6: 145-147.

28. Doi, R., A. Shirasaki, and M. Sasa. 1967. The mode of development of Japanese encephalitis virus in the mosquito Culex tritaensorhynchus summorosus as observed by the fluorescent antibody technique. Japanese J. Exp. Med. 37: 227-238.

29. Dunker, A. K., and R. R. Rueckert. 1969. Observations on molecular weight determinations on polyacrylamide gel. J. Biol. Chem. 244: 5074-5080.

30. Filshie, B. K., and J. Rehacek. 1968. Studies of the morphology of Murray Valley Encephalitis and Japanese Encephalitis viruses growing in cultured mosquito cells. Virology 34: 435-443.

31. Friedman, R. M. 1968. Replicative intermediate of an arbovirus. J. Virol. 2: 547-552.

32. Friedman, R. M., H. B. Levy, and W. B. Carter. 1966. Replication of Semliki Forest virus: Three forms of viral RNA produced during infection. Proc. Nat. Acad. Sci. U. S. A. 56: 440-446.

33. Grace, T. D. C. 1966. Establishment of a line of mosquito (Aedes aegypti) cells grown in vitro. Nature 211: 366-367.

34. Grant, J. L., M. C. Britton, and T. E. Kurtz. 1960. Measurement of red blood cell volume with the electronic cell counter. Am. J. Clin. Path. 33: 138-143.

35. Haruna, I., K. Nozu, Y. Ohtaka, and S. Spiegelman. 1963. An RNA "replicase" induced by and selective for a viral RNA. Proc. Nat. Acad. Sci. U. S. A. 50: 905-911.

36. Haruna, I., and S. Spiegelman. 1965. Specific template requirements of RNA replicases. Proc. Nat. Acad. Sci. U. S. A. 54: 579-587.

37. Haughton, G., J. Haot, L. Revesz, and G. Klein. 1965. Lymphoma growth in vivo: Electronic discrimination between tumor and stroma cells. Science 150: 769-771.

38. Heydrick, F. P., J. F. Comer, and R. F. Wachter. 1971. Phospholipid composition of Venezuelan equine encephalitis virus. Virology 7: 642-645.

39. Hobson, P. N., and S. O. Mann. 1970. Applications of the Coulter Counter in microbiology, p. 91. In A. Baillie, and R. J. Gilbert (eds.). Automation, mechanization, and data handling in microbiology. Academic Press, London, New York.

40. Janzen, H. G., A. J. Rhodes, and F. W. Doane. 1970. Chikungunya virus in salivary glands of Aedes aegypti (L.): An electron microscopy study. Can. J. Microbiol. 16: 581-586.

41. Johnson, J. W. 1969. Growth of Venezuelan, and Eastern equine encephalomyelitis viruses in tissue cultures of minced Aedes aegypti larvae. Am. J. Trop. Med. Hyg. 18: 103-114.

42. Johnson, J. W. 1971. Susceptibility of tissue cultures of minced Aedes aegypti pupae and adults to infection with Venezuelan equine encephalomyelitis virus. Am. J. Trop. Med. Hyg. 20: 761-764.

43. Kissling, R. E., R. W. Chamberlain, D. B. Nelson, and D. D. Stamm. 1956. Venezuelan equine encephalomyelitis in horses. Amer. J. Hyg. 63: 274-287.

44. Klimenko, S. M., F. I. Yershov, Y. P. Gofman, A. P. Nabatnikov, and V. M. Zhdanov. 1965. Architecture of Venezuelan equine encephalomyelitis virus. Virology 27: 125-128.

45. Kubas, V., and F. A. Rios. 1939. The causative agent of infectious equine encephalomyelitis in Venezuela. Science 90: 20-21.

46. Kubitschek. H. E. 1960. Electronic measurement of particle size. Research (London) 13: 128-135.

47. Kubitschek, H. E. 1969. Counting and sizing micro-organisms with the Coulter Counter, p. 593. In J. R. Norris, and D. W. Ribbons (eds.). Methods in microbiology, Vol. 1. Academic Press, London, New York.

48. Ladinsky, J. J., G. E. Sarto, and B. M. Peckham. 1964. Cell size distribution patterns as a means of uterine cancer detection. J. Lab. and Clin. Med. 64: 970-976.

49. Lam, K. S. K., and I. D. Marshall. 1968. Dual infections of Aedes aegypti with arboviruses. II. Salivary gland damage by Semliki Forest virus in relation to dual infections. Am. J. Trop. Med. Hyg. 17: 637-644.

50. LaMotte, L. C. 1960. Japanese B encephalitis virus in the organs of infected mosquitoes. Am. J. Hyg. 72: 73-87.

51. Larsen, J. R., and R. F. Ashley. 1971. Demonstration of Venezuelan equine encephalomyelitis virus in tissues of Aedes aegypti. Am. J. Trop. Med. Hyg. 20: 754-760.

52. Larson, D. R. 1971. Arboviruses in South Dakota mosquitoes and their pathogenicity to pheasants. M. S. Thesis. South Dakota State University.

53. Levin, J. G., and R. M. Friedman. 1971. Analysis of arbovirus ribonucleic acid forms by polyacrylamide gel electrophoresis. J. Virol. 7: 504-514.

54. Lockart, R. Z. 1964. The necessity for cellular RNA and protein synthesis for viral inhibition resulting from interferon. Biochem. Biophys. Res. Commun. 15: 513-518.

55. Loening, U. E. 1967. The fractionation of high-molecular-weight riobnucleic acid by polyacrylamide-gel electrophoresis. Biochem. J. 102: 251-257.

56. Martin, E. M., and J. A. Sonnabend. 1967. Ribonucleic acid polymerase catalyzing synthesis of double-stranded arbovirus ribonucleic acid. J. Virol. 1: 97-109.

57. Mattern, C. F. T., F. S. Brackett, and B. J. Olson. 1967. Determination of number and size of particles by electronic gating: Blood cells. J. Appl. Physiol. 10: 56-70.

58. Mitsuhashi, J., and K. Maramorosch. 1963. Aseptic cultivation of four virus transmitting species of leafhoppers (Cicadellidae). Contr. Boyce Thompson Inst. 22: 165-173.

59. Montagnier, L., and F. K. Sanders. 1963. Replicative form of encephalomyocarditis virus ribonucleic acid. Nature 199: 664-667.

60. Morgan, C., C. Howe, and H. M. Rose. 1961. Structure and development of viruses as observed in the electron microscope. V. Western equine encephalomyelitis virus. J. Exp. Med. 113: 219-223.

61. Mussgay, M., and J. Weibel. 1962. Electron microscopic and biological studies on the growth of Venezuelan equine encephalomyelitis virus. Virology 16: 52-62.

62. Nagle, S. C., W. C. Crothers, and N. L. Hall. 1967. Growth of

moth cells in suspension in hemolymph-free medium. Appl. Microbiol. 15: 1497-1498.

63. Olson, F. W. 1973. Detection of Staphylococcus aureus enterotoxin B by antibody coated latex particles using Coulter Counter channel shifts. M. S. Thesis. South Dakota State University.

64. Ota, Z. 1965. Electron microscopic study of the development of Japanese B encephalitis virus in porcine kidney stable (PS) cells. Virology 25: 372-378.

65. Pan American Health Organization. 1963. II. Recent arbovirus epidemics in the Americas and information exchange activities. RES report, 63.1, 15 October 1963, pp. 25-41.

66. Parikh, G. C., T. C. Sorenson, and C. S. Duvall. 1973. Identification and quantification of viruses and virus-specific antibodies utilizing latex particles and ^{125}I isotope. Presented at Symposium on Rapid Methods and Automation in Microbiology, Stockholm, Sweden, and to be published in Bio-Technology and Engineering.

67. Paul, S. D., and K. R. P. Singh. 1969. Comparative sensitivity of mosquito cell lines, VERO cell line and infant mice to infection with arboviruses. Curr. Sci. 38: 241-242.

68. Paul, S. D., K. R. P. Singh, and U. K. M. Bhat. 1969. A study on the cytopathic effect of arboviruses on cultures from Aedes albopictus cell line. Indian J. Med. Res. 57: 339-348.

69. Peacock, A. C., and C. W. Dingman. 1967. Resolution of multiple ribonucleic acid species by polyacrylamide gel electrophoresis. Biochemistry 6: 1818-1827.

70. Peacock, A. C., G. Z. Williams, and H. F. Mengoli. 1960. Rapid electronic measurement of cell volume and distribution. J. Natl. Cancer Inst. 25: 63-74.

71. Peleg, J. 1969. Inapparent persistent virus infection in continuously grown Aedes aegypti mosquito cells. J. Gen. Virol. 5: 463-471.

72. Pfefferkorn, E. R., B. W. Burge, and H. M. Coady. 1967. Intracellular conversion of the RNA of Sindbis virus to a double-stranded form. Virology 33: 239-249.

73. Pretlow, T. G., and C. W. Boone. 1969. Separation of mammalian cells using programmed gradient sedimentation. Exp. and Mol. Path. 11: 139-152.

74. Reed, L. V., and H. Muench. 1938. A simple method of estimating fifty per-cent endpoints. Amer. J. Hyg. 27: 493-497.

75. Reich, E., and R. M. Franklin. 1961. Effect of mitomycin C on the growth of some animal viruses. Proc. Nat. Acad. Sci. U. S. A. 47: 1212-1217.

76. Reich, E., R. M. Franklin, A. J. Shatkin, and E. L. Tatum. 1962. Effect of actinomycin D on cellular nucleic acid synthesis and virus production. Science 134: 556-557.

77. Rosemond, H., and T. Sreevalsan. 1973. Viral RNAs associated with ribosomes in Sindbis virus infected HeLa cells. J. Virol. 11: 399-415.

78. Sammartin-Barberi,C., H. Groot, and E. Osborno-Mesa. 1954. Human epidemic in Columbia caused by the Venezuelan equine encephalomyelitis virus. Am. J. Trop. Med. Hyg. 3: 283-293.

79. Santen, R. J. 1965. Automated estimation of diploid and tetraploid nuclei with an electronic particle counter. Exp. Cell Res. 40: 413-420.

80. Schneider, I. 1969. Establishment of three diploid cell lines of Anopheles stephensi (Diptera: Culicidae). J. Cell Biol. 42: 603-606.

81. Shatkin, A. J. 1962. Actinomycin inhibition of ribonucleic acid synthesis and poliovirus infection of HeLa cells. Biochem. Biophys. Acta. 61: 310-313.

82. Simon, E. H. 1961. Evidence for the nonparticipation of DNA in viral RNA synthesis. Virology 13: 105-118.

83. Sinarachatanant, P., and L. C. Olson. 1973. Replication of Dengue virus type 2 in Aedes albopictus cell culture. J. Virol. 12: 275-283.

84. Singh, K. R. P. 1967. Cell cultures derived from larvae of Aedes albopictus (Skuse) and Aedes aegypti (L.). Curr. Sci. 36: 506-508.

85. Singh, K. R. P., and S. D. Paul. 1968. Multiplication of arboviruses in cell lines from Aedes albopictus and Aedes aegypti. Curr. Sci. 37: 65-67.

86. Singh, K. R. P., and S. D. Paul. 1968. Susceptibility of Aedes albopictus and Aedes aegypti cell lines to infection by arbo and other viruses. Indian J. Med. Res. 56: 815-820.

87. Sonnabend, J., L. Dalgarno, R. M. Friedman, and E. M. Martin. 1964. A possible replicative form of Semliki Forest virus RNA. Biochem. Biophys. Res. Commun. 17: 455-460.

88. Sorensen, T. C. 1972. Detection and assay of viruses using latex particles. M. S. Thesis. South Dakota State University.

89. Sreevalsan, T., and Fay Hoh Yin. 1969. Sindbis virus-induced viral ribonucleic polymerase. J. Virol. 3: 599-604.

90. Sreevalsan, T., and R. Z. Lockart, Jr. 1966. Heterogeneous RNAs occurring during the replication of Western equine encephalomyelitis virus. Proc. Nat. Acad. Sci. U. S. A. 55: 974-981.

91. Stevens, T. M. 1970. Arbovirus replication in mosquito cell lines (Singh) grown in monolayer or suspension culture. Proc. Soc. Exp. Biol. 134: 356-361.

92. Stollar, V., R. W. Schlesinger, and T. M. Stevens. 1967. Studies on the nature of Dengue viruses. III. Three forms of viral RNA produced during infection. Proc. Nat. Acad. Sci. U. S. A. 56: 440-446.

93. Stollar, V., T. M. Stevens, and T. Shenk. 1970. RNA of uninfected and Sindbis virus infected mosquito cells (A. albopictus), p. 164. In E. Weiss (ed.). Current topics in microbiology and immunology, Vol. 55. Springer-Verlag, New York, Heidelberg, Berlin.

94. Sweet, B. H., and L. T. Dupree. 1968. Growth of cells derived from Culiseta inornata and Aedes vexans in tissue culture. A preliminary note. Mosquito News 28: 368-373.

95. Tiggertt, W. D., and W. G. Downs. 1962. Studies on the virus of Venezuelan equine encephalomyelitis in Trinidad, W.I.I. The 1943-1944 epizootic. Am. J. Trop. Med. Hyg. 11: 822-834.

96. Toennies, G., L. Iszard, N. B. Rogers, and G. D. Shockman. 1961. Cell multiplication studied with an electronic particle counter. J. Bact. 82: 857-866.

97. Trager, W. 1938. Multiplication of the virus of equine encephalomyelitis in surviving mosquito tissues. Amer. J. Trop. Med. 18: 387-393.

98. Trent, D. W., C. C. Swensen, and A. Q. Qureshi. 1969. Synthesis of Stain Louis encephalitis virus ribonucleic acid in BHK-21/13 cells. J. Virol. 3: 385-394.

99. Varma, M. G. R., and M. Pudney. 1969. The growth and serial passage of cell lines from Aedes aegypti (L.) larvae in different media. J. Med. Entomol. 6: 432-439.

100. Wachter, R. F., and E. W. Johnson. 1962. Lipid content of the equine encephalitis viruses. Federation Proc. 21: 461.

101. Wales, M., and J. N. Wilson. 1961. Theory of coincidence in Coulter particle counters. Rev. Sci. Inst. 32: 1132-1136.

102. Weismann, C., and G. Feix. 1966. Replication of viral RNA. XI. "Minus" strands in vitro. Proc. Nat. Acad. Sci. U. S. A. 55: 1264-1268.

103. Weismann, C., L. Simon, and S. Ochoa. 1963. Induction by an RNA phage of an enzyme catalyzing incorporation of ribonucleotides into ribonucleic acids. Proc. Nat. Acad. Sci. U. S. A. 49: 407-414.

104. Whitfield, S. G., F. A. Murphy, and W. D. Sudia. 1971. Eastern equine encephalomyelitis virus: An electron microscopic study of Aedes triseriatus (SAY) salivary gland infection. Virology 43: 110-122.

105. Yunker, C. E., W. Burgdorfer, and J. Cory. 1968. Growth of some group B arboviruses in two established insect cell lines. Proc. 23rd. Ann. Int. Northwest Conf. on Diseases in Nature Communicable to Man (19-21 Aug.). p. 79-82.

106. Zhdanov, V. M., F. I. Yershov, and L. V. Uryvayev. 1969. Ribonucleic acids synthesized in Venezuelan equine encephalomyelitis virus-infected cells. Virology 38: 355-358.